FINITE ELEMENT METHODS FOR AXISYMMETRIC PDES AND DIVERGENCE FREE FINITE ELEMENT PAIRS ON PARTICULAR MESH REFINEMENTS

by

Ahmed Zytoon

Bachelor of Science, Yarmouk University, 2009

Master of Science, University of Arkansas, 2015

Submitted to the Graduate Faculty of

the Dietrich School of Arts and Sciences in partial fulfillment

of the requirements for the degree of

Doctor of Philosophy

University of Pittsburgh

2021

UNIVERSITY OF PITTSBURGH

KENNETH P. DIETRICH SCHOOL OF ARTS AND SCIENCES

This dissertation was presented

by

Ahmed Zytoon

It was defended on

June 25, 2021

and approved by

Prof. Michael Neilan, Thesis Advisor

Prof. William Layton, Committee Member

Prof. Ivan Yotov, Committee Member

Prof. Catalin Trenchea, Committee Member

Prof. Vincent Ervin, External Committee Member

FINITE ELEMENT METHODS FOR AXISYMMETRIC PDES AND DIVERGENCE FREE FINITE ELEMENT PAIRS ON PARTICULAR MESH REFINEMENTS

Ahmed Zytoon, PhD

University of Pittsburgh, 2021

This dissertation discusses the following two main topics.

1. Finite element approximation for Partial Differential Equations (PDEs) defined on axisymmetric domains:

   We introduce the Darcy equations on axisymmetric domains and we show the stability of a low–order Raviart-Thomas element pair. We provide numerical experiments to support our theoretical results.

   Also, we introduce the Stokes equations on axisymmetric domains and show that the axisymmetric Stokes equations can fit within a commutative de Rham complex.

2. Connection between the grad-div stabilized and divergence-free Stokes finite element pairs and low–order divergence-free elements on particular mesh refinements:

   We introduce the most recent results that connect the grad-div stabilized Taylor–Hood (TH) finite element pair and divergence-free Scott–Vogelius (SV) finite element pairs, and we use these results to extend and generalize this connection to other Stokes finite element pairs.

   Finally, we provide numerical examples for low order divergence-free Stokes finite element pairs defined on particular mesh refinements. This research is focused on the numerical implementation aspects of these finite element pairs.

TABLE OF CONTENTS

LIST OF TABLES

LIST OF FIGURES

PREFACE

I would like to thank everyone who helped and supported me to make this dissertation possible.

1.0 INTRODUCTION

There are several papers and articles that investigate mixed methods for PDEs on axisymmetric domains that are subsets of $\mathbb{R}^3$ [7, 8, 20, 21, 43, 44]. Due to symmetry, the problems can be reduced from the original three-dimensional domain to a two-dimensional one. Hence, the computational complexity will be reduced significantly.

This reduction comes with the cost of dealing with weighted function spaces and modified (singular) differential operators which, in turn, complicates the study of the stability analysis of finite element pairs.

In [20], it was shown that the Raviart–Thomas (RT) finite element pair is stable under the axisymmetric variational formulation using a particular mesh discretization elements called "toroids". A polynomial degree condition was imposed on the RT element pair to achieve the stability result in [20]. Also, the same element was used in [43] to show that the Taylor–Hood finite element is stable for the Stokes problem defined on axisymmetric domain.

In our work, we generalize the stability result in [20] for any polynomial degree, and provide numerical examples to support the theoretical results. Also, we show that the axisymmetric Stokes problem is associated with a de Rham complex using commutative projections.

Next, we turn our attention to the connection between grad-div stabilized and divergence-free Stokes finite elements that were studied in [16]. We expand and generalized the results in [16]. In particular, we show that the results in [16] still hold true for higher degree Taylor–Hood finite element pairs with less restrictions on mesh construction. Also, we introduce a low–order divergence-free finite element pair with a particular mesh refinement that uses a linear Lagrange space for the velocity spaces and piecewise constants for the pressure space. We provide numerical experiments to support our theoretical results.

Finally, we introduce a low–order divergence-free finite element pair for the three–dimensional Stokes problem with a particular mesh refinement that uses a linear Lagrange space for the velocity spaces and piecewise constants for the pressure space. We provide

stability results for this pair, and we focus on the numerical implementation aspects for the finite element method.

2.0 THE AXISYMMETRIC DARCY PROBLEM

In this chapter, we introduce the Darcy problem on an axisymmetric domain and show that the lowest–order Raviart–Thomas finite element pair is stable and can be used to find an approximate solution to the Darcy equations.

2.1 Introduction

In this chapter, we study low–order mixed finite element approximations of three–dimensional Darcy flow in axisymmetric domains and with axisymmetric data. Due to the symmetry of the problem, the original three–dimensional problem is reduced to a two–dimensional one, and therefore this reduction offers considerable less computational effort to approximate the solutions. On the other hand, the axisymmetric formulation necessitates the use of weighted function spaces and modified (singular) differential operators leading to theoretical difficulties. This is especially true for mixed finite element methods because their structure–preserving properties often do not hold in the axisymmetric setting.

Nonetheless, there exists several references that propose and study mixed finite element methods for axisymmetric problems. These include the Stokes (and Navier–Stokes) problem (e.g., [43, 7, 8, 44]) and Maxwell equations (e.g., [19, 18, 41, 6]). On the other hand, the stability and error analysis for the mixed finite element methods for the axisymmetric Darcy problem is relatively less developed [20, 21]. In [20], both Brezzi–Douglas–Marini (BDM) and Raviart–Thomas (RT) mixed finite element methods are proposed for the axisymmetric Darcy problem, and it is shown that these discrete methods are well–posed. Assuming that an auxiliary problem inherits additional regularity (cf. [20, (3.34)]), optimal order error estimates for the pressure and velocity solutions are derived [20, Corollary 3.13]. However, the lowest–order case is noticeably absent from the analysis. Alternatively, one can add grad–div stabilization to the bilinear form to obtain optimal order estimates in the lowest–order case ([20, Corollary 3.7]); however, this modification leads to various computational

issues (e.g., conditioning, error dependence and optimality of grad–div parameter, etc.), and we show here that grad-div stabilization is unnecessary to guarantee convergence in the lowest–order case.

In this chapter, we follow the ideas in [51] and derive error estimates of the direct mixed finite element method using the lowest–order RT elements. The main difficulty in the analysis is that, in contrast to the Cartesian setting, the axisymmetric divergence operator acting on the RT space is not surjective onto the space of piecewise constants. Therefore, in this sense, the method is non-conforming.

The approach we take in the analysis is classical. We simply apply Strang's second lemma to obtain abstract error estimates in terms of the approximation properties of the RT space and the inconsistency (or non-conformity) of the method. We then derive several estimates of the (local) inconsistency of the method, each tailored for different regions of the domain. Using a convex combination of these estimates, and by applying a dyadic decomposition of the domain with respect to the r–variable, we show that the inconsistency of the method is almost first–order provided that the domain is convex. Strang's lemma and the approximation properties of the RT space then imply that pressure and velocity errors are both (almost) first order.

The organization of the chapter is as follows. After setting up the notation, we state the Darcy problem and its axisymmetric formulation in Section 4.2. We give the mixed finite element formulation in Section 4.3 and state some preliminary results. We then derive two estimates that measure the consistency error, and use these estimates to derive error estimates for the velocity and pressure solutions. Finally, in Section 4.4 we perform some numerical experiments which support the theoretical estimates.

2.2 Notation and Preliminaries

Let $\check{\Omega} \subset \mathbb{R}^3$ denote a three-dimensional domain obtained by rotating a simply-connected polygon $\Omega \subset \mathbb{R}^2$ about the z-axis. Namely, we assume that $\Omega = \check{\Omega} \cap \{(r, 0, z) : \ r > 0, z \in \mathbb{R}\}$, where (r, θ, z) denote the cylindrical coordinates. Let $\Gamma_0 = \partial\Omega \cap \{(0, z)\}$ denote the part

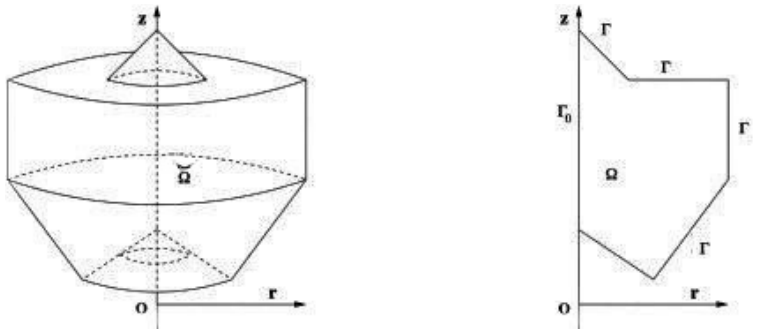

Figure 1: Axisymmetric domain $\breve{\Omega} \subset \mathbb{R}^3$ (left), and corresponding 2D domain $\Omega \subset \mathbb{R}^2$ (right).

of the boundary of Ω that intersects the z-axis and $\Gamma = \partial\Omega \setminus \Gamma_0$. We assume that Γ_0 is connected. The figure below [44] shows a two dimensional domain Ω and its corresponding three dimensional axisymmetric domain $\breve{\Omega}$.

The Darcy equations, in Cartesian coordinates defined on $\breve{\Omega}$, is given by the system of equations

$$\nu K^{-1}\breve{\boldsymbol{u}} + \breve{\nabla}\breve{p} = \breve{\boldsymbol{f}} \qquad \text{in } \breve{\Omega}, \tag{1a}$$

$$\breve{\nabla} \cdot \breve{\boldsymbol{u}} = \breve{g} \qquad \text{in } \breve{\Omega}, \tag{1b}$$

$$\breve{\boldsymbol{u}} \cdot \breve{\boldsymbol{n}} = 0 \qquad \text{on } \partial\breve{\Omega}, \tag{1c}$$

where the velocity $\breve{\boldsymbol{u}} = (\breve{u}_1, \breve{u}_2, \breve{u}_3)^\intercal$ and pressure $\breve{p}$ are functions of $\breve{x} = (\breve{x}_1, \breve{x}_2, \breve{x}_3)^\intercal$, and $\breve{\nabla}$ denotes the gradient operator with respect to $\breve{x}$. In (1), the matrix K denotes the permeability tensor, and ν is the viscosity. Similar to [20], we assume that $\breve{g} \equiv 0$, $K = kI_3$ for some constant $k > 0$, and set $\nu = \nu/k$. As explained in [20], the assumption that $\breve{g} = 0$ is equivalent to introducing a change of variable $\breve{\boldsymbol{u}} = \breve{\boldsymbol{u}}_0 + \breve{\boldsymbol{u}}_p$, where $\breve{\boldsymbol{u}}_p = \breve{\nabla}\breve{w}$ and $\breve{w}$ satisfies $\breve{\nabla} \cdot \breve{\nabla}\breve{w} = \breve{g}$ in $\breve{\Omega}$ and $\partial\breve{w}/\partial\breve{\boldsymbol{n}} = 0$ on $\partial\breve{\Omega}$.

For $\breve{U} \subset \mathbb{R}^d$, let

$$L^p(\breve{U}) := \{\breve{w} : \breve{U} \mapsto \mathbb{R} : \ \|\breve{w}\|_{L^p(\breve{U})} := \Big(\int_{\breve{U}} |\breve{w}|^p \, d\breve{x}\Big)^{1/p} < \infty\},$$

$$H^m(\breve{U}) := \{\breve{w} : \breve{U} \mapsto \mathbb{R} : \ \|\breve{w}\|_{H^m(\breve{U})} := \Big(\sum_{|\beta| \le m} \|\breve{D}^\beta \breve{w}\|^2_{L^2(\breve{U})}\Big)^{1/2} < \infty\},$$

We denote the analogous vector-valued function space in boldface; for example $\boldsymbol{H}^1(\check{U}) = H^1(\check{U})^d$ and $\boldsymbol{L}^2(\check{U}) = L^2(\check{U})^d$, $d = 2, 3$.

Defining

$$\boldsymbol{H}(\mathrm{div};\check{\Omega}) := \{\check{\boldsymbol{v}} \in \boldsymbol{L}^2(\check{\Omega}) : \ \|\check{\boldsymbol{v}}\|_{\boldsymbol{H}_0(\mathrm{div};\check{\Omega})} := (\|\check{\boldsymbol{v}}\|_{\boldsymbol{L}^2(\check{\Omega})} + \|\check{\nabla}\cdot\check{\boldsymbol{v}}\|_{L^2(\check{\Omega})})^{1/2} < \infty\},$$
$$L^2(\check{\Omega}) := \{\check{q} : \check{\Omega} \mapsto \mathbb{R} : \ \|\check{q}\|_{L^2(\check{\Omega})} := (\int_{\check{\Omega}} |\check{q}|^2 \, d\check{x})^{1/2} < \infty\},$$

and their variants

$$\boldsymbol{H}_0(\mathrm{div};\check{\Omega}) := \{\check{\boldsymbol{v}} \in \boldsymbol{H}(\mathrm{div};\check{\Omega}) : \ \check{\boldsymbol{v}}\cdot\check{\boldsymbol{n}}|_{\partial\check{\Omega}} = 0\}, \tag{2}$$
$$L^2_0(\check{\Omega}) := \{\check{q} \in L^2(\check{\Omega}) : \ \int_{\check{\Omega}} \check{q} \, d\check{x} = 0\}, \tag{3}$$

the weak formulation for (1) reads: Find $(\check{\boldsymbol{u}}, \check{p}) \in \boldsymbol{H}_0(\mathrm{div};\check{\Omega}) \times L^2_0(\check{\Omega})$ such that

$$\nu \int_{\check{\Omega}} \check{\boldsymbol{u}}\cdot\check{\boldsymbol{v}} \, d\check{x} - \int_{\check{\Omega}} (\check{\nabla}\cdot\check{\boldsymbol{v}})\check{p} \, d\check{x} = \int_{\check{\Omega}} \check{\boldsymbol{f}}\cdot\check{\boldsymbol{v}} \, d\check{x} \qquad \forall \check{\boldsymbol{v}} \in \boldsymbol{H}_0(\mathrm{div};\check{\Omega}), \tag{4a}$$
$$\int_{\check{\Omega}} (\check{\nabla}\cdot\check{\boldsymbol{u}})\check{q} \, d\check{x} = 0 \qquad \forall \check{q} \in L^2_0(\check{\Omega}). \tag{4b}$$

Theorem 2.2.1. *There exists a unique solution* $(\check{\boldsymbol{u}}, \check{p}) \in \boldsymbol{H}_0(\mathrm{div};\check{\Omega}) \times L^2_0(\check{\Omega})$ *to* (4).

Theorem 2.2.1 is well-known [30], but we provide a proof for completeness.

The proof of Theorem 2.2.1 relies on a few technical results. First, we state a general framework for saddle point problems. Its proof can be found in [30, CH. I,Sect. 4].

Proposition 2.2.2. *Let* $\boldsymbol{X}$ *and* Y *be two Hilbert spaces, and let* $\check{a} : \boldsymbol{X} \times \boldsymbol{X} \to \mathbb{R}$ *and* $\check{b} : \boldsymbol{X} \times Y \to \mathbb{R}$ *be bilinear forms. Let*

$$\boldsymbol{Z} = \{\check{\boldsymbol{v}} \in \boldsymbol{X} : \ \check{b}(\check{\boldsymbol{v}}, \check{q}) = 0, \ \forall \check{q} \in Y\},$$

and suppose that the following three conditions are satisfied:

1. $\check{a}(.,.)$ *and* $\check{b}(.,.)$ *are continuous on their domains.*
2. $\check{a}(.,.)$ *is symmetric for all* $\check{\boldsymbol{v}} \in \boldsymbol{X}$*, and there is a constant* $\alpha > 0$ *such that*

$$\check{a}(\check{\boldsymbol{v}}, \check{\boldsymbol{v}}) \geq \alpha \|\check{\boldsymbol{v}}\|^2_{\boldsymbol{X}} \quad \forall \check{\boldsymbol{v}} \in \boldsymbol{Z}.$$

3. There is $\check{\beta} > 0$ such that the following inf-sup condition is satisfied

$$\sup_{\check{\boldsymbol{v}} \in \boldsymbol{X} \setminus \{0\}} \frac{\check{b}(\check{\boldsymbol{v}}, \check{q})}{\|\check{\boldsymbol{v}}\|_{\boldsymbol{X}}} \geq \check{\beta} \|\check{q}\|_Y, \quad \forall \check{q} \in Y. \tag{5}$$

Then for any $\boldsymbol{F} \in \boldsymbol{X}'$, there exists a unique solution $(\check{\boldsymbol{u}}, \check{p}) \in \boldsymbol{X} \times Y$ such that

$$\begin{aligned} \check{a}(\check{\boldsymbol{u}}, \check{\boldsymbol{v}}) + \check{b}(\check{\boldsymbol{v}}, \check{p}) &= \boldsymbol{F}(\check{\boldsymbol{v}}) \qquad \forall \check{\boldsymbol{v}} \in \boldsymbol{X}, \\ \check{b}(\check{\boldsymbol{u}}, \check{q}) &= 0 \qquad \forall \check{q} \in Y. \end{aligned}$$

Lemma 2.2.3. *The operator $\check{\nabla} \cdot : \boldsymbol{H}_0(\mathrm{div}; \check{\Omega}) \to L_0^2(\check{\Omega})$ is surjective with a bounded right-inverse, namely, for any $\check{q} \in L_0^2(\check{\Omega})$, there exists $\check{\boldsymbol{v}} \in \boldsymbol{H}_0(\mathrm{div}; \check{\Omega})$ such that $\check{\nabla} \cdot \check{\boldsymbol{v}} = \check{q}$ and $\|\check{\boldsymbol{v}}\|_{\boldsymbol{H}_0(\mathrm{div};\check{\Omega})} \leq \check{\beta}^{-1} \|\check{q}\|_{L^2(\check{\Omega})}$, where $\check{\beta} > 0$ depends on $\check{\Omega}$.*

Proof. Let $\check{q} \in L_0^2(\check{\Omega})$. We assume that $\check{\Omega}$ is smooth, the result is still valid for non-smooth domains (see [15]).

Consider the following auxiliary problem in $\check{\Omega}$:

$$\begin{aligned} \check{\Delta} \hat{u} &= \tilde{q} \qquad \text{in } \check{\Omega}, \\ \frac{\partial \hat{u}}{\partial \check{\boldsymbol{n}}} &= 0 \qquad \text{on } \partial\check{\Omega}. \end{aligned}$$

By [49], there holds $\hat{u} \in H^2(\check{\Omega})$ and $\|\hat{u}\|_{H^2(\check{\Omega})} \leq C \|\tilde{q}\|_{L^2(\check{\Omega})} = C \|\check{q}\|_{L^2(\check{\Omega})}$. Now set $\check{\boldsymbol{v}} = \check{\nabla} \hat{u}|_{\check{\Omega}} \in \boldsymbol{H}^1(\check{\Omega})$, so that $\check{\nabla} \cdot \check{\boldsymbol{v}} = \check{\Delta} \hat{u} = \check{q}$ and $\|\check{\boldsymbol{v}}\|_{\boldsymbol{H}_0(\mathrm{div};\check{\Omega})} \leq \|\hat{u}\|_{H^2(\check{\Omega})} \leq C \|\check{q}\|_{L^2(\check{\Omega})}$. Furthermore, we have

$$\check{\boldsymbol{v}} \cdot \check{\boldsymbol{n}} = \check{\nabla} \hat{u} \cdot \check{\boldsymbol{n}} = \frac{\partial \hat{u}}{\partial \check{\boldsymbol{n}}} = 0 \qquad \text{on } \partial\check{\Omega}.$$

Therefore, we conclude that $\check{\boldsymbol{v}} \in \boldsymbol{H}_0(\mathrm{div}; \check{\Omega})$ and $\check{\nabla} \cdot \check{\boldsymbol{v}} = \check{q}$. □

Proof of Theorem 2.2.1. Letting $\boldsymbol{X} = \boldsymbol{H}_0(\mathrm{div}; \check{\Omega})$, $Y = L^2(\check{\Omega})$, $\check{a}(\check{\boldsymbol{u}}, \check{\boldsymbol{v}}) = \nu \int_{\check{\Omega}} \check{\boldsymbol{u}} \cdot \check{\boldsymbol{v}} \, d\check{x}$, $\check{b}(\check{\boldsymbol{v}}, \check{p}) = -\int_{\check{\Omega}} (\check{\nabla} \cdot \check{\boldsymbol{v}}) \check{p} \, d\check{x}$ and $\boldsymbol{F}(\check{\boldsymbol{v}}) = \int_{\check{\Omega}} \check{\boldsymbol{f}} \cdot \check{\boldsymbol{v}} \, d\check{x}$, problem (4) becomes: Find $(\check{\boldsymbol{u}}, \check{p}) \in \boldsymbol{H}_0(\mathrm{div}; \check{\Omega}) \times L_0^2(\check{\Omega})$ such that

$$\begin{aligned} \check{a}(\check{\boldsymbol{u}}, \check{\boldsymbol{v}}) + \check{b}(\check{\boldsymbol{v}}, \check{p}) &= \boldsymbol{F}(\check{\boldsymbol{v}}), \quad \forall \check{\boldsymbol{v}} \in \boldsymbol{H}_0(\mathrm{div}; \check{\Omega}), \\ \check{b}(\check{\boldsymbol{u}}, \check{q}) &= 0, \qquad \forall \check{q} \in L_0^2(\check{\Omega}). \end{aligned}$$

Hence, to proceed with the proof, we only need to verify the conditions stated in Proposition 2.2.2 with $\boldsymbol{Z} = \{\check{\boldsymbol{v}} \in \boldsymbol{H}_0(\mathrm{div}; \check{\Omega}) : \ \check{b}(\check{\boldsymbol{v}}, \check{q}) = 0, \ \forall \check{q} \in L^2(\check{\Omega})\}$.

1. Continuity of the bilinear forms $\check{a}(.,.)$ and $\check{b}(.,.)$ follow directly from the Cauchy-Schwarz inequality.
2. Let $\check{\boldsymbol{v}} \in \boldsymbol{Z}$, then $\check{\nabla} \cdot \check{\boldsymbol{v}} \in L^2(\check{\Omega})$. Since $\check{\boldsymbol{v}} \in \boldsymbol{Z}$, then we have that

$$\check{b}(\check{\boldsymbol{v}}, \check{\nabla} \cdot \check{\boldsymbol{v}}) = 0 = -\int_{\check{\Omega}} (\check{\nabla} \cdot \check{\boldsymbol{v}})(\check{\nabla} \cdot \check{\boldsymbol{v}})\, d\check{x} = -\|\check{\nabla} \cdot \check{\boldsymbol{v}}\|^2_{L^2(\check{\Omega})}.$$

   Hence, for $\check{\boldsymbol{v}} \in \boldsymbol{Z}$ we have that $\|\check{\boldsymbol{v}}\|_{\boldsymbol{H}_0(\mathrm{div};\check{\Omega})} = \|\check{\boldsymbol{v}}\|_{\boldsymbol{L}^2(\check{\Omega})}$. So

$$\check{a}(\check{\boldsymbol{v}}, \check{\boldsymbol{v}}) = \nu\|\check{\boldsymbol{v}}\|^2_{\boldsymbol{L}^2(\check{\Omega})} = \nu\|\check{\boldsymbol{v}}\|^2_{\boldsymbol{H}_0(\mathrm{div};\check{\Omega})} \qquad \forall \check{\boldsymbol{v}} \in \boldsymbol{Z}.$$

   Since $\check{a}(.,.)$ is clearly symmetric, we conclude that $\check{a}(.,.)$ satisfies 2 in Proposition 2.2.2.
3. Let $\check{q} \in L^2_0(\check{\Omega})$ with $\check{q} \neq 0$. Applying Lemma 2.2.3 there exists $\check{\boldsymbol{w}} \in \boldsymbol{H}_0(\mathrm{div};\check{\Omega})$ such that $\check{\nabla} \cdot \check{\boldsymbol{w}} = \check{q}$ and $\|\check{\boldsymbol{w}}\|_{\boldsymbol{H}_0(\mathrm{div};\check{\Omega})} \leq \check{\beta}^{-1}\|\check{q}\|_{L^2(\check{\Omega})}$. Consequently,

$$\check{\beta}\|\check{q}\|_{L^2(\check{\Omega})} = \frac{\check{b}(\check{\boldsymbol{w}}, \check{q})}{\check{\beta}^{-1}\|\check{q}\|_{L^2(\check{\Omega})}} \leq \frac{\check{b}(\check{\boldsymbol{w}}, \check{q})}{\|\check{\boldsymbol{w}}\|_{\boldsymbol{H}_0(\mathrm{div};\check{\Omega})}} \leq \sup_{\check{\boldsymbol{v}} \in \boldsymbol{H}_0(\mathrm{div};\check{\Omega})\setminus\{0\}} \frac{\check{b}(\check{\boldsymbol{v}}, \check{q})}{\|\check{\boldsymbol{v}}\|_{\boldsymbol{H}_0(\mathrm{div};\check{\Omega})}}.$$

   Therefore the inf-sup condition is satisfied.

Since we have confirmed all of the conditions in Proposition 2.2.2, we conclude that there exists a unique solution to (4). □

The solution pair $(\check{\boldsymbol{u}}, \check{p})$ to (4) enjoys the following regularity [24, 1].

Theorem 2.2.4. *There exists $\epsilon \in (0, 1]$ depending on the Lipschitz character of $\check{\Omega}$ such that the solution to (4) satisfies $\check{p} \in W^{1,t}(\check{\Omega})$ for all $2 \leq t < 3/(1-\epsilon)$ and $\check{\boldsymbol{u}} \in \boldsymbol{H}^s(\check{\Omega})$ for some $s > 1/2$, provided that $\check{\boldsymbol{f}} \in \boldsymbol{L}^t(\check{\Omega})$. If $\check{\Omega}$ is convex, then the solution satisfies $\check{p} \in W^{1,\infty}(\check{\Omega})$ and $\check{\boldsymbol{u}} \in \boldsymbol{H}^1(\check{\Omega})$ if $\check{\boldsymbol{f}} \in \boldsymbol{H}(\mathrm{div};\check{\Omega})$.*

Remark 2.2.5. We note that if $\check{\Omega}$ is convex, then so is Ω. However, the converse is not necessarily true.

Now, we introduce the cylindrical coordinate system (r, θ, z) with $r = \sqrt{\check{x}_1^2 + \check{x}_2^2}$, $\theta = \arctan(\check{x}_2/\check{x}_1)$, and $z = \check{x}_3$. For a vector field $\check{\boldsymbol{v}} = (\check{v}_1, \check{v}_2, \check{v}_3)^\intercal$, we denote by $\bar{v}_r$, $\bar{v}_\theta$, and $\bar{v}_z$ its radial, angular, and axial components, respectively, i.e.,

$$\begin{aligned}
\bar{v}_r &= \check{v}_1 \cos\theta + \check{v}_2 \sin\theta, \\
\bar{v}_\theta &= -\check{v}_1 \sin\theta + \check{v}_2 \cos\theta, \\
\bar{v}_z &= \check{v}_3.
\end{aligned}$$

We denote $\bar{\boldsymbol{v}} = \bar{\boldsymbol{v}}(r, \theta, z) = (\bar{v}_r, \bar{v}_\theta, \bar{v}_z)^\intercal$ so that

$$\bar{\boldsymbol{v}} = R_\theta \check{\boldsymbol{v}}, \tag{6}$$

where the rotation matrix R_θ is given by (7) (with $\eta = \theta(\check{x})$). Likewise, for a scalar function $\check{q} : \check{\Omega} \to \mathbb{R}$, we set $\bar{q} : \check{\Omega} \to \mathbb{R}$ such that $\check{q}(\check{x}) = \bar{q}(r, \theta, z)$.

For a fixed $\eta \in [-\pi, \pi]$, we define the rotation matrix

$$R_\eta = \begin{pmatrix} \cos\eta & \sin\eta & 0 \\ -\sin\eta & \cos\eta & 0 \\ 0 & 0 & 1 \end{pmatrix}. \tag{7}$$

Note the trivial identities $\det(R_\eta) = 1$ and $R_{-\eta} = (R_\eta)^{-1}$ for any $\eta \in [-\pi, \pi]$. These properties will be used often.

Definition 2.2.6.

1. A scalar function $\check{q} : \check{\Omega} \to \mathbb{R}$ is said to be *axisymmetric* if $\check{q} \circ R_\eta = \check{q}$ for all $\eta \in [-\pi, \pi]$.
2. A vector field $\check{\boldsymbol{v}} : \check{\Omega} \to \mathbb{R}^3$ is said to be *axisymmetric* if $\check{\boldsymbol{v}} = R_{-\eta} \check{\boldsymbol{v}} \circ R_\eta$ for all $\eta \in [-\pi, \pi]$.

Note that definition 2 along with the identity $R_{-\eta} = (R_\eta)^{-1}$ shows that $\bar{\boldsymbol{v}} = \check{\boldsymbol{v}} \circ R_\theta$ if $\check{\boldsymbol{v}}$ is axisymmetric. Since $R_\theta \check{x} = (r, 0, z)^\intercal$, we conclude that if $\check{\boldsymbol{v}}$ is axisymmetric (with respect to definition 2), then the components $\bar{v}_r, \bar{v}_\theta, \bar{v}_z$ are also axisymmetric (with respect to definition 1). Consequently there holds

$$\frac{\partial \bar{q}}{\partial \theta} = \frac{\partial \bar{v}_r}{\partial \theta} = \frac{\partial \bar{v}_\theta}{\partial \theta} = \frac{\partial \bar{v}_z}{\partial \theta} = 0 \tag{8}$$

for axisymmetric functions $\check{q}$ and $\check{\boldsymbol{v}}$.

If the source function $\check{\boldsymbol{f}}$ is axisymmetric, then the solution $(\check{\boldsymbol{u}}, \check{p})$ is axisymmetric as well [9]. Let $(\bar{u}_r, \bar{u}_\theta, \bar{u}_z)^\intercal$ and $\bar{p}$ be the cylindrical coordinate representation of $\check{\boldsymbol{u}}$ and $\check{p}$, respectively, and set $p(r,z) = \bar{p}(r,\theta,z)$, $u_\theta(r,z) = \bar{u}_\theta(r,\theta,z)$, and $\boldsymbol{u}(r,z) = (u_r(r,z), u_z(r,z))^\intercal$ with $u_r(r,z) = \bar{u}_r(r,\theta,z)$ and $\bar{u}_z(r,\theta,z)$. To state the axisymmetric problem and the corresponding variational formulation, we require some additional function space notation.

For $\alpha \in \mathbb{R}$, $p \in [1,\infty)$, and Lipschitz subdomain $D \subset \Omega$, we define the weighted L^p-space

$$\|v\|^p_{L^p_\alpha(D)} := \int_D r^\alpha |v|^p \, dr\, dz,$$

and set

$$L^p_\alpha(D) := \{v : D \to \mathbb{R} : \ \|v\|_{L^p_\alpha(D)} < \infty\}.$$

In the case that $\alpha = 0$, the subscript is omitted. We further define, for a non-negative integer m and number $p \in [1,\infty)$, the weighted norms and semi-norms

$$\|v\|^p_{W^{m,p}_\alpha(D)} = \sum_{|\beta| \le m} \int_D r^\alpha \Big| \frac{\partial^{|\beta|} v}{\partial^{\beta_1} r \partial^{\beta_2} z} \Big|^p \, dr\, dz,$$

$$|v|^p_{W^{m,p}_\alpha(D)} = \sum_{|\beta| = m} \int_D r^\alpha \Big| \frac{\partial^{|\beta|} v}{\partial^{\beta_1} r \partial^{\beta_2} z} \Big|^p \, dr\, dz,$$

and set

$$W^{m,p}_\alpha(D) = \{v : D \to \mathbb{R} : \ \|v\|_{W^{m,p}_\alpha(D)} < \infty\}.$$

In the case $p = 2$, we use the notation $H^m_\alpha(D) = W^{m,2}_\alpha(D)$.

Observe that the divergence of a vector field $\check{\boldsymbol{v}} = (\check{v}_1, \check{v}_2, \check{v}_3)^\intercal$ in cylindrical coordinates is given by

$$\check{\nabla} \cdot \check{\boldsymbol{v}} = \frac{1}{r}\Big(\frac{\partial (r \bar{v}_r)}{\partial r} + \frac{\partial \bar{v}_\theta}{\partial \theta}\Big) + \frac{\partial \bar{v}_z}{\partial z}.$$

If $\check{\boldsymbol{v}}$ is axisymmetric, then $\frac{\partial \bar{v}_\theta}{\partial \theta} = 0$. Hence, we define the axisymmetric divergence operator applied to a vector-valued function $\boldsymbol{v} = (v_r, v_z)^\intercal$ by

$$\nabla_{rz} \cdot \boldsymbol{v} := \frac{\partial v_r}{\partial r} + \frac{\partial v_z}{\partial z} + \frac{1}{r} v_r.$$

The two–dimensional gradient operator is defined as

$$\nabla_a w = (\frac{\partial w}{\partial r}, \frac{\partial w}{\partial z})^\intercal,$$

and note that $\nabla_{rz} \cdot \boldsymbol{v} = \nabla_a \cdot \boldsymbol{v} + \frac{1}{r} v_r$. We also have the integration-by-parts formula

$$\begin{aligned}\int_D (r\nabla_{rz} \cdot \boldsymbol{v}) w \, dr \, dz &= \int_D \big(r\nabla_a \cdot \boldsymbol{v} + v_r\big) w \, dr \, dz \\ &= \int_{\partial D} r(\boldsymbol{v} \cdot \boldsymbol{n}) w \, ds - \int_D r(\boldsymbol{v} \cdot \nabla_a w) \, dr \, dz\end{aligned}$$

for sufficiently smooth $\boldsymbol{v}$ and w. Here, $\boldsymbol{n}$ denotes the outward unit normal of ∂D.

Define

$$\begin{aligned}\boldsymbol{X}_1 :&= \mathring{\boldsymbol{H}}_1(\mathrm{div}; \Omega) := \{\boldsymbol{v} \in \boldsymbol{L}_1^2(\Omega) : \ \nabla_{rz} \cdot \boldsymbol{v} \in L_1^2(\Omega), \ \boldsymbol{v} \cdot \boldsymbol{n}|_{\partial\Omega} = 0\}, \\ Q :&= \mathring{L}_1(\Omega) := \{q \in L_1^2(\Omega), \ \int_\Omega rq \, dr \, dz = 0\},\end{aligned}$$

with corresponding norms

$$\begin{aligned}\|\boldsymbol{v}\|_{\boldsymbol{X}_1}^2 :&= \|\boldsymbol{v}\|_{L_1^2(\Omega)}^2 + \|\nabla_{rz} \cdot \boldsymbol{v}\|_{L_1^2(\Omega)}^2, \\ \|q\|_Q :&= \|q\|_{L_1^2(\Omega)}.\end{aligned}$$

Making a change of variables in (4), a calculation reveals that

$$\nu \int_\Omega r\boldsymbol{u} \cdot \boldsymbol{v} \, dr \, dz - \int_\Omega r(\nabla_{rz} \cdot \boldsymbol{v}) p \, dr \, dz = \int_\Omega r(\boldsymbol{f} \cdot \boldsymbol{v}) \, dr \, dz \qquad \forall \boldsymbol{v} \in \boldsymbol{X}_1, \tag{9a}$$

$$\int_\Omega r(\nabla_{rz} \cdot \boldsymbol{u}) q \, dr \, dz = 0 \qquad \forall q \in Q. \tag{9b}$$

Remark 2.2.7. The angular component u_θ satisfies

$$\nu \int_\Omega r u_\theta v_\theta \, dr \, dz = \int_\Omega r f_\theta v_\theta \, dr \, dz \qquad \forall v_\theta \in L_1^2(\Omega),$$

which is decoupled from the system (9).

Remark 2.2.8. The regularity results stated in Theorem 2.2.4 directly imply that the axisymmetric solution to (9) inherits elliptic regularity. If there holds $\check{p} \in W^{1,t}(\check{\Omega})$, then we deduce via a change of variables that $p \in W_1^{1,t}(\Omega)$.

2.3 Finite Element Method and Convergence Analysis

Denote by $\mathcal{T}_h$ a conforming, shape–regular, quasi-uniform, simplicial triangulation of Ω. For $\tau \in \mathcal{T}_h$, we denote by $h_\tau = \operatorname{diam}(\tau)$ and set $h = \max_{\tau\in\mathcal{T}_h} h_\tau$. The local, lowest–order Raviart–Thomas space is given by

$$\boldsymbol{X}(\tau) := \big\{\boldsymbol{v}_h = \boldsymbol{\alpha} + \beta(r,z)^\intercal : \ \boldsymbol{\alpha} \in \mathbb{R}^2,\ \beta \in \mathbb{R}\big\},$$

and the global version is defined as

$$\boldsymbol{X}_h := \big\{\boldsymbol{v}_h \in \boldsymbol{X}_1 : \ \boldsymbol{v}_h|_T \in \boldsymbol{X}(\tau)\ \forall \tau \in \mathcal{T}_h\big\}.$$

We further set Q_h to be the space of piecewise constants with vanishing mean, i.e.,

$$Q_h = \{q \in Q : \ q|_\tau \in \mathbb{R}\ \forall \tau \in \mathcal{T}_h\}.$$

The mixed finite element method for the axisymmetric Darcy problem (9) reads: Find $(\boldsymbol{u}_h, p_h) \in \boldsymbol{X}_h \times Q_h$ such that

$$\nu \int_\Omega r(\boldsymbol{u}_h \cdot \boldsymbol{v}_h)\,dr\,dz + \int_\Omega (r\nabla_{rz} \cdot \boldsymbol{v}_h) p_h\,dr\,dz = \int_\Omega r\boldsymbol{f} \cdot \boldsymbol{v}_h\,dr\,dz, \quad \forall \boldsymbol{v}_h \in \boldsymbol{X}_h, \tag{10a}$$

$$\int_\Omega r(\nabla_{rz} \cdot \boldsymbol{u}_h) q_h\,dr\,dz = 0, \qquad \forall q_h \in Q_h. \tag{10b}$$

The following theorems concern the well-possedness of (10) and the approximation properties of the discretely divergence–free space. Their proofs can be found in [20, Corollary 3.6] and [20, Corollary A.6]

Theorem 2.3.1. *The inf-sup condition*

$$\sup_{\boldsymbol{v}_h \in \boldsymbol{X}_h \setminus \{0\}} \frac{\int_\Omega (r\nabla_{rz} \cdot \boldsymbol{v}_h) q_h\,dr\,dz}{\|\boldsymbol{v}_h\|_X} \geq \beta \|q_h\|_Q \qquad \forall q_h \in Q_h \tag{11}$$

is satisfied with $\beta > 0$ independent of h. Consequently, there exists a unique solution to (10).

Theorem 2.3.2. *Define the space of discretely divergence–free functions:*

$$\boldsymbol{V}_h = \{\boldsymbol{v}_h \in \boldsymbol{X}_h : \int_\Omega r(\nabla_{rz} \cdot \boldsymbol{v}_h) q \, dr \, dz = 0 \ \forall q_h \in Q_h\}.$$

Then for any $\boldsymbol{u} \in \boldsymbol{H}^1_1(\Omega)$ *with* $\nabla_{rz} \cdot \boldsymbol{u} = 0$*, there exists* $\boldsymbol{v}_h \in \boldsymbol{V}_h$ *such that*

$$\|\boldsymbol{u} - \boldsymbol{v}_h\|_{L^2_1(\Omega)} \leq Ch|\boldsymbol{u}|_{H^1_1(\Omega)}.$$

Remark 2.3.3. Here and what follows, the letter C denotes a generic, h-independent, positive constant that may take different values at each occurrence.

Unlike the Cartesian setting, the axisymmetric divergence operator acting on the Raviart-Thomas space is not surjective onto the space of piecewise constants. As a result, the method is non-conforming in the sense that $\boldsymbol{V}_h \not\subset \boldsymbol{V} := \{\boldsymbol{v} \in \boldsymbol{X}_1 : \ \nabla_{rz} \cdot \boldsymbol{v} \equiv 0\}$. We follow the classical framework of non-conforming methods in order to obtain error estimates of the discrete approximation. In particular, Strang's Second Lemma [61] applied to (10) yields the following result.

Lemma 2.3.4. *The velocity error satisfies*

$$\nu\|\boldsymbol{u} - \boldsymbol{u}_h\|_{L^2_1(\Omega)} \leq \nu \inf_{\boldsymbol{w}_h \in \boldsymbol{V}_h} \|\boldsymbol{u} - \boldsymbol{w}_h\|_{L^2_1(\Omega)} + \sup_{\boldsymbol{v}_h \in \boldsymbol{V}_h \setminus \{0\}} \frac{\int_\Omega r(\nabla_{rz} \cdot \boldsymbol{v}_h) p \, dr \, dz}{\|\boldsymbol{v}_h\|_{L^2_1(\Omega)}}, \tag{12}$$

$$\|p - p_h\|_Q \leq C\big(\nu\|\boldsymbol{u} - \boldsymbol{u}_h\|_{L^2_1(\Omega)} + \inf_{q_h \in Q_h} \|p - q_h\|_Q\big), \tag{13}$$

where $C > 0$ *depends on the discrete inf–sup constant* $\beta > 0$ *in* (11)*.*

Proof. The proof of (12)–(13) is standard, but we provide it here for completeness.

Let $\tilde{\boldsymbol{u}}_h \in \boldsymbol{V}_h$ be the projection of $\boldsymbol{u}$ onto $\boldsymbol{V}_h$ with respect to the $L^2_1(\Omega)$ inner product, i.e.,

$$\int_\Omega r\tilde{\boldsymbol{u}}_h \cdot \boldsymbol{v}_h \, dr \, dz = \int_\Omega r\boldsymbol{u} \cdot \boldsymbol{v}_h \, dr \, dz, \quad \forall \boldsymbol{v}_h \in \boldsymbol{V}_h.$$

We then have $\|\boldsymbol{u}-\tilde{\boldsymbol{u}}_h\|_{L^2_1(\Omega)} = \inf_{\boldsymbol{w}_h\in\boldsymbol{V}_h}\|\boldsymbol{u}-\boldsymbol{w}_h\|_{L^2_1(\Omega)}$. We then find that, for all $\boldsymbol{v}_h\in\boldsymbol{V}_h$,

$$\begin{aligned}
\nu\int_\Omega r(\boldsymbol{u}_h-\tilde{\boldsymbol{u}}_h)\cdot\boldsymbol{v}_h\,dr\,dz &= \int_\Omega r(\boldsymbol{f}-\nu\tilde{\boldsymbol{u}}_h)\cdot\boldsymbol{v}_h\,dr\,dz\\
&= \int_\Omega r\big((\nu\boldsymbol{u}+\nabla_a p)-\nu\tilde{\boldsymbol{u}}_h\big)\cdot\boldsymbol{v}_h\,dr\,dz\\
&= \int_\Omega r\nabla_a p\cdot\boldsymbol{v}_h\,dr\,dz\\
&= -\int_\Omega r(\nabla_{rz}\cdot\boldsymbol{v}_h)p\,dr\,dz.
\end{aligned}$$

We then easy find that

$$\nu\|\boldsymbol{u}_h-\tilde{\boldsymbol{u}}_h\|_{L^2_1(\Omega)} \le \sup_{\boldsymbol{v}_h\in\boldsymbol{V}_h\setminus\{0\}}\frac{\int_\Omega(r\nabla_{rz}\cdot\boldsymbol{v}_h)p\,dr\,dz}{\|\boldsymbol{v}_h\|_{L^2_1(\Omega)}}.$$

Finally we apply the triangle inequality to get (12).

To obtain (13), we apply (11) to get, for any $q_h\in Q_h$,

$$\beta\|p_h-q_h\|_Q \le \sup_{\boldsymbol{v}_h\in\boldsymbol{X}_h\setminus\{0\}}\frac{\int_\Omega r(\nabla_{rz}\cdot\boldsymbol{v}_h)(p_h-q_h)\,dr\,dz}{\|\boldsymbol{v}_h\|_{\boldsymbol{X}_1}}. \tag{14}$$

Using (10) and (9), we write

$$\begin{aligned}
\int_\Omega r\nabla_{rz}\cdot\boldsymbol{v}_h(p_h-q_h)\,dr\,dz &= \nu\int_\Omega r\boldsymbol{u}_h\cdot\boldsymbol{v}_h\,dr\,dz-\int_\Omega r(\boldsymbol{f}\cdot\boldsymbol{v}_h)\,dr\,dz\\
&\quad-\int_\Omega r(\nabla_{rz}\cdot\boldsymbol{v}_h)q_h\,dr\,dz\\
&= \nu\int_\Omega r(\boldsymbol{u}_h-\boldsymbol{u})\cdot\boldsymbol{v}_h\,dr\,dz+\int_\Omega r(\nabla_{rz}\cdot\boldsymbol{v}_h)(p-q_h)\,dr\,dz\\
&\le \nu\|\boldsymbol{u}-\boldsymbol{u}_h\|_{L^2_1(\Omega)}\|\boldsymbol{v}_h\|_{L^2_1(\Omega)}+\|\nabla_{rz}\cdot\boldsymbol{v}_h\|_{L^2_1(\Omega)}\|p-q_h\|_{L^2_1(\Omega)}\\
&\le C\big(\nu\|\boldsymbol{u}-\boldsymbol{u}_h\|_{L^2_1(\Omega)}+\|p-q_h\|_{L^2_1(\Omega)}\big)\|\boldsymbol{v}_h\|_{\boldsymbol{X}_1}
\end{aligned}$$

for any $\boldsymbol{v}_h\in\boldsymbol{X}_h$. Applying this estimate to (14) yields

$$\beta\|p_h-q_h\|_Q \le C\big(\nu\|\boldsymbol{u}-\boldsymbol{u}_h\|_{L^2_1(\Omega)}+\|p-q_h\|_{L^2_1(\Omega)}\big)\quad\forall q_h\in Q_h,$$

and (13) follows from the triangle inequality. □

Remark 2.3.5. The error estimate for the velocity (12) shows that the error is bounded by the approximation properties of the discretely divergence–free space and the inconsistency of the method. In light of Theorem 2.3.2, one sees that the crux of the analysis is to estimate the inconsistency of the method, i.e., to estimate the second term in the right-hand side of (12).

2.3.1 Preliminary estimates

In this section we derive some identities that will be useful in estimating the inconsistency error in the error estimate (12). As a first step, we state a well-known identity [39].

Proposition 2.3.6. *Suppose that $\boldsymbol{v}_h \in \boldsymbol{V}_h$. Then there holds*

$$\int_\tau (r\nabla_{rz} \cdot \boldsymbol{v}_h)\, dr\, dz = 0 \qquad \forall \tau \in \mathcal{T}_h. \tag{15}$$

Proposition 2.3.7. *For $\tau \in \mathcal{T}_h$, let $r_{\min,\tau} \geq 0$ be the largest number such that $r_{\min,\tau} \leq r$ for all $(r,z) \in \tau$. We then have*

$$\|\boldsymbol{v}_h\|_{L^2(\tau)} \leq C \min\{h_\tau^{-1/2}, r_{\min,\tau}^{-1/2}\} \|\boldsymbol{v}_h\|_{L^2_1(\tau)} \qquad \forall \boldsymbol{v}_h \in \boldsymbol{X}_h$$

with the convention that $\min\{h_\tau^{-1/2}, r_{\min,\tau}^{-1/2}\} = h_\tau^{-1/2}$ if $r_{\min,\tau} = 0$.

Proof. For $\tau \in \mathcal{T}_h$ with $\operatorname{dist}(\partial\tau, \Gamma_0) \geq h_\tau$, we have $\min\{h_\tau^{-1/2}, r_{\min,\tau}^{-1/2}\} = r_{\min,\tau}^{-1/2}$, and the result is clearly true.

Let $\tau \in \mathcal{T}_h$ with $\operatorname{dist}(\partial\tau, \Gamma_0) \leq h_\tau$. Define $\hat{\tau} = \{\frac{1}{h_\tau}(r,z) : \ (r,z) \in \tau\}$, and set $\hat{\boldsymbol{v}}_h(\hat{r},\hat{z}) = \boldsymbol{v}_h(r,z)$ with $r = h_\tau \hat{r}$ and $z = h_\tau \hat{z}$. By equivalence of norms, and since $\hat{r} > 0$ on $\hat{\tau}$, we have $C_\tau = C_\tau(h_\tau, \Omega)$ such that

$$\int_{\hat{\tau}} |\hat{\boldsymbol{v}}_h(\hat{r},\hat{z})|^2\, d\hat{r}\, d\hat{z} \leq C_\tau \int_{\hat{\tau}} \hat{r} |\hat{\boldsymbol{v}}_h(\hat{r},\hat{z})|^2\, d\hat{r}\, d\hat{z}.$$

Since the mesh $\mathcal{T}_h$ is regular and quasi-uniform, and Ω is bounded, then there is C such that $C_\tau \leq C$ for all $\tau \in \mathcal{T}_h$, hence we have

$$\int_{\hat{\tau}} |\hat{\boldsymbol{v}}_h(\hat{r},\hat{z})|^2\, d\hat{r}\, d\hat{z} \leq C \int_{\hat{\tau}} \hat{r} |\hat{\boldsymbol{v}}_h(\hat{r},\hat{z})|^2\, d\hat{r}\, d\hat{z}.$$

Therefore, by a change of variables, we obtain

$$\begin{aligned} \|\boldsymbol{v}_h\|^2_{L^2(\tau)} &= h_\tau^2 \int_{\hat{\tau}} |\hat{\boldsymbol{v}}_h(\hat{r},\hat{z})|^2\, d\hat{r}\, d\hat{z} \\ &\leq C h_\tau^2 \int_{\hat{\tau}} \hat{r} |\hat{\boldsymbol{v}}_h(\hat{r},\hat{z})|^2\, d\hat{r}\, d\hat{z} = C h_\tau^{-1} \|\boldsymbol{v}_h\|^2_{L^2_1(\tau)}. \end{aligned}$$

Taking the square root of this inequality yields the desired result. □

Lemma 2.3.8. *For any $\boldsymbol{v}_h \in \boldsymbol{V}_h$ and $q \in L^1(\tau)$, there holds*

$$\Big| \int_\tau (r\nabla_{rz} \cdot \boldsymbol{v}_h) q \, dr \, dz \Big| \leq C h_\tau^{-2} \min\{h_\tau^{-1/2}, r_{\min,\tau}^{-1/2}\} \|\boldsymbol{v}_h\|_{L_1^2(\tau)} \Big| \int_\tau (r - \bar{r}_\tau)(q - \bar{q}_\tau) \, dr \, dz \Big|, \quad (16)$$

where $\bar{r}_\tau$ and $\bar{q}_\tau$ are the averages of r and q on τ, respectively.

Proof. Using the definition of the Raviart-Thomas space, we write

$$\boldsymbol{v}_h\big|_\tau = \boldsymbol{\alpha} + \beta \begin{pmatrix} r \\ z \end{pmatrix}$$

for some $\boldsymbol{\alpha} \in \mathbb{R}^2$ and $\beta \in \mathbb{R}$. We then have

$$\nabla_a \cdot \boldsymbol{v}_h = 2\beta, \qquad r\nabla_{rz} \cdot \boldsymbol{v}_h = r\nabla_a \cdot \boldsymbol{v}_h + v_h^{(1)} = (2\beta r) + \alpha^{(1)} + \beta r = 3\beta r + \alpha^{(1)}.$$

Thus, if $\boldsymbol{v}_h \in \boldsymbol{V}_h$ is discretely divergence-free, then

$$0 = \int_\tau r(\nabla_{rz} \cdot \boldsymbol{v}_h) \, dr \, dz = |\tau| \alpha^{(1)} + 3\beta \int_\tau r \, dr \, dz = |\tau| \alpha^{(1)} + 3\beta |\tau| \bar{r}_\tau.$$

We conclude that $\alpha^{(1)} = -3\beta \bar{r}_\tau$ and $(r\nabla_{rz} \cdot \boldsymbol{v}_h) = 3\beta(r - \bar{r}_\tau)$. We then have, for any $q \in L^1(\tau)$,

$$\int_\tau \big(r\nabla_{rz} \cdot \boldsymbol{v}_h\big) q \, dr \, dz = 3\beta \int_\tau (r - \bar{r}_\tau) q \, dr \, dz = 3\beta \int_\tau (r - \bar{r}_\tau)(q - \bar{q}_\tau) \, dr \, dz. \quad (17)$$

Finally, we apply standard inverse estimates and Proposition 2.3.7 to get

$$\begin{aligned} |\beta| &= \frac{1}{2} \|\nabla_a \cdot \boldsymbol{v}_h\|_{L^\infty(\tau)} \leq C h_\tau^{-1} \|\boldsymbol{v}_h\|_{L^\infty(\tau)} \\ &\leq C h_\tau^{-2} \|\boldsymbol{v}_h\|_{L^2(\tau)} \leq C h_\tau^{-2} \min\{h_\tau^{-1/2}, r_{\min,\tau}^{-1/2}\} \|\boldsymbol{v}_h\|_{L_1^2(\tau)}. \end{aligned}$$

Combining this last inequality with (17), we obtain (16). □

Remark 2.3.9. Applying the Cauchy-Schwarz inequality to (16) and assuming that $q \in H^1(\tau)$, we have

$$\begin{aligned}\Big|\int_\tau (r\nabla_{rz}\cdot \boldsymbol{v}_h) q\,dr\,dz\Big| &\le Ch_\tau^{-2}\min\{h_\tau^{-1/2}, r_{\min,\tau}^{-1/2}\}\|\boldsymbol{v}_h\|_{L_1^2(\tau)}\|r-\bar{r}_\tau\|_{L^2(\tau)}\|q-\bar{q}_\tau\|_{L^2(\tau)}\\ &\le C\min\{h_\tau^{-1/2}, r_{\min,\tau}^{-1/2}\}\|\boldsymbol{v}_h\|_{L_1^2(\tau)}\|\nabla_a r\|_{L^2(\tau)}\|\nabla_a q\|_{L^2(\tau)}\\ &\le Ch_\tau^{1/2}\|\boldsymbol{v}_h\|_{L_1^2(\tau)}\|\nabla_a q\|_{L^2(\tau)}.\end{aligned}$$

Thus, we conclude from this estimate and from (12), that if the pressure solution has regularity $p \in H^1(\Omega)$, then the L^2 error of the velocity is bounded by $Ch^{1/2}$. However, as far as we are aware, the pressure function does not generically enjoy such regularity. In what follows, we derive estimates under the assumption that the pressure solution lies in a weighted Sobolev space and improve this rate of convergence provided that p is sufficiently regular. As a first step, we prove an estimate that is useful for $\tau \in \mathcal{T}_h$ that is close to the z-axis.

Lemma 2.3.10. *For $\tau \in \mathcal{T}_h$, let $r_{\max,\tau} > 0$ denote the smallest number such that $r \le r_{\max,\tau}$ for all $(r,z) \in \tau$. Suppose that $q \in W_1^{1,t}(\tau)$ for some $t \ge 2$, and let $\boldsymbol{v}_h \in \boldsymbol{V}_h$. Then there holds*

$$\Big|\int_\tau (r\nabla_{rz}\cdot \boldsymbol{v}_h) q\,dr\,dz\Big| \le Ch_\tau^{1/2-2/t} r_{\max,\tau}^{1-1/t}\|\boldsymbol{v}_h\|_{L_1^2(\tau)}|q|_{W_1^{1,t}(\tau)}. \tag{18}$$

Remark 2.3.11. There holds $W_1^{1,t}(\tau) \hookrightarrow L^1(\tau)$ [40, pg. 15].

Proof. Applying Hölder's inequality and [52, Corollary 3.2], we have

$$\begin{aligned}\Big|\int_\tau (r-\bar{r}_\tau)(q-\bar{q}_\tau)\,dr\,dz\Big| &= \Big|\int_\tau r(q-\bar{q}_\tau)\,dr\,dz\Big|\\ &= \Big|\int_\tau r^{1/t'} r^{1/t}(q-\bar{q}_\tau)\,dr\,dz\Big|\\ &\le \Big(\int_\tau r\,dr\,dz\Big)^{1/t'}\Big(\int_\tau r|q-\bar{q}_\tau|^t\,dr\,dz\Big)^{1/t}\\ &\le Ch_\tau^{1+2/t'} r_{\max,\tau}^{1/t'}|q|_{W_1^{1,t}(\tau)},\end{aligned}$$

where $t' \in [1,2]$ is the Hölder conjugate of t. Therefore, by Lemma 2.3.8,

$$\begin{aligned}\Big|\int_\tau (r\nabla_{rz}\cdot \boldsymbol{v}_h) q\,dr\,dz\Big| &\le Ch_\tau^{-5/2}\|\boldsymbol{v}_h\|_{L_1^2(\tau)}\Big|\int_\tau (r-\bar r_\tau)(q-\bar q_\tau)\,dr\,dz\Big| \\ &\le Ch_\tau^{(-3/2+2/t')} r_{\max,\tau}^{1/t'}\|\boldsymbol{v}_h\|_{L_1^2(\tau)}|q|_{W_1^{1,t}(\tau)} \\ &= Ch_\tau^{(1/2-2/t)} r_{\max,\tau}^{(1-1/t)}\|\boldsymbol{v}_h\|_{L_1^2(\tau)}|q|_{W_1^{1,t}(\tau)}.\end{aligned}$$

□

Remark 2.3.12. Such an estimate is useful for τ near Γ_0. Indeed for such $\tau \in \mathcal{T}_h$ with $\operatorname{dist}\{\partial\tau,\Gamma_0\} \le Ch_\tau$, we have $r_{\max,\tau} = \mathcal{O}(h_\tau)$, and so

$$\Big|\int_\tau (r\nabla_{rz}\cdot \boldsymbol{v}_h) q\,dr\,dz\Big| \le Ch^{3/2-3/t}\|\boldsymbol{v}_h\|_{L_1^2(\tau)}|q|_{W_1^{1,t}(\tau)}.$$

However, Lemma 2.3.10 does not yield a meaningful estimate for $r_{\max,\tau} = \mathcal{O}(1)$. Instead, we have the following result.

Lemma 2.3.13. *Suppose that* $\operatorname{dist}\{\partial\tau,\Gamma_0\} \ge h_\tau$. *Then under the same assumptions of Lemma 2.3.10, we have*

$$\Big|\int_\tau (r\nabla_{rz}\cdot \boldsymbol{v}_h) q\,dr\,dz\Big| \le Ch_\tau^{2-2/t} r_{\min,\tau}^{-1/2-1/t}\|\boldsymbol{v}_h\|_{L_1^2(\tau)}|q|_{W_1^{1,t}(\tau)}. \tag{19}$$

Proof. We apply Lemma 2.3.8, the Cauchy-Schwarz inequality, standard interpolation estimates, and Hölder's inequality to get

$$\begin{aligned}\Big|\int_\tau (r\nabla_{rz}\cdot \boldsymbol{v}_h) q\,dr\,dz\Big| &\le Ch_\tau^{-2}\|\boldsymbol{v}_h\|_{L^2(\tau)}\Big|\int_\tau (r-\bar r_\tau)(q-\bar q_\tau)\,dr\,dz\Big| \\ &\le C\|\boldsymbol{v}_h\|_{L^2(\tau)}\|\nabla_a r\|_{L^2(\tau)}\|\nabla_a q\|_{L^2(\tau)} \\ &\le Ch_\tau\|\boldsymbol{v}_h\|_{L^2(\tau)}\|\nabla_a q\|_{L^2(\tau)} \\ &\le Ch_\tau^{2-2/t}\|\boldsymbol{v}_h\|_{L^2(\tau)}\|\nabla_a q\|_{L^t(\tau)} \\ &\le Ch_\tau^{2-2/t} r_{\min,\tau}^{-1/2-1/t}\|\boldsymbol{v}_h\|_{L_1^2(\tau)}|q|_{W_1^{1,t}(\tau)}.\end{aligned}$$

□

2.3.2 Error estimates

In this section, we combine the estimates in Lemmas 2.3.10 and 2.3.13 to estimate the inconsistency error appearing in (12). As alluded to before, the idea is to apply the estimate (18) for $\tau \in \mathcal{T}_h$ with $\operatorname{dist}\{\partial\tau, \Gamma_0\} \leq Ch$, while using the estimate (19) for $\tau \in \mathcal{T}_h$ satisfying $\operatorname{dist}\{\partial\tau, \Gamma_0\} = \mathcal{O}(1)$. For intermediate elements $\tau \in \mathcal{T}_h$, we simply take a convex combination of the two estimates.

To carry out this methodology, we require a decomposition of Ω. To this end, we define the subdomains

$$\begin{aligned}\Omega_{-1} &:= \{(r,z) \in \Omega : \ 0 \leq r \leq h\},\\ \Omega_j &:= \{(r,z) \in \Omega : \ 2^j h \leq r \leq 2^{j+1} h\}, \qquad j = 0, 1, \ldots, J,\end{aligned}$$

where $J = \mathcal{O}(|\log h|)$ is chosen such that

$$\Omega = \bigcup_{j=-1}^{J} \Omega_j.$$

We also set

$$\mathcal{T}_h^{(j)} := \{\tau \in \mathcal{T}_h : \ \tau \cap \Omega_j \neq \emptyset\}, \qquad \Omega_j^h := \bigcup_{\tau \in \mathcal{T}_h^{(j)}} \tau.$$

Lemma 2.3.14. *Suppose that $q \in W_1^{1,t}(\Omega)$ with $t \geq 2$ and that $\boldsymbol{v}_h \in \boldsymbol{V}_h$. We then have*

$$\Big| \int_{\Omega_j^h} (r \nabla_{rz} \cdot \boldsymbol{v}_h) q \, dr \, dz \Big| \leq C h^{1-2/t} \|\boldsymbol{v}_h\|_{L_1^2(\Omega_j^h)} |q|_{W_1^{1,t}(\Omega_j^h)}.$$

Proof. Combining Lemmas 2.3.10 and 2.3.13, we conclude that for $\operatorname{dist}(\Gamma_0, \tau) \geq h_\tau$ and for any $\alpha \in [0,1]$,

$$\Big| \int_{\tau} (r \nabla_{rz} \cdot \boldsymbol{v}_h) q \, dr \, dz \Big| \leq C \big(h^{(1/2-2/t)} r_{\max,\tau}^{(1-1/t)} \big)^{1-\alpha} \big(h^{(2-2/t)} r_{\min,\tau}^{(-1/2-1/t)} \big)^{\alpha} \|\boldsymbol{v}_h\|_{L_1^2(\tau)} |q|_{W_1^{1,t}(\tau)}.$$

Consider the case $j \geq 0$. If $\tau \in \mathcal{T}_h^{(j)}$, then $r_{\min,\tau} \geq 2^{(j-1)}h$ and $r_{\max,\tau} \leq 2^{(j+2)}h$. Hence,

$$\begin{aligned}
&\Big| \int_\tau (r\nabla_{rz} \cdot \boldsymbol{v}_h) q \, dr \, dz \Big| \qquad (20)\\
&\quad \leq C\big(h^{(1/2-2/t)}(2^{j+1}h)^{1/t'}\big)^{1-\alpha}\big(h^{(2-2/t)}(2^j h)^{(-1/2-1/t)}\big)^{\alpha}\|\boldsymbol{v}_h\|_{L_1^2(\tau)}|q|_{W_1^{1,t}(\tau)}\\
&\quad = C\big(h^{(1/2-2/t+1/t')}2^{(j+1)/t'}\big)^{1-\alpha}\big(h^{(2-2/t-1/2-1/t)}2^{j(-1/2-1/t)}\big)^{\alpha}\|\boldsymbol{v}_h\|_{L_1^2(\tau)}|q|_{W_1^{1,t}(\tau)}\\
&\quad = Ch^{(3/2-3/t)}\big(2^{(j+1)(1-\alpha)/t'}\big)\big(2^{j\alpha(-1/2-1/t)}\big)\|\boldsymbol{v}_h\|_{L_1^2(\tau)}|q|_{W_1^{1,t}(\tau)}
\end{aligned}$$

for all $\tau \in \mathcal{T}_h^{(j)}$.

Summing the estimate (20) over $\tau \in \mathcal{T}_h^{(j)}$, and applying Hölder's inequality results in

$$\begin{aligned}
&\sum_{\tau\in\mathcal{T}_h^{(j)}} \Big| \int_\tau (r\nabla_{rz} \cdot \boldsymbol{v}_h) q \, dr \, dz \Big|\\
&\quad \leq Ch^{(3/2-3/t)}\big(2^{(j+1)(1-\alpha)/t'}\big)\big(2^{j\alpha(-1/2-1/t)}\big)\|\boldsymbol{v}_h\|_{L_1^2(\Omega_j^h)}|q|_{W_1^{1,t}(\Omega_j^h)}\Big(\sum_{\tau\in\mathcal{T}_h^{(j)}} 1\Big)^{1/2-1/t}.
\end{aligned}$$

Since the cardinality of $\mathcal{T}_h^{(j)}$ is $\mathcal{O}(2^j h^{-1})$, we conclude that

$$\begin{aligned}
&\sum_{\tau\in\mathcal{T}_h^{(j)}} \Big| \int_\tau (r\nabla_{rz} \cdot \boldsymbol{v}_h) q \, dr \, dz \Big|\\
&\quad \leq Ch^{(3/2-3/t)}\big(2^{(j+1)(1-\alpha)/t'}\big)\big(2^{j\alpha(-1/2-1/t)}\big)\big(2^j h^{-1}\big)^{1/2-1/t}\|\boldsymbol{v}_h\|_{L_1^2(\Omega_j^h)}|q|_{W_1^{1,t}(\Omega_j^h)}.
\end{aligned}$$

We choose α such that

$$\frac{1}{t'}(j+1)(1-\alpha) + j(-\frac{1}{2}-\frac{1}{t})\alpha + j(\frac{1}{2}-\frac{1}{t}) = 0,$$

that is,

$$\alpha = \frac{3jt-4j+2t-2}{3jt+2t-2}.$$

Clearly, we have $\alpha \leq 1$. Furthermore, using that $t \geq 2$,

$$\alpha \geq \frac{6j-4j+2(2)-2}{3jt+2t-2} = \frac{2j+2}{3jt+2t-2} \geq 0.$$

For this choice of α, we get

$$\Big| \int_{\Omega_j^h} (r\nabla_{rz} \cdot \boldsymbol{v}_h) q \, dr \, dz \Big| \leq Ch^{1-2/t}\|\boldsymbol{v}_h\|_{L_1^2(\Omega_j^h)}|q|_{W_1^{1,t}(\Omega_j^h)}, \quad j \geq 0.$$

For the other case $j=-1$, we have that $r_{\max,\tau} \le 2h$. Therefore, by Lemma 2.3.10,

$$\begin{aligned}\Big| \int_{\Omega_j^h} (r\nabla_{rz}\cdot \boldsymbol{v}_h) q \, dr\, dz \Big| &\le Ch^{1/2-2/t} \sum_{\tau\in\mathcal{T}_h^{(j)}} r_{\max,\tau}^{1-1/t} \|\boldsymbol{v}_h\|_{L_1^2(\tau)} |q|_{W_1^{1,t}(\tau)} \\ &\le Ch^{3/2-3/t} \|\boldsymbol{v}_h\|_{L^2(\Omega_j^h)} |q|_{W_1^{1,t}(\Omega_j^h)} \Big(\sum_{\tau\in\mathcal{T}_h^{(j)}} 1 \Big)^{1/2-1/t} \\ &= Ch^{1-2/t} \|\boldsymbol{v}_h\|_{L^2(\Omega_j^h)} |q|_{W_1^{1,t}(\Omega_j^h)}.\end{aligned}$$

□

Theorem 2.3.15. *Suppose that the pressure solution satisfies $p \in W_1^{1,t}(\Omega)$, where $t \ge 2$ is given in Theorem 2.2.4. Then there holds*

$$\|\boldsymbol{u}-\boldsymbol{u}_h\|_{L_1^2(\Omega)} \le C\big(\inf_{\boldsymbol{v}_h\in\boldsymbol{V}_h} \|\boldsymbol{u}-\boldsymbol{v}_h\|_{L_1^2(\Omega)} + h^{1-2/t} |\log h|^{1/2-1/t} |p|_{W_1^{1,t}(\Omega)} \big), \tag{21}$$

$$\|p-p_h\|_{L_1^2(\Omega)} \le C\big(\|\boldsymbol{u}-\boldsymbol{u}_h\|_{L_1^2(\Omega)} + h|p|_{H_1^1(\Omega)} \big). \tag{22}$$

If $\check{\Omega}$ is convex, then there holds

$$\|\boldsymbol{u}-\boldsymbol{u}_h\|_{L_1^2(\Omega)} + \|p-p_h\|_{L_1^2(\Omega)} \le Ch|\log h|^{1/2}. \tag{23}$$

Proof. Summing the estimate in Lemma 2.3.14 over j, and recalling that $J = \mathcal{O}(|\log h|)$, we have

$$\begin{aligned}\Big| \int_{\Omega} (r\nabla_{rz}\cdot \boldsymbol{v}_h) p \, dr\, dz \Big| &\le \sum_{j=-1}^{J} \Big| \int_{\Omega_j^h} (r\nabla_{rz}\cdot \boldsymbol{v}_h) p \, dr\, dz \Big| \\ &\le Ch^{1-2/t} \sum_{j=-1}^{J} \|\boldsymbol{v}_h\|_{L^2(\Omega_j^h)} |p|_{W_1^{1,t}(\Omega_j^h)} \\ &\le Ch^{1-2/t} \Big(\sum_{j=-1}^{J} 1 \Big)^{1/2-1/t} \|\boldsymbol{v}_h\|_{L^2(\Omega)} |p|_{W_1^{1,t}(\Omega)} \\ &\le Ch^{1-2/t} |\log h|^{1/2-1/t} \|\boldsymbol{v}_h\|_{L^2(\Omega)} |p|_{W_1^{1,t}(\Omega)}.\end{aligned}$$

Combining this estimate with Lemma 2.3.4 and Theorem 2.3.2, we obtain the desired result (21)–(22). The estimate (23) follows from (21), Theorem 2.2.4, and Theorem 2.3.2. □

2.4 Numerical Examples

In this section, we perform some simple numerical experiments and compare the results with the theoretical ones given in the previous sections. We consider the example such that the data is taken to be $\Omega = (0,1)^2$, the viscosity is $\nu = 10^{-1}$, and the source function is chosen such that the exact velocity and pressure solutions are given respectively as

$$\boldsymbol{u}(r,z) = \begin{pmatrix} r\cos(\frac{\pi r}{2})\sin(\pi z + \frac{\pi}{2}) \\ \cos(\pi z + \frac{\pi}{2})((\frac{2}{\pi})\cos((\frac{\pi r}{2})) - (\frac{r}{2})\sin(\frac{\pi r}{2}) \end{pmatrix}, \quad p = r^s - \frac{2}{2+s} \quad (s > 0). \tag{24}$$

We then find that $p \in W_1^{1,t}(\Omega)$ provided that $t(s-1) > -2$. In particular, if $s \in (0,1)$, then $p \in W_1^{1,t}(\Omega)$ provided that $t < 2/(1-s)$. Consequently, Theorem 2.3.15 shows that the error is bounded by Ch^s modulo logarithmic terms.

The resulting rates of convergence of the numerical experiments are listed in Tables 1 and 2 for the cases $s = 1/2$ and $s = 1/4$, respectively. While the exact (asymptotic) rates of convergence of the velocity are not clear from the tests, the observed rates are close to the theoretical results stated in Theorem 2.3.15. For example, the average rate of convergence for the velocity error for the three finest meshes are 0.245 for the case $s = 1/4$ and 0.501 for the case $s = 1/2$. On the other hand, we see from Tables 1–2 that the pressure approximation converges with order one in both cases. These results indicate that the pressure estimate given in (22)–(23) may not be sharp.

Table 1: Errors and rates of convergence for example (84) with $s = 1/2$.

h	$\|\boldsymbol{u} - \boldsymbol{u}_h\|_{L^2_1(\Omega)}$	rate	$\|p - p_h\|_{L^2_1(\Omega)}$	rate
2^{-2}	4.99E-01	–	3.68E-01	–
2^{-3}	5.50E-02	3.182	1.25E-02	4.877
2^{-4}	4.49E-02	0.291	6.50E-03	0.947
2^{-5}	2.79E-02	0.689	3.24E-03	1.004
2^{-6}	1.70E-02	0.709	1.64E-03	0.984
2^{-7}	1.23E-02	0.465	8.21E-04	0.998
2^{-8}	8.82E-03	0.486	4.12E-04	0.996
2^{-9}	6.00E-03	0.555	2.06E-04	0.998

Table 2: Errors and rates of convergence for example (84) with $s = 1/4$.

h	$\|\boldsymbol{u} - \boldsymbol{u}_h\|_{L^2_1(\Omega)}$	rate	$\|p - p_h\|_{L^2_1(\Omega)}$	rate
2^{-2}	4.79E-01		2.60E-01	
2^{-3}	5.34E-02	3.165	8.34E-03	4.962
2^{-4}	4.96E-02	0.105	4.37E-03	0.932
2^{-5}	3.66E-02	0.438	2.21E-03	0.983
2^{-6}	2.68E-02	0.452	1.13E-03	0.968
2^{-7}	2.31E-02	0.213	5.71E-04	0.986
2^{-8}	1.98E-02	0.222	2.87E-04	0.992
2^{-9}	1.61E-02	0.300	1.44E-04	0.993

3.0 THE AXISYMMETRIC STOKES PROBLEM AND THE DE RHAM COMPLEX

In this chapter, we introduce the Stokes problem on an axisymmetric domain and show how the axisymmetric Stokes problem fits within a commutative de Rham complex. We also prove the stability of various Stokes finite element pairs under the axisymmetric variational formulation.

3.1 The Stokes Problem

We consider the Stokes problem on a three-dimensional domain

$$-\nu\check{\Delta}\check{\boldsymbol{u}} + \check{\nabla}\check{p} = \check{\boldsymbol{f}} \qquad \text{in } \check{\Omega}, \tag{25a}$$

$$\check{\nabla}\cdot\check{\boldsymbol{u}} = 0 \qquad \text{in } \check{\Omega}, \tag{25b}$$

$$\check{\boldsymbol{u}} = 0 \qquad \text{on } \partial\check{\Omega}, \tag{25c}$$

where $\check{\boldsymbol{u}} = \check{\boldsymbol{u}}(\check{x}) = (\check{u}_1(\check{x}), \check{u}_2(\check{x}), \check{u}_3(\check{x}))^\intercal$ denote the velocity, $\check{p} = \check{p}(\check{x})$ denotes the pressure, and $\check{\boldsymbol{f}} = \check{\boldsymbol{f}}(\check{x}) = (\check{f}_1(\check{x}), \check{f}_2(\check{x}), \check{f}_3(\check{x}))^\intercal$ is the (given) source function. As in the previous chapter, we use hats over the differential operators to indicate derivatives with respect to the $\check{x} = (\check{x}_1, \check{x}_2, \check{x}_3)^\intercal$ variable. For simplicity, we assume that the viscosity $\nu > 0$ is constant.

We assume that $\check{\Omega} \subset \mathbb{R}^3$ is open, bounded, simply connected, and is obtained by rotating a two dimensional polygon Ω in the (r, z)-plane around the z-axis. We say that Ω is the meridian domain. We further assume that if an endpoint of two segments of Ω is in the z-axis, then at least one of the segments lies entirely in the z-axis. This excludes the case where $\partial\Omega$ meets with the z-axis at one point.

3.1.1 Variational formulation

In this section we state the variational problem of (25) and show that the problem is well-posed. These results are standard (see, e.g., [30]), but we include the proofs for completeness. We start by defining the following function space on $\check{\Omega}$:

$$H_0^m(\check{\Omega}) := \{\check{w} \in H^m(\check{\Omega}) : \ D^\beta w|_{\partial\check{\Omega}} = 0, \forall \beta : \ |\beta| \leq m-1\}.$$

Suppose for the moment that there is a sufficiently regular pair $(\check{\boldsymbol{u}}, \check{p})$ satisfying (25). Taking the dot product of (25a) with a function $\check{\boldsymbol{v}} \in \boldsymbol{H}_0^1(\check{\Omega})$ and integrating over $\check{\Omega}$ yields

$$-\int_{\check{\Omega}} \nu \check{\Delta}\check{\boldsymbol{u}} \cdot \check{\boldsymbol{v}} \, d\check{x} + \int_{\check{\Omega}} \check{\nabla}\check{p} \cdot \check{\boldsymbol{v}} \, d\check{x} = \int_{\check{\Omega}} \check{\boldsymbol{f}} \cdot \check{\boldsymbol{v}} \, d\check{x}. \tag{26}$$

Integrating the left hand side of (26) by parts, we get

$$-\int_{\check{\Omega}} \nu \check{\Delta}\check{\boldsymbol{u}} \cdot \check{\boldsymbol{v}} \, d\check{x} = -\nu \int_{\partial\check{\Omega}} (\check{\nabla}\check{\boldsymbol{u}}\check{\boldsymbol{v}}) \cdot \check{\boldsymbol{n}} \, d\check{s} + \nu \int_{\check{\Omega}} \check{\nabla}\check{\boldsymbol{u}} : \check{\nabla}\check{\boldsymbol{v}} \, d\check{x},$$

and

$$\int_{\check{\Omega}} \check{\nabla}\check{p} \cdot \check{\boldsymbol{v}} \, d\check{x} = \int_{\partial\check{\Omega}} \check{p}(\check{\boldsymbol{v}} \cdot \check{\boldsymbol{n}}) \, d\check{s} - \int_{\check{\Omega}} \check{p}\check{\nabla} \cdot \check{\boldsymbol{v}} \, d\check{x},$$

where $\check{\boldsymbol{n}}$ is the outward normal vector to $\partial\check{\Omega}$, and " : " is the Frobenius inner product. Because $\check{\boldsymbol{v}}$ vanishes on $\partial\check{\Omega}$, we have

$$-\int_{\check{\Omega}} \nu \check{\Delta}\check{\boldsymbol{u}} \cdot \check{\boldsymbol{v}} \, d\check{x} = \nu \int_{\check{\Omega}} \check{\nabla}\check{\boldsymbol{u}} : \check{\nabla}\check{\boldsymbol{v}} \, d\check{x}, \tag{27a}$$

and

$$\int_{\check{\Omega}} \check{\nabla}\check{p} \cdot \check{\boldsymbol{v}} \, d\check{x} = -\int_{\check{\Omega}} \check{p}\check{\nabla} \cdot \check{\boldsymbol{v}} \, d\check{x}. \tag{27b}$$

We use equations (27) to define the bilinear forms $\check{a}(.,.)$ and $\check{b}(.,.)$ on $\boldsymbol{H}_0^1(\check{\Omega}) \times \boldsymbol{H}_0^1(\check{\Omega})$ and $\boldsymbol{H}_0^1(\check{\Omega}) \times L_0^2(\check{\Omega})$ respectively:

$$\check{a}(\check{\boldsymbol{u}}, \check{\boldsymbol{v}}) := \nu \int_{\check{\Omega}} \check{\nabla}\check{\boldsymbol{u}} : \check{\nabla}\check{\boldsymbol{v}} \, d\check{x}, \tag{28}$$

$$\check{b}(\check{\boldsymbol{v}}, \check{q}) := -\int_{\check{\Omega}} \check{q}\check{\nabla} \cdot \check{\boldsymbol{v}} \, d\check{x}. \tag{29}$$

The weak formulation for problem (25) reads: Find $(\check{\boldsymbol{u}}, \check{p}) \in \boldsymbol{H}_0^1(\check{\Omega}) \times L_0^2(\check{\Omega})$ such that, for all $(\check{\boldsymbol{v}}, \check{q}) \in \boldsymbol{H}_0^1(\check{\Omega}) \times L_0^2(\check{\Omega})$, we have

$$\check{a}(\check{\boldsymbol{u}}, \check{\boldsymbol{v}}) + \check{b}(\check{\boldsymbol{v}}, \check{p}) = \int_{\check{\Omega}} \check{\boldsymbol{f}} \cdot \check{\boldsymbol{v}} \, d\check{x}, \tag{30a}$$

$$\check{b}(\check{\boldsymbol{u}}, \check{q}) = 0. \tag{30b}$$

Theorem 3.1.1. *There exists a unique solution* $(\check{\boldsymbol{u}}, \check{p}) \in \boldsymbol{H}_0^1(\check{\Omega}) \times L_0^2(\check{\Omega})$ *to* (30).

Theorem 3.1.1 is well-known [30], but we provide a proof for completeness.

The proof of Theorem 3.1.1 is very similar to the proof of Theorem 2.2.1. We will show that the bilinear forms defined in (28) and (29) satisfy the hypotheses in Theorem 2.2.2 with $\boldsymbol{X} = \boldsymbol{H}_0^1(\check{\Omega})$ and $Y = L_0^2(\check{\Omega})$.

Lemma 3.1.2. *The operator* $\check{\nabla}\cdot : \boldsymbol{H}_0^1(\check{\Omega}) \to L_0^2(\check{\Omega})$ *is surjective with a bounded right-inverse, namely, for any* $\check{q} \in L_0^2(\check{\Omega})$*, there exists* $\check{\boldsymbol{v}} \in \boldsymbol{H}_0^1(\check{\Omega})$ *such that* $\check{\nabla}\cdot\check{\boldsymbol{v}} = \check{q}$ *and* $\|\check{\boldsymbol{v}}\|_{H^1(\check{\Omega})} \le \check{\beta}^{-1}\|\check{q}\|_{L^2(\check{\Omega})}$*, where* $\check{\beta} > 0$ *depends on* $\check{\Omega}$*.*

Proof. Let $\check{q} \in L_0^2(\check{\Omega})$. Since $\check{\Omega}$ is bounded, there exist an open bounded set $\check{U} \subset \mathbb{R}^3$ such that $\check{U}$ has smooth boundary and $\check{\Omega} \subset\subset \check{U}$. Define $\tilde{q}$ on $\check{U}$ such that $\tilde{q}|_{\check{\Omega}} = \check{q}$ and $\tilde{q} = 0$ in $\check{U} \setminus \check{\Omega}$. Then $\tilde{q} \in L^2(\check{U})$.

Consider the following auxiliary problem in $\check{U}$:

$$\begin{aligned} \check{\Delta}\hat{u} &= \tilde{q} \qquad \text{in } \check{U}, \\ \hat{u} &= 0 \qquad \text{on } \partial\check{U}. \end{aligned}$$

By [22, Sect. 6.3, Theorem 1], there holds $\hat{u} \in H^2(\check{U})$ and $\|\hat{u}\|_{H^2(\check{U})} \le C\|\tilde{q}\|_{L^2(\check{U})} = C\|\check{q}\|_{L^2(\check{\Omega})}$. Now set $\check{\boldsymbol{v}}_1 = \check{\nabla}\hat{u}|_{\check{\Omega}} \in \boldsymbol{H}^1(\check{\Omega})$, so that $\check{\nabla}\cdot\check{\boldsymbol{v}}_1 = \check{\Delta}\hat{u} = \check{q}$ and $\|\check{\boldsymbol{v}}_1\|_{H^1(\check{\Omega})} \le \|\hat{u}\|_{H^2(\check{\Omega})} \le C\|\hat{q}\|_{L^2(\check{\Omega})}$. Furthermore, we have

$$\int_{\partial\check{\Omega}} \check{\boldsymbol{v}}_1 \cdot \check{\boldsymbol{n}}\, d\check{s} = \int_{\check{\Omega}} \check{\nabla}\cdot\check{\boldsymbol{v}}_1\, d\check{x} = \int_{\check{\Omega}} \check{q}\, d\check{x} = 0.$$

Therefore, we conclude from [30, Theorem 3.5] that there exits $\check{\boldsymbol{w}}_1 \in \boldsymbol{H}^1(\check{\Omega})$ such that $\check{\boldsymbol{w}}_1|_{\partial\check{\Omega}} = \check{\boldsymbol{v}}_1|_{\partial\check{\Omega}}$ and $\check{\nabla}\cdot\check{\boldsymbol{w}}_1 = 0$. Setting $\check{\boldsymbol{v}} = \check{\boldsymbol{v}}_1 - \check{\boldsymbol{w}}_1$, we have $\check{\boldsymbol{v}} \in \boldsymbol{H}_0^1(\check{\Omega})$ and $\check{\nabla}\cdot\check{\boldsymbol{v}} = \check{q}$. □

Proof of Theorem 3.1.1. We verify the conditions stated in Proposition 2.2.2 with $\boldsymbol{X} = \boldsymbol{H}_0^1(\check{\Omega})$ and $Y = L_0^2(\check{\Omega})$.

1. Continuity of the bilinear forms $\check{a}(.,.)$ and $\check{b}(.,.)$ follow directly from the Cauchy-Schwarz inequality.

2. Denote by $C_p = C_p(\check{\Omega}) > 0$ the Poincare-Friedrichs' inequality constant, i.e., $\|\check{\boldsymbol{v}}\|_{L^2(\check{\Omega})} \leq C_p \|\check{\nabla}\check{\boldsymbol{v}}\|_{L^2(\check{\Omega})}$ for all $\check{\boldsymbol{v}} \in \boldsymbol{H}_0^1(\check{\Omega})$. We then have $\|\check{\boldsymbol{v}}\|^2_{H^1(\check{\Omega})} \leq (1 + C_p^2)\|\check{\nabla}\check{\boldsymbol{v}}\|^2_{L^2(\check{\Omega})}$, and so

$$\check{a}(\check{\boldsymbol{v}}, \check{\boldsymbol{v}}) = \nu \|\check{\nabla}\check{\boldsymbol{v}}\|^2_{L^2(\check{\Omega})} \geq \nu(1 + C_p^2)^{-1} \|\check{\nabla}\check{\boldsymbol{v}}\|^2_{L^2(\check{\Omega})}.$$

Letting $\alpha = \nu(1 + C_p^2)^{-1}$ we get

$$\check{a}(\check{\boldsymbol{v}}, \check{\boldsymbol{v}}) \geq \alpha \|\check{\boldsymbol{v}}\|^2_{H^1(\check{\Omega})} \qquad \forall \check{\boldsymbol{v}} \in \boldsymbol{H}_0^1(\check{\Omega}).$$

Since $\check{a}(.,.)$ is clearly symmetric, we conclude that $\check{a}(.,.)$ satisfies 2 in Proposition 2.2.2.

3. Let $\check{q} \in L_0^2(\check{\Omega})$ with $\check{q} \neq 0$. Applying Lemma 3.1.2 there exists $\check{\boldsymbol{w}} \in \boldsymbol{H}_0^1(\check{\Omega})$ such that $\check{\nabla} \cdot \check{\boldsymbol{w}} = \check{q}$ and $\|\check{\boldsymbol{w}}\|_{H^1(\check{\Omega})} \leq \check{\beta}^{-1} \|\check{q}\|_{L^2(\check{\Omega})}$. Consequently,

$$\check{\beta}\|\check{q}\|_{L^2(\check{\Omega})} = \frac{\check{b}(\check{\boldsymbol{w}}, \check{q})}{\check{\beta}^{-1}\|\check{q}\|_{L^2(\check{\Omega})}} \leq \frac{\check{b}(\check{\boldsymbol{w}}, \check{q})}{\|\check{\boldsymbol{w}}\|_{H^1(\check{\Omega})}} \leq \sup_{\check{\boldsymbol{v}} \in \boldsymbol{H}_0^1(\check{\Omega}) \setminus \{0\}} \frac{\check{b}(\check{\boldsymbol{v}}, \check{q})}{\|\check{\boldsymbol{v}}\|_{H^1(\check{\Omega})}}.$$

Therefore the inf-sup condition is satisfied.

Since we have confirmed all of the conditions in Proposition 2.2.2, we conclude that there exists a unique solution to (30). □

3.2 The Axisymmetric Stokes Problem

In this section we derive the formulation of the Stokes problem on axisymmetric functions and show that the resulting problem is well-posed.

We introduce the Hilbert spaces

$$\hat{\boldsymbol{H}}_0^1(\check{\Omega}) := \{\check{\boldsymbol{v}} \in \boldsymbol{H}_0^1(\check{\Omega}) : \ \check{\boldsymbol{v}} \text{ is axisymmetric}\},$$
$$\hat{L}_0^2(\check{\Omega}) := \{\check{q} \in L_0^2(\check{\Omega}) : \ \check{q} \text{ is axisymmetric}\},$$

and consider the following problem: Find $(\check{\boldsymbol{u}}, \check{p}) \in \hat{\boldsymbol{H}}_0^1(\check{\Omega}) \times \hat{L}_0^2(\check{\Omega})$ such that

$$\check{a}(\check{\boldsymbol{u}}, \check{\boldsymbol{v}}) + \check{b}(\check{\boldsymbol{v}}, \check{p}) = \int_{\check{\Omega}} \check{\boldsymbol{f}} \cdot \check{\boldsymbol{v}} \, d\check{x} \qquad \forall \check{\boldsymbol{v}} \in \hat{\boldsymbol{H}}_0^1(\check{\Omega}), \tag{31a}$$

$$\check{b}(\check{\boldsymbol{u}}, \check{q}) = 0 \qquad \forall \check{q} \in \hat{L}_0^2(\check{\Omega}). \tag{31b}$$

Note that this problem is nearly identical to (30); the only difference being that the functions in the formulation are assumed to be axisymmetric.

Proposition 3.2.1 (Theorem 2.1 in [43]). *Given $\check{q} \in \hat{L}^2_0(\check{\Omega})$, there exists $\check{\boldsymbol{v}} \in \hat{\boldsymbol{H}}^1_0(\check{\Omega})$ such that $\check{\nabla} \cdot \check{\boldsymbol{v}} = \check{q}$ and $\|\check{\boldsymbol{v}}\|_{H^1(\check{\Omega})} \leq \check{\beta}^{-1} \|\check{q}\|_{L^2(\check{\Omega})}$.*

Proof. We repeat the arguments given in [43] for completeness.

Let $\check{q} \in \hat{L}^2_0(\check{\Omega})$. By Proposition 3.1.2, there is $\tilde{\boldsymbol{v}} \in \boldsymbol{H}^1_0(\check{\Omega})$ such that $\check{\nabla} \cdot \tilde{\boldsymbol{v}} = \check{q}$ and $\|\tilde{\boldsymbol{v}}\|_{H^1(\Omega)} \leq \check{\beta}^{-1} \|\check{q}\|_{L^2(\check{\Omega})}$.

We then define $\check{\boldsymbol{v}}$ as follows:

$$\check{\boldsymbol{v}} = \frac{1}{2\pi} \int_{-\pi}^{\pi} R_{-\eta} \tilde{\boldsymbol{v}} \circ R_\eta \, d\eta.$$

By definition, $\check{\boldsymbol{v}}$ is axisymmetric. By the chain rule we have

$$\check{\nabla} \cdot \big(R_{-\eta} \tilde{\boldsymbol{v}} \circ R_\eta \big) = (\check{\nabla} \cdot \tilde{\boldsymbol{v}}) \circ R_\eta = \check{q} \circ R_\eta,$$

and therefore

$$\check{\nabla} \cdot \check{\boldsymbol{v}} = \frac{1}{2\pi} \int_{-\pi}^{\pi} \check{q} \circ R_\eta \, d\eta = \check{q}.$$

□

Theorem 3.2.2 (Proposition I.2.7 in [9]). *There exists a unique $(\check{\boldsymbol{u}}, \check{p}) \in \hat{\boldsymbol{H}}^1_0(\check{\Omega}) \times \hat{L}^2_0(\check{\Omega})$ satisfying* (31)*. Moreover, if $\check{\boldsymbol{f}}$ is axisymmetric, then $(\check{\boldsymbol{u}}, \check{p})$ coincides with the solution to* (30)*.*

Proof. Proposition 3.2.1 implies that the inf-sup condition on axisymmetric functions

$$\sup_{\check{\boldsymbol{v}} \in \hat{\boldsymbol{H}}^1_0(\check{\Omega}) \setminus \{0\}} \frac{\check{b}(\check{\boldsymbol{v}}, \check{q})}{\|\check{\boldsymbol{v}}\|_{H^1(\check{\Omega})}} \geq \check{\beta} \|\check{q}\|_{L^2(\check{\Omega})} \qquad \forall \check{q} \in \hat{L}^2_0(\check{\Omega})$$

is satisfied. Therefore the existence and and uniqueness of (31) follows from the general theory of saddle point problems (see Proposition 2.2.2 and the proof of Theorem 3.1.1). It suffices to show that if the data vector field $\check{\boldsymbol{f}}$ is axisymmetric, then so is the solution pair $(\check{\boldsymbol{u}}, \check{p})$.

Let $\check{\boldsymbol{v}} \in \boldsymbol{H}_0^1(\check{\Omega})$ and fix $\eta \in [-\pi, \pi]$. Assume that the pair $(\check{\boldsymbol{u}}, \check{p})$ solve (30), and the data vector field $\check{\boldsymbol{f}}$ is axisymmetric. Observe that the vector field $R_\eta \check{\boldsymbol{v}} \circ R_{-\eta} \in \boldsymbol{H}_0^1(\check{\Omega})$, so we have

$$\check{a}(\check{\boldsymbol{u}}, R_\eta \check{\boldsymbol{v}} \circ R_{-\eta}) + \check{b}(R_\eta \check{\boldsymbol{v}} \circ R_{-\eta}, \check{p}) = \int_{\check{\Omega}} \check{\boldsymbol{f}} \cdot R_\eta \check{\boldsymbol{v}} \circ R_{-\eta} \, d\check{x} \qquad \forall \check{\boldsymbol{v}} \in \boldsymbol{H}_0^1(\check{\Omega}), \tag{32a}$$

$$\check{b}(\check{\boldsymbol{u}}, \check{q}) = 0 \qquad \forall \check{q} \in L_0^2(\check{\Omega}). \tag{32b}$$

Let A, B and C be any square matrices. Observe that $A : (BC) = (B^\intercal A) : C$, and so we have

$$\check{a}(\check{\boldsymbol{u}}, R_\eta \check{\boldsymbol{v}}) = \check{a}(R_{-\eta} \check{\boldsymbol{u}}, \check{\boldsymbol{v}}) \quad \forall \check{\boldsymbol{u}}, \check{\boldsymbol{v}} \in \boldsymbol{H}_0^1(\check{\Omega}).$$

The proof of Proposition 3.2.1 shows that $\check{\nabla} \cdot (R_\eta \check{\boldsymbol{v}} \circ R_{-\eta}) = (\check{\nabla} \cdot \check{\boldsymbol{v}}) \circ R_{-\eta}$ and so we have

$$\check{b}(R_\eta \check{\boldsymbol{v}} \circ R_{-\eta}, \hat{p}) = \check{b}(\check{\boldsymbol{v}} \circ R_{-\eta}, \check{p}).$$

Hence, using the change of variables $\check{y} = R_{-\eta} \check{x}$, and the fact that $\check{\boldsymbol{f}} \cdot R_\eta \check{\boldsymbol{v}} = R_{-\eta} \check{\boldsymbol{f}} \cdot \check{\boldsymbol{v}}$ and $\check{\boldsymbol{f}}$ is axisymmetric, we get that

$$\int_{\check{\Omega}} \check{\boldsymbol{f}} \cdot R_\eta \check{\boldsymbol{v}} \circ R_{-\eta} \, d\check{x} = \int_{\check{\Omega}} R_{-\eta} \check{\boldsymbol{f}} \circ R_\eta \cdot \check{\boldsymbol{v}} \, d\hat{y} = \int_{\check{\Omega}} \check{\boldsymbol{f}} \cdot \check{\boldsymbol{v}} \, d\check{x}, \qquad \forall \check{\boldsymbol{v}} \in \boldsymbol{H}_0^1(\check{\Omega}).$$

Hence, the system (32) becomes

$$\check{a}(R_{-\eta} \check{\boldsymbol{u}} \circ R_\eta, \check{\boldsymbol{v}}) + \check{b}(\check{\boldsymbol{v}}, \check{p} \circ R_\eta) = \int_{\check{\Omega}} \check{\boldsymbol{f}} \cdot \check{\boldsymbol{v}} \, d\check{x}, \qquad \forall \check{\boldsymbol{v}} \in \boldsymbol{H}_0^1(\check{\Omega}), \tag{33a}$$

$$\check{b}(R_{-\eta} \check{\boldsymbol{u}} \circ R_\eta, \check{q}) = 0, \qquad \forall \check{q} \in L_0^2(\check{\Omega}). \tag{33b}$$

Since (30) has a unique solution and $\eta \in [-\pi, \pi]$ was taken arbitrary, we conclude that $(\check{\boldsymbol{u}}, \check{p}) = (R_{-\eta} \check{\boldsymbol{u}} \circ R_\eta, \check{p} \circ R_\eta)$, hence $(\check{\boldsymbol{u}}, \check{p}) \in \hat{\boldsymbol{H}}_0^1(\check{\Omega}) \times \hat{L}_0^2(\check{\Omega})$ and solves (31). This completes the proof. □

3.3 The Axisymmetric Stokes Problem in Cylindrical Coordinates

In this section we formulate the axisymmetric Stokes problem and its variational formulation in cylindrical coordinates. To this end, we recall some notation from the previous chapter.

We take into consideration the cylindrical coordinate system (r, θ, z) with $r = \sqrt{\check{x}_1^2 + \check{x}_2^2}$, $\theta = \arctan(\check{x}_2/\check{x}_1)$, and $z = \check{x}_3$. For a vector field $\check{\boldsymbol{v}} = (\check{v}_1, \check{v}_2, \check{v}_3)^\intercal$, we denote by $\bar{v}_r$, $\bar{v}_\theta$, and $\bar{v}_z$ its radial, angular, and axial components, respectively, i.e.,

$$\begin{aligned}
\bar{v}_r &= \check{v}_1 \cos\theta + \check{v}_2 \sin\theta, \\
\bar{v}_\theta &= -\check{v}_1 \sin\theta + \check{v}_2 \cos\theta, \\
\bar{v}_z &= \check{v}_3.
\end{aligned}$$

We denote $\bar{\boldsymbol{v}} = \bar{\boldsymbol{v}}(r, \theta, z) = (\bar{v}_r, \bar{v}_\theta, \bar{v}_z)^\intercal$ so that

$$\bar{\boldsymbol{v}} = R_\theta \check{\boldsymbol{v}}, \tag{34}$$

where the rotation matrix R_θ is given by (7) (with $\eta = \theta(\check{x})$). Likewise, for a scalar function $\check{q} : \check{\Omega} \to \mathbb{R}$, we set $\bar{q} : \check{\Omega} \to \mathbb{R}$ such that $\check{q}(\check{x}) = \bar{q}(r, \theta, z)$.

Proposition 3.3.1. *Let $\check{\boldsymbol{v}}, \bar{\boldsymbol{v}} : \check{\Omega} \to \mathbb{R}^3$ and $\check{q}, \bar{q} : \check{\Omega} \to \mathbb{R}$ be related via $\bar{\boldsymbol{v}}(r, \theta, z) = R_\theta \check{\boldsymbol{v}}(\hat{x})$ and $\bar{q}(r, \theta, z) = \check{q}(\check{x})$. Then there holds*

$$\begin{aligned}
\check{\nabla} \check{q} &= R_{-\theta} \begin{pmatrix} \frac{\partial \bar{q}}{\partial r} \\ \frac{1}{r}\frac{\partial \bar{q}}{\partial \theta} \\ \frac{\partial \bar{q}}{\partial z} \end{pmatrix}, \\
\check{\nabla} \check{\boldsymbol{v}} &= R_{-\theta} \begin{pmatrix} \frac{\partial \bar{v}_r}{\partial r} & \frac{1}{r}\frac{\partial \bar{v}_r}{\partial \theta} & \frac{\partial \bar{v}_r}{\partial z} \\ \frac{\partial \bar{v}_\theta}{\partial r} & \frac{1}{r}\frac{\partial \bar{v}_\theta}{\partial \theta} & \frac{\partial \bar{v}_\theta}{\partial z} \\ \frac{\partial \bar{v}_z}{\partial r} & \frac{1}{r}\frac{\partial \bar{v}_z}{\partial \theta} & \frac{\partial \bar{v}_z}{\partial z} \end{pmatrix} R_\theta + I_\theta(\bar{\boldsymbol{v}} \otimes \check{\nabla}\theta), \\
\check{\Delta} \check{\boldsymbol{v}} &= R_{-\theta}\Big(\frac{\partial^2 \bar{\boldsymbol{v}}}{\partial r^2} + \frac{1}{r}\frac{\partial \bar{\boldsymbol{v}}}{\partial r} + \frac{1}{r^2}\frac{\partial^2 \bar{\boldsymbol{v}}}{\partial \theta^2} + \frac{\partial^2 \bar{\boldsymbol{v}}}{\partial z^2}\Big) + \frac{1}{r^2}\Big(\frac{d^2}{d\theta^2} R_{-\theta}\Big)\bar{\boldsymbol{v}}, \\
\hat{\nabla} \times \hat{\boldsymbol{v}} &= R_{-\theta}\Big(\frac{1}{r}\frac{\partial \bar{v}_z}{\partial \theta} - \frac{\partial \bar{v}_\theta}{\partial z}, \frac{\partial \bar{v}_r}{\partial z} - \frac{\partial \bar{v}_z}{\partial r}, \frac{1}{r}\Big(\frac{\partial (r\bar{v}_\theta)}{\partial r} - \frac{\partial \bar{v}_r}{\partial \theta}\Big)\Big)^\intercal,
\end{aligned}$$

where

$$I_\theta := \frac{d}{d\theta} R_{-\theta} = \begin{pmatrix} -\sin\theta & -\cos\theta & 0 \\ \cos\theta & -\sin\theta & 0 \\ 0 & 0 & 0 \end{pmatrix}, \quad \check{\nabla}\theta = \frac{1}{r} \begin{pmatrix} -\sin\theta \\ \cos\theta \\ 0 \end{pmatrix}.$$

Proof. The identities readily follow from the chain rule and the identities $\frac{\partial r}{\partial \check{x}_j} = (R_\theta)_{1,j}$, $\frac{\partial \theta}{\partial \check{x}_j} = \frac{1}{r}(R_\theta)_{2,j}$, and $\frac{\partial z}{\partial \check{x}_j} = (R_\theta)_{3,j}$. □

3.3.1 Cylindrical strong form derivation

Throughout this section, we assume that the source function $\check{\boldsymbol{f}}$ is axisymmetric so that the solution to the Stokes problem is axisymmetric (cf. Theorem 3.2.2), i.e., $\check{\boldsymbol{u}} \in \hat{\boldsymbol{H}}^1_0(\check{\Omega})$ and $\check{p} \in \hat{L}^2_0(\check{\Omega})$. In this case we conclude from Proposition 3.3.1 and (8) that

$$\begin{aligned}
\check{\nabla}\check{p} &= R_{-\theta} \begin{pmatrix} \frac{\partial \bar{p}}{\partial r} \\ 0 \\ \frac{\partial \bar{p}}{\partial z} \end{pmatrix}, \\
\check{\nabla}\check{\boldsymbol{u}} &= R_{-\theta} \begin{pmatrix} \frac{\partial \bar{u}_r}{\partial r} & 0 & \frac{\partial \bar{u}_r}{\partial z} \\ \frac{\partial \bar{u}_\theta}{\partial r} & 0 & \frac{\partial \bar{u}_\theta}{\partial z} \\ \frac{\partial \bar{u}_z}{\partial r} & 0 & \frac{\partial \bar{u}_z}{\partial z} \end{pmatrix} R_\theta + I_\theta(\bar{\boldsymbol{u}} \otimes \check{\nabla}\theta), \qquad (35) \\
\check{\Delta}\check{\boldsymbol{u}} &= R_{-\theta}\Big(\frac{\partial^2 \bar{\boldsymbol{u}}}{\partial r^2} + \frac{1}{r}\frac{\partial \bar{\boldsymbol{u}}}{\partial r} + \frac{\partial^2 \bar{\boldsymbol{u}}}{\partial z^2}\Big) + \frac{1}{r^2}\big(\frac{d^2}{d\theta^2} R_{-\theta}\big)\bar{\boldsymbol{u}} \\
&= R_{-\theta}\left(\frac{\partial^2 \bar{\boldsymbol{u}}}{\partial r^2} + \frac{1}{r}\frac{\partial \bar{\boldsymbol{u}}}{\partial r} + \frac{\partial^2 \bar{\boldsymbol{u}}}{\partial z^2} - \frac{1}{r^2}\begin{pmatrix} \bar{u}_r \\ \bar{u}_\theta \\ 0 \end{pmatrix}\right).
\end{aligned}$$

Consequently, the momentum equations of the Stokes problem (25a) reduce to

$$\begin{aligned}
\bar{\boldsymbol{f}} = R_\theta \check{\boldsymbol{f}} &= R_\theta\big(-\nu\check{\Delta}\check{\boldsymbol{u}} + \check{\nabla}\check{p}\big) \qquad (36) \\
&= -\nu\Big(\frac{\partial^2 \bar{\boldsymbol{u}}}{\partial r^2} + \frac{1}{r}\frac{\partial \bar{\boldsymbol{u}}}{\partial r} + \frac{\partial^2 \bar{\boldsymbol{u}}}{\partial z^2} - \frac{1}{r^2}\begin{pmatrix} \bar{u}_r \\ \bar{u}_\theta \\ 0 \end{pmatrix}\Big) + \begin{pmatrix} \frac{\partial \bar{p}}{\partial r} \\ 0 \\ \frac{\partial \bar{p}}{\partial z} \end{pmatrix}.
\end{aligned}$$

For the divergence constraint $\check{\nabla} \cdot \check{\boldsymbol{u}} = 0$, we compute the trace of $\check{\nabla}\check{\boldsymbol{u}}$ in (35) to get

$$\begin{aligned} \check{\nabla} \cdot \check{\boldsymbol{u}} &= \frac{\partial \bar{u}_r}{\partial r} + \frac{\partial \bar{u}_z}{\partial z} + \operatorname{tr}\Big(I_\theta(\bar{\boldsymbol{u}} \otimes \check{\nabla}\theta)\Big) \\ &= \frac{\partial \bar{u}_r}{\partial r} + \frac{\partial \bar{u}_z}{\partial z} + \frac{1}{r}\bar{u}_r =: \nabla_{rz} \cdot \bar{\boldsymbol{u}}. \end{aligned} \tag{37}$$

From (36)–(37), we conclude that, assuming $\check{\boldsymbol{u}}$ and $\check{p}$ are axisymmetric, the Stokes problem (25) in cylindrical coordinates reduces to the following system:

$$-\nu\Big(\frac{\partial^2 \bar{u}_r}{\partial r^2} + \frac{1}{r}\frac{\partial \bar{u}_r}{\partial r} + \frac{\partial^2 \bar{u}_r}{\partial z^2} - \frac{1}{r^2}\bar{u}_r\Big) + \frac{\partial \bar{p}}{\partial r} = \bar{f}_r, \tag{38a}$$

$$-\nu\Big(\frac{\partial^2 \bar{u}_\theta}{\partial r^2} + \frac{1}{r}\frac{\partial \bar{u}_\theta}{\partial r} + \frac{\partial^2 \bar{u}_\theta}{\partial z^2} - \frac{1}{r^2}\bar{u}_\theta\Big) = \bar{f}_\theta, \tag{38b}$$

$$-\nu\Big(\frac{\partial^2 \bar{u}_z}{\partial r^2} + \frac{1}{r}\frac{\partial \bar{u}_z}{\partial r} + \frac{\partial^2 \bar{u}_z}{\partial z^2}\Big) + \frac{\partial \bar{p}}{\partial z} = \bar{f}_z, \tag{38c}$$

$$\nabla_{rz} \cdot \bar{\boldsymbol{u}} = \frac{\partial \bar{u}_r}{\partial r} + \frac{\bar{u}_r}{r} + \frac{\partial \bar{u}_z}{\partial z} = 0. \tag{38d}$$

Similar to (25), this system involves four unknowns on a three-dimensional domain. However, since u_θ does not appear in the divergence constraint, it is decoupled from the system. Furthermore, if $f_\theta = 0$ then $u_\theta = 0$ (see [7, 9]). Finally since $\bar{p}$ and $\bar{\boldsymbol{u}}$ do not depend on θ (cf. (8)), the problem can be posed on the two-dimensional domain Ω. This feature will be explored in subsequent sections.

3.3.2 Bilinear forms in cylindrical coordinates

In this section we derive expressions of the bilinear forms $\check{a}(.,.)$ and $\check{b}(.,.)$ in cylindrical coordinates. While this can be done based on the system (38), we instead make a change of variables in (28)–(29) and apply the identities (8).

Without loss of generality we assume that $\bar{f}_\theta \equiv 0$ so that the angular component of $\check{\boldsymbol{u}}$ vanishes. In this case, Proposition 3.3.1 shows that

$$\check{\nabla}\check{\boldsymbol{u}} = R_{-\theta}\nabla_{rz}\bar{\boldsymbol{u}}R_\theta + I_\theta(\bar{\boldsymbol{u}} \otimes \check{\nabla}\theta),$$

where $\nabla_{rz}\bar{\boldsymbol{u}} := \begin{pmatrix} \partial_r \bar{u}_r & 0 & \partial_r \bar{u}_z \\ 0 & 0 & 0 \\ \partial_z \bar{u}_r & 0 & \partial_z \bar{u}_z \end{pmatrix}$. Let $\check{\boldsymbol{v}}$ be an axisymmetric function with zero angular component. We then compute

$$\begin{aligned} \check{\nabla}\check{\boldsymbol{u}} : \check{\nabla}\check{\boldsymbol{v}} &= \big(R_{-\theta}\nabla_{rz}\bar{\boldsymbol{u}}R_\theta + I_\theta(\bar{\boldsymbol{u}} \otimes \check{\nabla}\theta)\big) : \big(R_{-\theta}\nabla_{rz}\bar{\boldsymbol{v}}R_\theta + I_\theta(\bar{\boldsymbol{v}} \otimes \check{\nabla}\theta)\big) \\ &= \big(R_{-\theta}\nabla_{rz}\bar{\boldsymbol{u}}R_\theta\big) : \big(R_{-\theta}\nabla_{rz}\bar{\boldsymbol{v}}R_\theta\big) + \big(I_\theta(\bar{\boldsymbol{u}} \otimes \check{\nabla}\theta)\big) : \big(I_\theta(\bar{\boldsymbol{v}} \otimes \check{\nabla}\theta)\big) \\ &\quad + \big(R_{-\theta}\nabla_{rz}\bar{\boldsymbol{u}}R_\theta\big) : \big(I_\theta(\bar{\boldsymbol{v}} \times \check{\nabla}\theta)\big). \end{aligned} \tag{39}$$

Using the property $A : B = \operatorname{tr}(AB)$ for matrices A and B, we easily find that

$$\begin{aligned} \big(R_{-\theta}\nabla_{rz}\bar{\boldsymbol{u}}R_\theta\big) : \big(R_{-\theta}\nabla_{rz}\bar{\boldsymbol{v}}R_\theta\big) &= \operatorname{tr}\big(R_{-\theta}\nabla_{rz}\bar{\boldsymbol{u}}\nabla_{rz}\bar{\boldsymbol{v}}R_\theta\big) \\ &= \operatorname{tr}(\nabla_{rz}\bar{\boldsymbol{u}}\nabla_{rz}\bar{\boldsymbol{v}}) = \nabla_{rz}\bar{\boldsymbol{u}} : \nabla_{rz}\bar{\boldsymbol{v}}. \end{aligned} \tag{40}$$

Next we write

$$\begin{aligned} \big(R_{-\theta}\nabla_{rz}\bar{\boldsymbol{u}}R_\theta\big) : \big(I_\theta(\bar{\boldsymbol{v}} \otimes \check{\nabla}\theta)\big) &= \operatorname{tr}\Big(R_{-\theta}\nabla_{rz}\bar{\boldsymbol{u}}R_\theta I_\theta(\bar{\boldsymbol{v}} \otimes \check{\nabla}\theta)\Big) \\ &= \operatorname{tr}\Big(R_{-\theta}\big((\nabla_{rz}\bar{\boldsymbol{u}}R_\theta I_\theta\bar{\boldsymbol{v}}) \otimes \check{\nabla}\theta\big)\Big). \end{aligned}$$

A calculation shows that

$$R_\theta I_\theta = \begin{pmatrix} 0 & -1 & 0 \\ 1 & 0 & 0 \\ 0 & 0 & 0 \end{pmatrix} \quad\Longrightarrow\quad R_\theta I_\theta \bar{\boldsymbol{v}} = \begin{pmatrix} 0 \\ \bar{v}_r \\ 0 \end{pmatrix}.$$

Because the second column of $\nabla_{rz}\bar{\boldsymbol{u}}$ is the zero vector, we conclude that $\nabla_{rz}\bar{u}R_\theta I_\theta\bar{\boldsymbol{v}} = \boldsymbol{0}$ and

$$\big(R_{-\theta}\nabla_{rz}\bar{\boldsymbol{u}}R_\theta\big) : \big(I_\theta(\bar{\boldsymbol{v}} \otimes \check{\nabla}\theta)\big) = 0. \tag{41}$$

Finally, another calculation shows that

$$\big(I_\theta(\bar{\boldsymbol{u}} \otimes \check{\nabla}\theta)\big) : \big(I_\theta(\bar{\boldsymbol{v}} \otimes \check{\nabla}\theta)\big) = (I_\theta\bar{\boldsymbol{u}}) \cdot (I_\theta\bar{\boldsymbol{v}})|\check{\nabla}\theta|^2 = \frac{1}{r^2}\bar{u}_r\bar{v}_r. \tag{42}$$

Applying the identities (40)–(42) to (39) gives us

$$\check{\nabla}\check{\boldsymbol{u}} : \check{\nabla}\check{\boldsymbol{v}} = \nabla_{rz}\bar{\boldsymbol{u}} : \nabla_{rz}\bar{\boldsymbol{v}} + \frac{1}{r^2}\bar{u}_r\bar{v}_r.$$

We now apply this identity and the identity (37) in the definition of the bilinear forms $\check{a}(.,.)$, $\check{b}(.,.)$ and make a change of variables to conclude that the bilinear forms in cylindrical coordinates reduce to

$$\check{a}(\check{\boldsymbol{u}},\check{\boldsymbol{v}}) = \int_0^{2\pi}\int_\Omega (\nabla_{rz}\bar{\boldsymbol{u}} : \nabla_{rz}\bar{\boldsymbol{v}} + \frac{\bar{u}_r\bar{v}_r}{r^2})r\,dr\,dz\,d\theta, \tag{43a}$$

$$\check{b}(\check{\boldsymbol{u}},\check{q}) = -\int_0^{2\pi}\int_\Omega (\nabla_{rz}\cdot\bar{\boldsymbol{u}})\bar{q}r\,dr\,dz\,d\theta. \tag{43b}$$

3.4 Dimension Reduction

For an axisymmetric function $\check{\boldsymbol{v}}$ we set $\boldsymbol{v}:\Omega\to\mathbb{R}^2$ as

$$\boldsymbol{v}(r,z) = (v_r(r,z), v_z(r,z))^\intercal = (\bar{v}_r(r,0,z), \bar{v}_z(r,0,z))^\intercal, \tag{44}$$

where we recall that $(\bar{v}_r,\bar{v}_\theta,\bar{v}_z)^\intercal$ is the cylindrical representation of $\check{\boldsymbol{v}}$. Likewise, for an axisymmetric function $\check{q}$, we set $q:\Omega\to\mathbb{R}$ as

$$q(r,z) = \bar{q}(r,\theta,z). \tag{45}$$

We then define the following bilinear forms on Ω:

$$a(\boldsymbol{u},\boldsymbol{v}) = \int_\Omega \Big(\nabla_{rz}\boldsymbol{u} : \nabla_{rz}\boldsymbol{v} + \frac{u_rv_r}{r^2}\Big)r\,dr\,dz, \tag{46a}$$

$$b(\boldsymbol{v},q) = -\int_\Omega (\nabla_{rz}\cdot\boldsymbol{v})qr\,dr\,dz. \tag{46b}$$

Since the cylindrical components of an axisymmetric function does not depend on the variable θ, we conclude from (43) that

$$\check{a}(\check{\boldsymbol{u}},\check{\boldsymbol{v}}) = 2\pi a(\boldsymbol{u},\boldsymbol{v}), \qquad \check{b}(\check{\boldsymbol{v}},\check{q}) = 2\pi b(\boldsymbol{v},q) \tag{47}$$

for all $\check{q}\in\hat{L}^2_0(\check{\Omega})$ and $\check{\boldsymbol{u}},\check{\boldsymbol{v}}\in\hat{\boldsymbol{H}}^1_0(\check{\Omega})$ with zero angular component.

Due to a change of variables into cylindrical coordinates, the measure $d\check{x}_1d\check{x}_2d\check{x}_3$ is transformed into $rdrd\theta dz$, and therefore it is natural to seek solutions in weighted Sobolev

spaces on Ω associated with the measure $rdrdz$ [43]. To this end, we define the following variants of the spaces $L^2_\alpha(\Omega)$ and $H^m_\alpha(\Omega)$:

$$V^1_1(\Omega) = \{w : w \in L^2_{-1}(\Omega) \cap H^1_1(\Omega)\},$$
$$V^1_{1,0}(\Omega) = \{w \in H^1_{-1}(\Omega) : \ w|_\Gamma = 0\},$$
$$H^1_{1,0}(\Omega) = \{w : \ w \in H^1_1(\Omega), w|_\Gamma = 0\},$$

where Γ is the part of $\partial\Omega$ that does not intersect with the z-axis.

We define the norm on $V^1_1(\Omega)$ by $\|w\|_{V^1_1(\Omega)} = (\|w\|^2_{L^2_{-1}(\Omega)} + |w|^2_{H^1_1(\Omega)})^{1/2}$, where $|w|_{H^m_\alpha(\Omega)} = (\sum_{|\beta|=m} \|D^\beta w\|^2_{L^2_\alpha(\Omega)})^{1/2}$. Finally we set

$$\boldsymbol{V}(\Omega) := V^1_{1,0}(\Omega) \times H^1_{1,0}(\Omega), \qquad Q(\Omega) := \{q \in L^2_1(\Omega) : \int_\Omega qr\, dr\, dz = 0\}. \tag{48}$$

Proposition 3.4.1 (Proposition 1 in [7])**.**

1. *The space* $\{\check{\boldsymbol{v}} \in \hat{\boldsymbol{H}}^1_0(\check{\Omega}) : \ \bar{v}_\theta = 0\}$ *is isomorphic to* $\boldsymbol{V}(\Omega)$ *via the mapping* $\check{\boldsymbol{v}} \to \boldsymbol{v}$ *given by* (44)*.*
2. *The space* $\hat{L}^2_0(\check{\Omega})$ *is isomorphic to* $Q(\Omega)$ *via the mapping* $\check{q} \to q$ *given by* (45)*.*

This result immediately gives us the following theorem.

Theorem 3.4.2. *There exists a unique* $(\boldsymbol{u}, p) \in \boldsymbol{V}(\Omega) \times Q(\Omega)$ *satisfying*

$$a(\boldsymbol{u}, \boldsymbol{v}) + b(\boldsymbol{v}, p) = \int_\Omega r\boldsymbol{f} \cdot \boldsymbol{v}\, dr\, dz \qquad \forall \boldsymbol{v} \in \boldsymbol{V}(\Omega), \tag{49a}$$
$$b(\boldsymbol{u}, q) = 0 \qquad \forall q \in Q(\Omega). \tag{49b}$$

Moreover, the pair $(\check{\boldsymbol{u}}, \check{p})$ *given by the (inverse) mappings* $\boldsymbol{u} \to \check{\boldsymbol{u}}$ *and* $p \to \check{p}$ *solve the system* (31) *provided that* $\bar{f}_\theta = 0$*.*

Proof. We verify the conditions stated in Proposition 2.2.2 with $\boldsymbol{X} = \boldsymbol{V}(\Omega)$ and $Y = Q(\Omega)$.

1. Proposition 3.4.1 shows that the continuity of the bilinear forms $a(.,.)$ and $b(.,.)$ follow directly from (47) and the continuity of $\check{a}(.,.)$ and $\check{b}(.,.)$.
2. Proposition 3.4.1 shows that the coercivity of the bilinear form $a(.,.)$ follows directly from (47) and the coercivity of the bilinear form $\check{a}(.,.)$.

3. Let $\check{\boldsymbol{v}} \in \hat{\boldsymbol{H}}_0^1(\check{\Omega})$ and $\check{q} \in \hat{L}_0^2(\check{\Omega})$. Let $\boldsymbol{v} \in \boldsymbol{V}(\Omega)$ and $q \in Q(\Omega)$ be the images of $\check{\boldsymbol{v}}$ and $\check{q}$ under the mapping defined in(44) and (45) respectively. Recall that the following inf-sup condition

$$\sup_{\check{\boldsymbol{v}} \in \hat{\boldsymbol{H}}_0^1(\check{\Omega}) \setminus \{0\}} \frac{\check{b}(\check{\boldsymbol{v}}, \check{q})}{\|\check{\boldsymbol{v}}\|_{H^1(\check{\Omega})}} \geq \beta \|\check{q}\|_{L^2(\check{\Omega})} \qquad \forall \check{q} \in \hat{L}_0^2(\check{\Omega})$$

holds. Since $\check{\nabla} \cdot \check{\boldsymbol{v}} = \nabla_{rz} \cdot \boldsymbol{v}$ and $\|\boldsymbol{v}\|_{\boldsymbol{V}(\Omega)} \leq \|\check{\boldsymbol{v}} \circ R_\theta\|_{H^1(\check{\Omega})} = \|\check{\boldsymbol{v}}\|_{H^1(\check{\Omega})}$, we have

$$\sup_{\boldsymbol{v} \in \boldsymbol{V}(\Omega) \setminus \{0\}} \frac{2\pi b(\boldsymbol{v}, q)}{\|\boldsymbol{v}\|_{\boldsymbol{V}(\Omega)}} \geq \sup_{\check{\boldsymbol{v}} \in \hat{\boldsymbol{H}}_0^1(\check{\Omega}) \setminus \{0\}} \frac{\check{b}(\check{\boldsymbol{v}}, \check{q})}{\|\check{\boldsymbol{v}}\|_{H^1(\check{\Omega})}} \qquad \forall \check{q} \in \hat{L}_0^2(\check{\Omega}).$$

Consequently, there is $C > 0$ so that $\forall q \in Q(\Omega)$ we have

$$2\pi C \|q\|_{Q(\Omega)} = C \|\check{q}\|_{L^2(\check{\Omega})} \leq \sup_{\check{\boldsymbol{v}} \in \hat{\boldsymbol{H}}_0^1(\check{\Omega}) \setminus \{0\}} \frac{\check{b}(\check{\boldsymbol{v}}, \check{q})}{\|\check{\boldsymbol{v}}\|_{H^1(\check{\Omega})}} \leq \sup_{\boldsymbol{v} \in \boldsymbol{V}(\Omega) \setminus \{0\}} \frac{b(\boldsymbol{v}, q)}{\|\boldsymbol{v}\|_{\boldsymbol{V}(\Omega)}}.$$

Therefore the inf-sup condition is satisfied.

Since we have confirmed all of the conditions in Proposition 2.2.2, we conclude that there exists a unique solution to (49). We consider the following problem: Find $(\check{\boldsymbol{u}}, \check{p}) \in \{\check{\boldsymbol{v}} \in \hat{\boldsymbol{H}}_0^1(\hat{\Omega}) : \ \bar{v}_\theta = 0\} \times \hat{L}_0^2(\check{\Omega})$ such that

$$\check{a}(\check{\boldsymbol{u}}, \check{\boldsymbol{v}}) + \check{b}(\check{\boldsymbol{v}}, \check{p}) = \int_{\check{\Omega}} \check{\boldsymbol{f}} \cdot \check{\boldsymbol{v}} \, d\check{x} \qquad \forall \check{\boldsymbol{v}} \in \{\check{\boldsymbol{v}} \in \hat{\boldsymbol{H}}_0^1(\check{\Omega}) : \ \bar{v}_\theta = 0\}, \tag{50a}$$

$$\check{b}(\check{\boldsymbol{u}}, \check{q}) = 0 \qquad \forall \check{q} \in \hat{L}_0^2(\check{\Omega}). \tag{50b}$$

Recall that $\bar{f}_\theta = 0$ implies $\bar{u}_\theta = 0$, so we narrow our search to be in the space $\{\check{\boldsymbol{v}} \in \hat{\boldsymbol{H}}_0^1(\check{\Omega}) : \bar{v}_\theta = 0\}$. Hence, the system (31) becomes equivalent to (50). It is easy to check (by going backwards in cylindrical coordinates change of variables) that the image of the solution to (49) under the inverse mapping $(\check{\boldsymbol{u}}, \check{p})$ solves (50). This completes the proof. □

3.5 A Commutative Diagram

In this section we expand the results of the previous sections, and show how the axisymmetric Stokes problem fits within a commutative de Rham complexes in both the two and three dimensional domains. In addition we draw connections between these complexes via commutative projections.

Recall the space $\boldsymbol{H}_0(\mathrm{div};\check{\Omega})$ defined in (2) and define the auxiliary function space

$$\boldsymbol{H}_0(\mathbf{curl};\check{\Omega}) := \{\check{\boldsymbol{v}} \in \boldsymbol{L}^2(\check{\Omega}) :\ \check{\nabla}\times\check{\boldsymbol{v}} \in \boldsymbol{L}^2(\check{\Omega}),\ \check{\boldsymbol{v}}\times\check{\boldsymbol{n}}|_{\partial\check{\Omega}} = 0\}.$$

The three dimensional de Rham complex with minimal L^2-smoothness is given by [23]

$$0 \longrightarrow H_0^1(\check{\Omega}) \xrightarrow{\check{\nabla}} \boldsymbol{H}_0(\mathbf{curl};\check{\Omega}) \xrightarrow{\check{\nabla}\times} \boldsymbol{H}_0^1(\check{\Omega}) \xrightarrow{\check{\nabla}\cdot} L_0^2(\check{\Omega}) \longrightarrow 0. \tag{51}$$

If the domain $\check{\Omega}$ is contractible then the sequence is exact, i.e., the image of each map is the kernel of the succeeding map [23]. In more detail, the exactness property gives

1. Functions $\check{v} \in H_0^1(\check{\Omega})$ with vanishing gradient are identically zero;
2. If $\check{\boldsymbol{v}} \in \boldsymbol{H}_0(\mathbf{curl};\check{\Omega})$ is curl–free, then there exists a unique $\check{w} \in H_0^1(\check{\Omega})$ such that $\check{\nabla}\check{w} = \check{\boldsymbol{v}}$;
3. If $\check{\boldsymbol{v}} \in \boldsymbol{H}_0(\mathrm{div};\check{\Omega})$ is divergence-free, then there exists $\check{\boldsymbol{w}} \in \boldsymbol{H}_0(\mathbf{curl};\check{\Omega})$, unique up to a gradient, such that $\check{\boldsymbol{v}} = \check{\nabla}\times\check{\boldsymbol{w}}$;
4. The divergence operator $\check{\nabla}\cdot : \boldsymbol{H}_0(\mathrm{div};\check{\Omega}) \to L_0^2(\check{\Omega})$ is surjective.

Here we study a three-dimensional de Rham complex with additional smoothness so that it is suitable for the Stokes problem (25). To this end, we define

$$\boldsymbol{H}_0(\mathbf{curl};\check{\Omega}) := \{\boldsymbol{v} \in \boldsymbol{H}_0(\mathbf{curl};\check{\Omega}) :\ \check{\nabla}\times\boldsymbol{v} \in \boldsymbol{H}_0^1(\check{\Omega})\},$$

and consider the sequence of mappings (see [23])

$$0 \longrightarrow H_0^1(\check{\Omega}) \xrightarrow{\check{\nabla}} \boldsymbol{H}_0(\mathbf{curl};\check{\Omega}) \xrightarrow{\check{\nabla}\times} \boldsymbol{H}_0^1(\check{\Omega}) \xrightarrow{\check{\nabla}\cdot} L_0^2(\check{\Omega}) \longrightarrow 0. \tag{52}$$

Proposition 3.5.1. *If $\check{\Omega}$ is contractible, the sequence* (52) *is exact.*

Proof. Lemma 3.1.2 establishes that $\check{\nabla}\cdot : \boldsymbol{H}_0^1(\check{\Omega}) \to L_0^2(\check{\Omega})$ is surjective. Moreover, it is clear that if $\check{v} \in H_0^1(\check{\Omega})$ satisfies $\check{\nabla}\check{v} = 0$, then $v = 0$.

Now suppose that $\check{\boldsymbol{v}} \in \boldsymbol{H}_0(\mathbf{curl}; \check{\Omega})$ is curl–free. By the exactness of (51) and since $\boldsymbol{H}_0(\mathbf{curl}; \check{\Omega}) \subset \boldsymbol{H}_0(\mathbf{curl}; \check{\Omega})$, there exists a unique $\check{w} \in H_0^1(\check{\Omega})$ such that $\check{\boldsymbol{v}} = \check{\nabla}\check{w}$.

Now suppose that $\check{\boldsymbol{v}} \in \boldsymbol{H}_0^1(\check{\Omega}) \subset \boldsymbol{H}_0(\mathrm{div}; \check{\Omega})$ is divergence-free. Then again, by the exactness of (51) there exists $\check{\boldsymbol{w}} \in \boldsymbol{H}_0(\mathbf{curl}; \check{\Omega})$ such that $\check{\boldsymbol{v}} = \check{\nabla} \times \check{\boldsymbol{w}}$. This implies that $\check{\nabla} \times \check{\boldsymbol{w}} \in \boldsymbol{H}_0^1(\check{\Omega})$, and so $\check{\boldsymbol{w}} \in \boldsymbol{H}_0(\mathbf{curl}; \check{\Omega})$. This completes the proof. □

To draw connections between the three-dimensional complex (52) and a two-dimensional one defined on Ω, we first discuss an intermediary complex consisting of axisymmetric functions. In particular, we shall construct an analogous complex of (52) with axisymmetric function spaces. Motivated by Proposition 3.2.1, this will be done using "averaged pullback operators" defined as follows.

Definition 3.5.2.

1. We define $\boldsymbol{\phi} : \boldsymbol{L}^2(\check{\Omega}) \to \hat{\boldsymbol{L}}^2(\check{\Omega})$ such that

$$\boldsymbol{\phi}(\check{\boldsymbol{v}}) = \frac{1}{2\pi} \int_{-\pi}^{\pi} R_{-\eta} \check{\boldsymbol{v}} \circ R_\eta \, d\eta.$$

2. We define $\phi : L^2(\check{\Omega}) \to \hat{L}^2(\check{\Omega})$ such that

$$\phi(\check{q}) = \frac{1}{2\pi} \int_{-\pi}^{\pi} \check{q} \circ R_\eta \, d\eta.$$

Remark 3.5.3. It is clear from their definitions that $\boldsymbol{\phi}(\check{\boldsymbol{v}})$ and $\phi(\check{q})$ are axisymmetric, and if $\check{\boldsymbol{v}}$ and $\check{q}$ are axisymmetric, then $\boldsymbol{\phi}(\check{\boldsymbol{v}}) = \check{\boldsymbol{v}}$ and $\phi(\check{q}) = \check{q}$.

Lemma 3.5.4. *The operators $\phi, \boldsymbol{\phi}$ are idempotent. Moreover, there holds*

1. $\check{\nabla}\phi(\check{q}) = \boldsymbol{\phi}(\check{\nabla}\check{q})$.
2. $\check{\nabla} \times \boldsymbol{\phi}(\check{\boldsymbol{w}}) = \boldsymbol{\phi}(\check{\nabla} \times \check{\boldsymbol{w}})$.
3. $\check{\nabla} \cdot \boldsymbol{\phi}(\check{\boldsymbol{v}}) = \phi(\check{\nabla} \cdot \check{\boldsymbol{v}})$.

Proof. We assume that the functions $\check{q}$, $\check{\boldsymbol{w}}$, and $\check{\boldsymbol{v}}$ are smooth. The general setting may then be obtained by a standard density argument.

1. The chain rule shows that, for a fixed $\eta \in [-\pi, \pi]$,

$$\check{\nabla}\big(\check{q} \circ R_\eta\big) = R_\eta^{\intercal} \check{\nabla} \check{q} \circ R_\eta = R_{-\eta} \check{\nabla} \check{q} \circ R_\eta,$$

   and therefore

$$\check{\nabla} \phi(\check{q}) = \frac{1}{2\pi} \int_{-\pi}^{\pi} R_{-\eta} \check{\nabla} \check{q} \circ R_\eta \, d\eta = \boldsymbol{\phi}(\check{\nabla} \check{q}).$$

2. The chain rule shows that (cf. [50])

$$\begin{aligned} \check{\nabla} \times \big(R_{-\eta} \check{\boldsymbol{w}} \circ R_\eta\big) = \check{\nabla} \times (R_\eta^{\intercal} \check{\boldsymbol{w}} \circ R_\eta) &= \det(R_\eta) R_\eta^{-1} (\check{\nabla} \times \check{\boldsymbol{w}}) \circ R_\eta \\ &= R_{-\eta} (\check{\nabla} \times \check{\boldsymbol{w}}) \circ R_\eta, \end{aligned}$$

   and it readily follows that $\check{\nabla} \times \boldsymbol{\phi}(\check{\boldsymbol{w}}) = \boldsymbol{\phi}(\check{\nabla} \times \check{\boldsymbol{w}})$.

3. Let $\check{\boldsymbol{v}} \in \boldsymbol{L}^2(\check{\Omega})$. By [Lemma 3.59 in [50]], we conclude that

$$\check{\nabla} \cdot (R_{-\eta} \check{\boldsymbol{v}} \circ R_\eta) = (\check{\nabla} \cdot \check{\boldsymbol{v}}) \circ R_\eta,$$

   hence the result follows.

□

Theorem 3.5.5. *The diagram*

$$\begin{array}{ccccccccc} 0 & \longrightarrow & H_0^1(\check{\Omega}) & \xrightarrow{\check{\nabla}} & \boldsymbol{H}_0(\mathbf{curl}; \check{\Omega}) & \xrightarrow{\check{\nabla}\times} & \boldsymbol{H}_0^1(\check{\Omega}) & \xrightarrow{\check{\nabla}\cdot} & L_0^2(\check{\Omega}) & \longrightarrow & 0 \\ \downarrow & & \downarrow{\scriptstyle \phi} & & \downarrow{\scriptstyle \boldsymbol{\phi}} & & \downarrow{\scriptstyle \boldsymbol{\phi}} & & \downarrow{\scriptstyle \phi} & & \downarrow \\ 0 & \longrightarrow & \hat{H}_0^1(\check{\Omega}) & \xrightarrow{\check{\nabla}} & \hat{\boldsymbol{H}}_0(\mathbf{curl}; \check{\Omega}) & \xrightarrow{\check{\nabla}\times} & \hat{\boldsymbol{H}}_0^1(\check{\Omega}) & \xrightarrow{\check{\nabla}\cdot} & \hat{L}_0^2(\check{\Omega}) & \longrightarrow & 0 \end{array} \tag{53}$$

commutes. If $\check{\Omega}$ is contractible, then each horizontal sequence is exact.

Proof. The commutative property is established in Lemma 3.5.4.

If $\check{\Omega}$ is contractible, then the first horizontal sequence is exact (cf. Proposition 3.5.1). To prove exactness of the second sequence we show:

1. If $\check{q} \in \hat{H}_0^1(\check{\Omega})$ satisfies $\check{\nabla} \check{q} = 0$, then $\check{q} = 0$;
2. If $\check{\boldsymbol{w}} \in \hat{\boldsymbol{H}}_0(\mathbf{curl}; \check{\Omega})$ is curl-free, then $\check{\boldsymbol{w}} = \check{\nabla} \check{q}$ for some $\check{q} \in \hat{H}_0^1(\check{\Omega})$.
3. If $\check{\boldsymbol{v}} \in \hat{\boldsymbol{H}}_0^1(\check{\Omega})$ is divergence-free, then $\check{\boldsymbol{v}} = \check{\nabla} \times \check{\boldsymbol{w}}$ for some $\check{\boldsymbol{w}} \in \hat{\boldsymbol{H}}_0(\mathbf{curl}; \check{\Omega})$.
4. The divergence operator $\check{\nabla} \cdot : \hat{\boldsymbol{H}}_0^1(\check{\Omega}) \to \hat{L}_0^2(\check{\Omega})$ is surjective.

Property 1 is obvious. Moreover, 4 is shown in Proposition 3.4.1.

Now suppose that $\check{\boldsymbol{w}} \in \hat{\boldsymbol{H}}_0(\mathbf{curl};\check{\Omega}) \subset \boldsymbol{H}_0(\mathbf{curl};\check{\Omega})$ satisfies $\check{\nabla}\times\check{\boldsymbol{w}} = 0$. By the exactness of the first sequence, there exists $\check{q} \in H^1_0(\check{\Omega})$, not necessarily axisymmetric, such that $\check{\boldsymbol{w}} = \check{\nabla}\check{q}$. We then have $\phi(\check{q}) \in \hat{H}^1_0(\check{\Omega})$ and

$$\check{\nabla}\phi(\check{q}) = \boldsymbol{\phi}(\check{\nabla}\check{q}) = \boldsymbol{\phi}(\check{\boldsymbol{w}}) = \check{\boldsymbol{w}}.$$

This establishes 2.

Likewise, suppose that suppose $\check{\boldsymbol{v}} \in \hat{\boldsymbol{H}}^1_0(\check{\Omega})$ with $\check{\nabla}\cdot\check{\boldsymbol{v}} = 0$. Then the exactness of the first horizontal row in (53) implies the existence of $\check{\boldsymbol{w}} \in \boldsymbol{H}_0(\mathbf{curl};\check{\Omega})$ such that $\check{\boldsymbol{v}} = \check{\nabla}\times\check{\boldsymbol{w}}$. We then have $\boldsymbol{\phi}(\check{\boldsymbol{w}}) \in \hat{\boldsymbol{H}}_0(\mathbf{curl};\check{\Omega})$ and

$$\check{\nabla}\times\boldsymbol{\phi}(\check{\boldsymbol{w}}) = \boldsymbol{\phi}(\check{\nabla}\times\check{\boldsymbol{w}}) = \boldsymbol{\phi}(\check{\boldsymbol{v}}) = \check{\boldsymbol{v}}.$$

Thus, we have shown 3, and the proof is complete. □

3.5.1 Reduction operators

We define the following function space

$$W(\Omega) = \{w \in L^2_1(\Omega) : \frac{\partial w}{\partial z}, \frac{1}{r}\frac{\partial(rw)}{\partial r} \in H^1_{1,0}(\Omega), w_{|\Gamma} = 0\},$$

with norm

$$\|w\|_{W(\Omega)} = (\|w\|^2_{L^2_1(\Omega)} + \|\frac{\partial w}{\partial z}\|^2_{H^1_1(\Omega)} + \|\frac{1}{r}\frac{\partial(rw)}{\partial r}\|^2_{H^1_1(\Omega)})^{1/2}.$$

Observe that the space $W(\Omega)$ is defined so that it is isomorphic to the subspace of $\hat{\boldsymbol{H}}_0(\mathbf{curl};\check{\Omega})$ consisting of vector fields with zero radial and axial components. Indeed, if $\check{\boldsymbol{w}} \in \hat{\boldsymbol{H}}_0(\mathbf{curl};\check{\Omega})$ with $\bar{\boldsymbol{w}} = (0,\bar{w}_\theta,0)^\intercal$ then we have that

$$\begin{aligned}\check{\nabla}\times\check{\boldsymbol{w}} &= (\frac{1}{r}\frac{\partial\bar{w}_z}{\partial\theta} - \frac{\partial\bar{w}_\theta}{\partial z}, \frac{\partial\bar{w}_r}{\partial z} - \frac{\partial\bar{w}_z}{\partial r}, \frac{1}{r}(\frac{\partial(r\bar{w}_\theta)}{\partial r} - \frac{\partial\bar{w}_r}{\partial\theta}))^\intercal,\\ &= (-\frac{\partial\bar{w}_\theta}{\partial z}, 0, \frac{1}{r}\frac{\partial(r\bar{w}_\theta)}{\partial r})^\intercal.\end{aligned}$$

Since $\check{\boldsymbol{w}}\times\check{\boldsymbol{n}} = \mathbf{0}$ and $\check{\nabla}\times\check{\boldsymbol{w}} \in \boldsymbol{H}^1_0(\check{\Omega})$, we conclude that $\bar{w}_\theta \in L^2_1(\Omega)$ with $\bar{w}_\theta|_\Gamma = 0$, and $\frac{\partial\bar{w}_\theta}{\partial z}, \frac{1}{r}\frac{\partial(r\bar{w}_\theta)}{\partial r} \in H^1_{1,0}(\Omega)$.

Now, we inroduce some definitions. In what follows, $\boldsymbol{V}(\Omega)$ and $Q(\Omega)$ are given by (48).

Definition 3.5.6. Define

1. $\mathcal{T}_1 : \hat{\boldsymbol{H}}_0(\mathbf{curl};\check{\Omega}) \to W(\Omega)$ such that

$$(\mathcal{T}_1\check{\boldsymbol{w}})(r,z) = \bar{w}_\theta(r,0,z)$$

2. $\mathcal{T}_2 : \hat{\boldsymbol{H}}^1_0(\check{\Omega}) \to \boldsymbol{V}(\Omega)$ such that

$$(\mathcal{T}_2\check{\boldsymbol{v}})(r,z) = (\bar{v}_r(r,0,z), \bar{v}_z(r,0,z))^\intercal.$$

3. $\mathcal{T}_3 : \hat{L}^2_0(\check{\Omega}) \to Q(\Omega)$ such that

$$(\mathcal{T}_3\check{q})(r,z) = \bar{q}(r,0,z).$$

In addition, we define

$$\nabla_{rz} \times w = \begin{pmatrix} -\frac{\partial w}{\partial z} \\ \frac{1}{r}\frac{\partial (rw)}{\partial r} \end{pmatrix}.$$

Lemma 3.5.7. *There holds*

1. $\nabla_{rz} \times \mathcal{T}_1(\check{\boldsymbol{w}}) = \mathcal{T}_2(\check{\nabla} \times \check{\boldsymbol{w}})$ *for all* $\check{\boldsymbol{w}} \in \hat{\boldsymbol{H}}_0(\mathbf{curl};\check{\Omega})$;
2. $\nabla_{rz} \cdot \mathcal{T}_2(\check{\boldsymbol{v}}) = \mathcal{T}_3(\check{\nabla} \cdot \check{\boldsymbol{v}})$ *for all* $\check{\boldsymbol{v}} \in \hat{\boldsymbol{H}}^1_0(\check{\Omega})$.

Proof. By Proposition 3.3.1 we have

$$\begin{aligned} R_\theta \check{\nabla} \times \check{\boldsymbol{w}} &= \Big(\frac{1}{r}\frac{\partial \bar{w}_z}{\partial \theta} - \frac{\partial \bar{w}_\theta}{\partial z}, \frac{\partial \bar{w}_r}{\partial z} - \frac{\partial \bar{w}_z}{\partial r}, \frac{1}{r}\big(\frac{\partial (r\bar{w}_\theta)}{\partial r} - \frac{\partial \bar{w}_r}{\partial \theta}\big)\Big)^\intercal \\ &= \Big(-\frac{\partial \bar{w}_\theta}{\partial z}, \frac{\partial \bar{w}_r}{\partial z} - \frac{\partial \bar{w}_z}{\partial r}, \frac{1}{r}\frac{\partial (r\bar{w}_\theta)}{\partial r}\Big)^\intercal \end{aligned}$$

for all $\check{\boldsymbol{w}} \in \hat{\boldsymbol{H}}_0(\mathbf{curl};\check{\Omega})$. It then follows from the definition of $\mathcal{T}_2$, $\mathcal{T}_1$, and $\nabla_{rz}\times$ that

$$\mathcal{T}_2(\check{\nabla} \times \check{\boldsymbol{w}}) = = \Big(-\frac{\partial \bar{w}_\theta}{\partial z}, \frac{1}{r}\frac{\partial (r\bar{w}_\theta)}{\partial r}\Big)^\intercal = \nabla_{rz} \times \mathcal{T}_1(\check{\boldsymbol{w}}).$$

Finally, by (37) we have

$$\check{\nabla} \cdot \check{\boldsymbol{v}} = \frac{\partial \bar{v}_r}{\partial r} + \frac{\partial \bar{v}_z}{\partial z} + \frac{1}{r}\bar{v}_r,$$

and it readily follows that $\mathcal{T}_3(\check{\nabla} \cdot \check{\boldsymbol{v}}) = \nabla_{rz} \cdot \mathcal{T}_2(\check{\boldsymbol{v}})$. □

Theorem 3.5.8. *The following diagram is commutative. If $\check{\Omega}$ is contractible, then each horizontal sequence is exact.*

$$\begin{array}{ccccccccccc}
0 & \longrightarrow & H_0^1(\check{\Omega}) & \xrightarrow{\check{\nabla}} & \boldsymbol{H}_0(\mathbf{curl};\check{\Omega}) & \xrightarrow{\check{\nabla}\times} & \boldsymbol{H}_0^1(\check{\Omega}) & \xrightarrow{\check{\nabla}\cdot} & L_0^2(\check{\Omega}) & \longrightarrow & 0 \\
\downarrow & & \downarrow{\scriptstyle \phi} & & \downarrow{\scriptstyle \boldsymbol{\phi}} & & \downarrow{\scriptstyle \boldsymbol{\phi}} & & \downarrow{\scriptstyle \phi} & & \downarrow \\
0 & \longrightarrow & \hat{H}_0^1(\check{\Omega}) & \xrightarrow{\check{\nabla}} & \hat{\boldsymbol{H}}_0(\mathbf{curl};\check{\Omega}) & \xrightarrow{\check{\nabla}\times} & \hat{\boldsymbol{H}}_0^1(\check{\Omega}) & \xrightarrow{\check{\nabla}\cdot} & \hat{L}_0^2(\check{\Omega}) & \longrightarrow & 0 \\
\downarrow & & \downarrow & & \downarrow{\scriptstyle \mathcal{T}_1} & & \downarrow{\scriptstyle \mathcal{T}_2} & & \downarrow{\scriptstyle \mathcal{T}_3} & & \downarrow \\
0 & \longrightarrow & 0 & \longrightarrow & W(\Omega) & \xrightarrow{\nabla_{rz}\times} & \boldsymbol{V}(\Omega) & \xrightarrow{\nabla_{rz}\cdot} & Q(\Omega) & \longrightarrow & 0
\end{array}$$

Proof. The commutative property follows from Lemmas 3.5.4 and 3.5.7. The exactness of the first two horizontal sequences follow from Theorem 3.5.5.

Suppose that $w \in W(\Omega)$ is smooth enough with $\nabla_{rz} \times w = 0$. Observe that the rectangular vector representation of w is $\check{\boldsymbol{w}} = (\check{w}_1, \check{w}_2, 0)^\intercal$ with $w = \bar{w}_\theta = \check{w}_2 \cos(\theta) - \check{w}_1 \sin(\theta)$ and $0 = \bar{w}_r = \check{w}_1 \cos(\theta) + \check{w}_2 \sin(\theta)$. The equation $0 = \bar{w}_r$ yields $\check{w}_1 = -\tan(\theta)\check{w}_2$. Also, the normal vector reads $\check{\boldsymbol{n}} = (\hat{n}_1, 0, \hat{n}_3)^\intercal$ on Γ with $\hat{n}_1^2 + \hat{n}_3^2 = 1$. Hence, the condition $\check{\boldsymbol{w}} \times \check{\boldsymbol{n}} = 0$ gives us $(\check{w}_2\hat{n}_3, -\check{w}_1\hat{n}_3, -\check{w}_2\hat{n}_1) = (0,0,0)$. Hence, we conclude that either $\check{w}_1 = 0$ or $\check{w}_2 = 0$, and hence by the fact that $\check{w}_1 = -\tan(\theta)\check{w}_2$ we have that $w_{|\Gamma} = 0$.

By the definition of $\nabla_{rz}\times$, we conclude that $\frac{\partial w}{\partial z} = 0$ and hence $w(r,z) = w(r)$. Moreover, we have that $\frac{1}{r}\frac{\partial (rw)}{\partial r} = 0$ and hence $w = \frac{c}{r}$ for some constant c. But $w_{|\Gamma} = 0$, hence $w(r_0) = \frac{c}{r_0} = 0$ for some $r_0 > 0$. Hence, we conclude that $c = 0$ and we have that $w = 0$.

Now suppose that $\boldsymbol{v} \in \boldsymbol{V}(\Omega)$ with $\nabla_{rz} \cdot \boldsymbol{v} = 0$. Define $\check{\boldsymbol{v}} \in \hat{\boldsymbol{H}}_0^1(\check{\Omega})$ such that its cylindrical representation is $\bar{\boldsymbol{v}}(r,\theta,z) = (v_r(r,z), 0, v_z(r,z))^\intercal$, and note that $\mathcal{T}_2(\check{\boldsymbol{v}}) = \boldsymbol{v}$. We also have $\check{\nabla} \cdot \check{\boldsymbol{v}} = 0$ (cf. (37)), and so $\check{\boldsymbol{v}} = \check{\nabla} \times \check{\boldsymbol{w}}$ for some $\check{\boldsymbol{w}} \in \hat{\boldsymbol{H}}_0(\mathbf{curl};\Omega)$. Let $w = \mathcal{T}_1(\check{\boldsymbol{w}})$. Then Lemma 3.5.7 shows that

$$\nabla_{rz} \times w = \nabla_{rz} \times (\mathcal{T}_1(\check{\boldsymbol{w}})) = \mathcal{T}_2(\check{\nabla} \times \check{\boldsymbol{w}}) = \mathcal{T}_2(\check{\boldsymbol{v}}) = \boldsymbol{v}.$$

Finally, suppose that $q \in Q(\Omega)$, then there is $\check{q} \in \hat{L}_0^2(\check{\Omega})$ with $\mathcal{T}_3(\check{q}) = q$. Proposition 3.4.1 shows that there is $\check{\boldsymbol{v}} \in \hat{\boldsymbol{H}}_0^1(\hat{\Omega})$ with $\check{\nabla} \cdot \check{\boldsymbol{v}} = \check{q}$. Let $\boldsymbol{v} = \mathcal{T}_2(\check{\boldsymbol{v}})$. Then Lemma 3.5.7 shows that

$$\nabla_{rz} \cdot \boldsymbol{v} = \nabla_{rz} \cdot (\mathcal{T}_2(\check{\boldsymbol{v}})) = \mathcal{T}_3(\check{\nabla} \cdot \check{\boldsymbol{v}}) = \mathcal{T}_3(\check{q}) = q.$$

This completes the proof. □

4.0 CONNECTION BETWEEN GRAD-DIV STABILIZED STOKES FINITE ELEMENTS AND DIVERGENCE-FREE STOKES FINITE ELEMENTS

In this chapter, we use recently developed theories of divergence–free finite element schemes to analyze methods for the Stokes problem with grad-div stabilization. For example, we show that, if the polynomial degree is sufficiently large, the solutions of the Taylor–Hood finite element scheme with a grad-div stabilization term converges to an optimal convergence exactly divergence–free solution as the grad-div parameter tends to infinity. In addition, we introduce and analyze a stable first-order scheme that does not exhibit locking phenomenon for large grad-div parameters

4.1 Introduction

grad-div stabilization is a well-known and simple stabilization technique in numerical discretizations to improve mass conservation in simulations of incompressible flow. In its simplest form, the methodology adds the consistent term (written in strong form)

$$-\gamma\nabla(\nabla\cdot\boldsymbol{u})$$

to the momentum equations of the (Navier-)Stokes equations. Here, $\gamma > 0$ is a user-defined constant, which is referred to as the grad-div parameter. In addition to improving conservation of mass of the scheme, this stabilization technique may also improve the coupling errors of the velocity and pressure solutions. This can be advantageous for situations with large pressure gradients, e.g., in natural convection problems.

While enjoying many benefits, the use of grad-div stabilization comes with several practical disadvantages. These include a deterioration of the condition number and reduced sparsity of the algebraic system. Another disadvantage is the possible emergence of 'locking' for large grad-div parameters. Indeed, simply energy arguments show the discrete velocity

solution satisfies $\|\nabla \cdot \boldsymbol{u}_h\| = O(\gamma^{-1})$, and therefore, in the limiting case, the discrete solution is divergence–free. If the discrete divergence–free subspace does not have rich enough approximation properties, then grad-div stabilization, while improving mass conservation, may lead to poor approximations.

The stability and convergence analysis for grad-div stabilization for incompressible flow have been explored in, e.g., [54, 27, 28, 38, 2]. These estimates, together with numerical simulations, provide a guide to choose optimal γ-values. For example, references [53, 48, 54, 13] suggests $\gamma = O(1)$ as the optimal value. On the other hand, numerical experiments in [29] and the analysis in [38, 2] suggest that the optimal choice may be much larger and depend on the finite element spaces, the mesh, and/or the viscosity of the model.

In another direction, and the path taken in this chapter, is to identify and characterize the limiting solution as the grad-div parameter tends to infinity. For example, in [16, 46], it is shown that the Taylor–Hood finite element scheme on special (Clough-Tocher) triangulations, no locking occurs in the limiting case $\gamma \to \infty$, and the Taylor–Hood grad-div solution converges to the analogous (divergence–free) Scott–Vogelius solution.

The purpose of this chapter is to extend and generalize the results in [16] by incorporating the recent theories of divergence–free finite element Stokes pairs. In this regard, we make two main contributions. First we show the absence of locking for the two-dimensional Taylor–Hood pair for a general class of meshes. In particular, we show that high–order Taylor–Hood pairs are generally locking-free. In addition, we show that the limiting (Taylor-Hood) solutions converge to the solution of the divergence–free Scott-Vogelius scheme, defined on general triangulations. The second contribution of the chapter is the introduction and analysis of a new low–order and stable finite element pair that is locking–free. The velocity space is simply the linear Lagrange finite element space, and the pressure space consists of piecewise constants with respect to an auxiliary coarsened mesh.

The chapter is organized as follows. In the next section, we introduce the notation and a framework for the grad-div finite element method for the Stokes problem. We show that the discrete solutions converge to a solution of a divergence–free method with rate $O(\gamma^{-1})$. In Section 4.3, we apply this framework to the two-dimensional Taylor–Hood elements. The general theme of the results is that additional mesh constraints are imposed for lower degree

polynomial spaces. In Section 4.4, we define a stable first-order scheme for the Stokes problem, and show that the solutions converge to a divergence–free method as $\gamma \to \infty$. Finally, in Section 4.5 we provide some numerical experiments.

4.2 Notation and Framework

The Stokes equations defined on a polytope domain $\Omega \subset \mathbb{R}^2$ with Lipschitz continuous boundary $\partial\Omega$ is given by the system of equations

$$-\nu\Delta \boldsymbol{u} + \nabla p = \boldsymbol{f} \qquad \text{in } \Omega, \tag{54a}$$

$$\nabla \cdot \boldsymbol{u} = 0 \qquad \text{in } \Omega, \tag{54b}$$

$$\boldsymbol{u} = 0 \qquad \text{on } \partial\Omega, \tag{54c}$$

where the $\boldsymbol{u}$ is the velocity, p the pressure, and ∇, Δ denote the gradient operator and vector Laplacian operators, respectively. In (54a), ν is the viscosity.

We define the following function spaces on Ω:

$$L^2(\Omega) := \{w : \Omega \mapsto \mathbb{R} : \ \|w\|_{L^2(\Omega)} := (\int_\Omega |w|^2\, dx)^{1/2} < \infty\},$$
$$H^m(\Omega) := \{w : \Omega \mapsto \mathbb{R} : \ \|w\|_{H^m(\Omega)} := (\sum_{|\beta|\le m} \|D^\beta w\|^2_{L^2(\Omega)})^{1/2} < \infty\},$$

and set $(\cdot,\cdot)$ denote the inner product on $L^2(\Omega)$ and set $\|\cdot\| = \|\cdot\|_{L^2(\Omega)}$. The analogous spaces with boundary conditions are given by

$$L^2_0(\Omega) := \{w \in L^2(\Omega) : \ \int_\Omega w\, dx = 0\},$$
$$H^m_0(\Omega) := \{w \in H^m(\Omega) : \ D^\beta w|_{\partial\Omega} = 0, \forall \beta : \ |\beta| \le m-1\}.$$

We denote the analogous vector-valued function spaces in boldface; for example $\boldsymbol{H}^1(\Omega) = H^1(\Omega)^2$ and $\boldsymbol{L}^2(\Omega) = L^2(\Omega)^2$. We also define the space of $\boldsymbol{H}^1_0(\Omega)$ divergence–free vector fields

$$\boldsymbol{V} := \{\boldsymbol{v} \in \boldsymbol{H}^1_0(\Omega) : (\nabla \cdot \boldsymbol{v}, q) = 0, \forall q \in L^2_0(\Omega)\}.$$

The weak formulation for (54) reads: Find $(\boldsymbol{u}, p) \in \boldsymbol{H}_0^1(\Omega) \times L_0^2(\Omega)$ such that $\forall (\boldsymbol{v}, q) \in \boldsymbol{H}_0^1(\Omega) \times L_0^2(\Omega)$ we have

$$\nu(\nabla \boldsymbol{u}, \nabla \boldsymbol{v}) - (\nabla \cdot \boldsymbol{v}, p) = (\boldsymbol{f}, \boldsymbol{v}), \tag{55a}$$

$$(\nabla \cdot \boldsymbol{u}, q) = 0. \tag{55b}$$

It was shown in the previous chapter that problem (55) has a unique solution [30].

Let $\boldsymbol{X}_h \times Y_h \subset \boldsymbol{H}_0^1(\Omega) \times L_0^2(\Omega)$ be a conforming finite element pair with respect to mesh parameter $h > 0$. For each such a pair, we define the space of discretely divergence–free vector fields as follows

$$\boldsymbol{V}_h := \{\boldsymbol{v} \in \boldsymbol{X}_h : (\nabla \cdot \boldsymbol{v}, q_h) = 0, \forall q_h \in Y_h\}.$$

We note, for many finite element pairs, there holds the non–inclusion $\boldsymbol{V}_h \not\subset \boldsymbol{V}$.

The discrete Stokes problem corresponding to the pair $\boldsymbol{X}_h \times Y_h$ reads: Find $(\boldsymbol{u}_h, p_h) \in \boldsymbol{X}_h \times Y_h$ such that $\forall (\boldsymbol{v}, q) \in \boldsymbol{X}_h \times Y_h$ we have

$$\nu(\nabla \boldsymbol{u}_h, \nabla \boldsymbol{v}) - (\nabla \cdot \boldsymbol{v}, p_h) = (\boldsymbol{f}, \boldsymbol{v}), \tag{56a}$$

$$(\nabla \cdot \boldsymbol{u}_h, q) = 0. \tag{56b}$$

Problem (56) has a unique solution provided that the pair $\boldsymbol{X}_h \times Y_h$ satisfies the inf-sup condition, that is, there exists a constant $\beta > 0$ independent of the mesh parameter h such that

$$\sup_{\boldsymbol{v} \in \boldsymbol{X}_h \setminus \{0\}} \frac{(\nabla \cdot \boldsymbol{v}, q)}{\|\nabla \boldsymbol{v}\|} \geq \beta \|q\| \qquad \forall q \in Y_h. \tag{57}$$

We introduce the corresponding grad-div stabilized problem, which reads: For given $\gamma \in \mathbb{R}$ with $\gamma > 0$, find $(\boldsymbol{u}_h^\gamma, p_h^\gamma) \in \boldsymbol{X}_h \times Y_h$ such that $\forall (\boldsymbol{v}, q) \in \boldsymbol{X}_h \times Y_h$ we have

$$\nu(\nabla \boldsymbol{u}_h^\gamma, \nabla \boldsymbol{v}) + \gamma(\nabla \cdot \boldsymbol{u}_h^\gamma, \nabla \cdot \boldsymbol{v}) - (\nabla \cdot \boldsymbol{v}, p_h^\gamma) = (\boldsymbol{f}, \boldsymbol{v}), \tag{58a}$$

$$(\nabla \cdot \boldsymbol{u}_h^\gamma, q) = 0. \tag{58b}$$

Again, standard arguments show that (58) is well-posed provided the inf-sup condition (57) is satisfied. Adding the term $\gamma(\nabla \cdot \boldsymbol{u}_h^\gamma, \nabla \cdot \boldsymbol{v}_h)$ improves mass conservation and can reduce the effect of the pressure error on the velocity approximation. The limiting case $\gamma \to \infty$ is studied in the following two theorems.

Theorem 4.2.1. *Let $\boldsymbol{X}_h \times Y_h$ be a conforming finite element pair satisfying the inf-sup condition. Let $\{\gamma_i\}_{i=1}^{\infty} \subset \mathbb{R}$ with $\gamma_i \to \infty$, and let $(\boldsymbol{u}_i, p_i) \in \boldsymbol{X}_h \times Y_h$ be the solution for (58) corresponding to γ_i. Then the sequence $\{\boldsymbol{u}_i\}_{i=1}^{\infty} \subset \boldsymbol{X}_h$ converges to some $\boldsymbol{w}_h \in \boldsymbol{X}_h \cap \boldsymbol{V}$. Moreover,*

$$\|\nabla(\boldsymbol{u} - \boldsymbol{w}_h)\| = \inf_{\boldsymbol{v} \in \boldsymbol{X}_h \cap \boldsymbol{V}} \|\nabla(\boldsymbol{u} - \boldsymbol{v})\|. \tag{59}$$

Proof. We follow the ideas in [16, Theorem 3.1] and begin with an a priori bound which is obtained by taking $\boldsymbol{v} = \boldsymbol{u}_i$ and $q = p_i$ in (58):

$$\nu\|\nabla \boldsymbol{u}_i\|^2 + \gamma_i\|\nabla \cdot \boldsymbol{u}_i\|^2 = |(\boldsymbol{f}, \boldsymbol{u}_i)|. \tag{60}$$

Thus, we have the following inequality

$$\nu\|\nabla \boldsymbol{u}_i\| \leq \|\boldsymbol{f}\|_{*,h} \quad \forall i \in \mathbb{N},$$

where $\|\boldsymbol{f}\|_{*,h} = \sup_{\boldsymbol{v} \in \boldsymbol{X}_h \setminus \{0\}} \frac{|(\boldsymbol{f}, \boldsymbol{v})|}{\|\nabla \boldsymbol{v}\|}$. The above inequality shows that the sequence $\{\boldsymbol{u}_i\}_{i=1}^{\infty}$ is a uniformly bounded sequence in the finite dimensional space $\boldsymbol{X}_h$. Hence, $\{\boldsymbol{u}_i\}_{i=1}^{\infty}$ has a convergent subsequence $\{\boldsymbol{u}_{i_j}\}_j$ that converges to some $\boldsymbol{w}_h \in \boldsymbol{X}_h$.

To show $\boldsymbol{w}_h \in \boldsymbol{V}$, i.e., $\nabla \cdot \boldsymbol{w}_h = 0$, we use (60) and the Cauchy-Schwarz inequality to obtain

$$\|\nabla \cdot \boldsymbol{u}_{i_j}\| \leq \frac{1}{\sqrt{2\nu\gamma_{i_j}}}\|\boldsymbol{f}\|_{*,h} \quad \forall j \in \mathbb{N}. \tag{61}$$

Because $\|\nabla \cdot \boldsymbol{v}\| \leq \sqrt{2}\|\nabla \boldsymbol{v}\|$ for all $\boldsymbol{v} \in \boldsymbol{H}_0^1(\Omega)$ and $\boldsymbol{u}_{i_j} \to \boldsymbol{w}_h$, it follows that

$$\begin{aligned}
\|\nabla \cdot \boldsymbol{w}_h\| &= \|\nabla \cdot (\boldsymbol{w}_h - \boldsymbol{u}_{i_j} + \boldsymbol{u}_{i_j})\| \\
&\leq \|\nabla \cdot (\boldsymbol{w}_h - \boldsymbol{u}_{i_j})\| + \|\nabla \cdot \boldsymbol{u}_{i_j}\| \\
&\leq \sqrt{2}\|\nabla(\boldsymbol{w}_h - \boldsymbol{u}_{i_j})\| + \frac{1}{\sqrt{2\nu\gamma_{i_j}}}\|\boldsymbol{f}\|_{*,h} \to 0 \text{ as } j \to \infty.
\end{aligned}$$

Hence, we conclude that $\|\nabla \cdot \boldsymbol{w}_h\| = 0$, and so $\boldsymbol{w}_h \in \boldsymbol{V}$.

To show the estimate (59) and the uniqueness of $\boldsymbol{w}_h$, we observe that for $\boldsymbol{v} \in \boldsymbol{X}_h \cap \boldsymbol{V}$ we have

$$\begin{aligned}\nu(\nabla \boldsymbol{w}_h, \nabla \boldsymbol{v}) - (\boldsymbol{f}, \boldsymbol{v}) &= \lim_{j\to\infty} \nu(\nabla \boldsymbol{u}_{i_j}, \nabla \boldsymbol{v}) + \lim_{j\to\infty} \gamma_{i_j}(\nabla \cdot \boldsymbol{u}_{i_j}, \nabla \cdot \boldsymbol{v}) - (\boldsymbol{f}, \boldsymbol{v}) \\ &= \lim_{j\to\infty} (\nu(\nabla \boldsymbol{u}_{i_j}, \nabla \boldsymbol{v}) + \gamma_{i_j}(\nabla \cdot \boldsymbol{u}_{i_j}, \nabla \cdot \boldsymbol{v}) - (\boldsymbol{f}, \boldsymbol{v})) \\ &= 0.\end{aligned}$$

Hence, $\boldsymbol{w}_h$ satisfies

$$\nu(\nabla \boldsymbol{w}_h, \nabla \boldsymbol{v}) = (\boldsymbol{f}, \boldsymbol{v}) \qquad \forall \boldsymbol{v} \in \boldsymbol{X}_h \cap \boldsymbol{V}, \tag{62}$$

and (59) immediately follows by Cea's lemma.

By the Lax-Milgram theorem, problem (62) has a unique solution. If $\{\boldsymbol{u}_{i_k}\}_k$ is another convergent subsequence of $\{\boldsymbol{u}_i\}_{i=1}^{\infty}$ that converges to some $\boldsymbol{z}_h \in \boldsymbol{X}_h$, then $\boldsymbol{z}_h$ is a solution to the problem (62). Since the problem (62) has a unique solution, we conclude that $\boldsymbol{w}_h = \boldsymbol{z}_h$, which means any convergent subsequence of $\{\boldsymbol{u}_i\}_{i=1}^{\infty}$ converges to the same element in $\boldsymbol{X}_h$. Hence the entire sequence $\{\boldsymbol{u}_i\}_{i=1}^{\infty}$ converges to $\boldsymbol{w}_h$. □

Theorem 4.2.2. *Suppose that the conditions of Theorem 4.2.1 are satisfied. Set*

$$Q_h := \nabla \cdot \boldsymbol{X}_h = \{\nabla \cdot \boldsymbol{v} : \ \boldsymbol{v} \in \boldsymbol{X}_h\},$$

and suppose that $Y_h \subset Q_h$ and $\boldsymbol{X}_h \times Q_h$ is an inf-sup stable pair, i.e.,

$$\sup_{\boldsymbol{v}\in\boldsymbol{X}_h\setminus\{0\}} \frac{(\nabla \cdot \boldsymbol{v}, q)}{\|\nabla \boldsymbol{v}\|} \geq \beta_Q \|q\| \qquad \forall q \in Q_h, \quad \exists \beta_Q > 0. \tag{63}$$

Then the sequence $\{(\boldsymbol{u}_i, p_i - \gamma_i \nabla \cdot \boldsymbol{u}_i)\}_{i=1}^{\infty} \subset \boldsymbol{X}_h \times Q_h$ converges to $(\boldsymbol{w}_h, p_h) \in (\boldsymbol{X}_h \cap \boldsymbol{V}) \times Q_h$ satisfying

$$\nu(\nabla \boldsymbol{w}_h, \nabla \boldsymbol{v}) - (\nabla \cdot \boldsymbol{v}, p_h) = (\boldsymbol{f}, \boldsymbol{v}) \qquad \forall \boldsymbol{v} \in \boldsymbol{X}_h, \tag{64a}$$

$$(\nabla \cdot \boldsymbol{w}_h, q) = 0 \qquad \forall q \in Q_h. \tag{64b}$$

There also holds

$$\begin{aligned}\beta_Q^2 \nu^{-1} \|p_h - (p_i - \gamma_i \nabla \cdot \boldsymbol{u}_i)\| &\leq \beta_Q \|\nabla(\boldsymbol{w}_h - \boldsymbol{u}_i)\| \\ &\leq \|\nabla \cdot \boldsymbol{u}_i\| \leq \min\{2\beta_Q^{-1}\gamma_i^{-1}, (2\nu\gamma_i)^{-1/2}\} \|\boldsymbol{f}\|_{*,h}.\end{aligned} \tag{65}$$

Proof. The convergence $\boldsymbol{u}_i \to \boldsymbol{w}_h$ for some $\boldsymbol{w}_h \in \boldsymbol{X}_h \cap \boldsymbol{V}$ is established in Theorem 4.2.1. Since $\boldsymbol{w}_h$ is divergence–free, it clearly satisfies (64b).

To show the convergence of the modified pressure sequence, we first use with the inf-sup condition for the pair $\boldsymbol{X}_h \times Q_h$ (63) and the inclusion $Y_h \subset Q_h$ to obtain

$$\begin{aligned}\beta_Q \|p_i - \gamma_i \nabla \cdot \boldsymbol{u}_i\| &\leq \sup_{\boldsymbol{v} \in \boldsymbol{X}_h \setminus \{0\}} \frac{-(\nabla \cdot \boldsymbol{v}, p_i) + \gamma_i (\nabla \cdot \boldsymbol{u}_i, \nabla \cdot \boldsymbol{v})}{\|\nabla \boldsymbol{v}\|} \\ &= \frac{(\boldsymbol{f}, \boldsymbol{v}) - \nu (\nabla \boldsymbol{u}_i, \nabla \boldsymbol{v})}{\|\nabla \boldsymbol{v}\|} \leq \|\boldsymbol{f}\|_{*,h} + \nu \|\nabla \boldsymbol{u}_i\|.\end{aligned}$$

Thus, $\{p_i - \gamma_i \nabla \cdot \boldsymbol{u}_i\}_{i=1}^{\infty} \subset Q_h$ is a bounded sequence, and thus has a convergent subsequence: $p_{i_j} - \gamma_{i_j} \nabla \cdot \boldsymbol{u}_{i_j} \to p_h$ for some $p_h \in Q_h$. We then find that, for any $\boldsymbol{v} \in \boldsymbol{X}_h$,

$$\begin{aligned}(\nabla \boldsymbol{w}_h, \nabla \boldsymbol{v}) - (\nabla \cdot \boldsymbol{v}, p_h) &= \lim_{j \to \infty} \big((\nabla \boldsymbol{u}_{i_j}, \nabla \boldsymbol{v}) - (p_{i_j}, \nabla \cdot \boldsymbol{v}) + \gamma_{i_j} (\nabla \cdot \boldsymbol{u}_{i_j}, \nabla \cdot \boldsymbol{v}) \big) \\ &= (\boldsymbol{f}, \boldsymbol{v}).\end{aligned}$$

We conclude that $(\boldsymbol{w}_h, p_h) \in \boldsymbol{X}_h \times Q_h$ satisfies (64). The convergence of the entire sequence $\{(\boldsymbol{u}_i, p_i - \gamma_i \nabla \cdot \boldsymbol{u}_i)\}_{i=1}^{\infty}$ follows directly from the arguments in Theorem 4.2.1.

Next we establish the rate of convergence given in (65). As a first step, we first note that $\|\nabla \boldsymbol{w}_h\| \leq \nu^{-1} \|f\|_{*,h}$. Consequently, by the inf–sup condition (63),

$$\beta_Q \|p_h\| \leq \sup_{\boldsymbol{v} \in \boldsymbol{X}_h \setminus \{0\}} \frac{(\nabla \cdot \boldsymbol{v}, p_h)}{\|\nabla \boldsymbol{v}\|} = \sup_{\boldsymbol{v} \in \boldsymbol{X}_h \setminus \{0\}} \frac{(\boldsymbol{f}, \boldsymbol{v}) - \nu (\nabla \boldsymbol{w}_h, \nabla \boldsymbol{v})}{\|\nabla \boldsymbol{v}\|} \leq 2 \|\boldsymbol{f}\|_{*,h}. \tag{66}$$

Write $\boldsymbol{e}_i = \boldsymbol{w}_h - \boldsymbol{u}_i \in \boldsymbol{V}_h$ and note that

$$\nu (\nabla \boldsymbol{e}_i, \nabla \boldsymbol{v}) - (p_h - p_i, \nabla \cdot \boldsymbol{v}) + \gamma_i (\nabla \cdot \boldsymbol{e}_i, \nabla \cdot \boldsymbol{v}) = 0 \qquad \forall \boldsymbol{v} \in \boldsymbol{X}_h. \tag{67}$$

Consequently, by setting $\boldsymbol{v} = \boldsymbol{e}_i$ and using $\nabla \cdot \boldsymbol{w}_h = 0$, we find

$$\nu \|\nabla \boldsymbol{e}_i\|^2 + \gamma_i \|\nabla \cdot \boldsymbol{u}_i\|^2 = (\nabla \cdot \boldsymbol{e}_i, p_h - p_i) = (\nabla \cdot \boldsymbol{e}_i, p_h) \leq \|\nabla \cdot \boldsymbol{u}_i\| \|p_h\|.$$

Therefore by (66),

$$\|\nabla \cdot \boldsymbol{u}_i\| \leq \frac{2}{\gamma_i \beta_Q} \|\boldsymbol{f}\|_{*,h}.$$

Combined with (61), this establishes the last inequality in (65).

To derive a convergence rate for $\|\nabla \boldsymbol{e}_i\|$ with respect to γ_i, we introduce the space

$$\boldsymbol{R}_h = (\boldsymbol{X}_h \cap \boldsymbol{V})^{\perp} = \{\boldsymbol{v} \in \boldsymbol{X}_h : \ (\nabla \boldsymbol{v}, \nabla \boldsymbol{w}) = 0 \ \forall \boldsymbol{w} \in \boldsymbol{X}_h \cap \boldsymbol{V}\}.$$

Because $\boldsymbol{X}_h \cap \boldsymbol{V} = \{\boldsymbol{v} \in \boldsymbol{X}_h : \ (\nabla \cdot \boldsymbol{v}, q) = 0, \forall q \in Q_h\}$, and $\boldsymbol{X}_h \times Y_h$ is assumed to be inf-sup stable, there holds [45]

$$\|\nabla \boldsymbol{v}\| \leq \beta_Q^{-1} \|\nabla \cdot \boldsymbol{v}\| \qquad \forall \boldsymbol{v} \in \boldsymbol{R}_h. \tag{68}$$

Write $\boldsymbol{e}_i = \boldsymbol{e}_i^0 + \boldsymbol{e}_i^R$ with $\boldsymbol{e}_i^0 \in \boldsymbol{X}_h \cap \boldsymbol{V}$ and $\boldsymbol{e}_i^R \in \boldsymbol{R}_h$. Because $\|\nabla \boldsymbol{e}_i\|^2 = \|\nabla \boldsymbol{e}_i^0\|^2 + \|\nabla \boldsymbol{e}^R\|^2$ and $\nabla \cdot \boldsymbol{e}_i^0 = 0$, there holds by (68)

$$\|\nabla \boldsymbol{e}_i^R\| \leq \beta_Q^{-1} \|\nabla \cdot \boldsymbol{e}_i^R\| = \beta_Q^{-1} \|\nabla \cdot \boldsymbol{e}_i\| = \beta_Q^{-1} \|\nabla \cdot \boldsymbol{u}_i\|.$$

On the other hand, by taking $\boldsymbol{v} = \boldsymbol{e}_i^0 \in \boldsymbol{X}_h \cap \boldsymbol{V}$ in (67), we get

$$\begin{aligned} 0 &= \nu(\nabla \boldsymbol{e}_i, \nabla \boldsymbol{e}_i^0) - (p_h - p_i, \nabla \cdot \boldsymbol{e}_i^0) + \gamma_i (\nabla \cdot \boldsymbol{e}_i, \nabla \cdot \boldsymbol{e}_i^0) \\ &= \nu(\nabla \boldsymbol{e}_i^R, \nabla \boldsymbol{e}_i^0) + \nu \|\nabla \boldsymbol{e}_i^0\|^2 = \nu \|\nabla \boldsymbol{e}_i^0\|^2. \end{aligned}$$

Thus $\boldsymbol{e}_i^0 \equiv 0$, and therefore

$$\|\nabla \boldsymbol{e}_i\| = \|\nabla \boldsymbol{e}_i^R\| \leq \beta_Q^{-1} \|\nabla \cdot \boldsymbol{u}_i\|.$$

Finally, we use the inf-sup condition on $\boldsymbol{X}_h \times Q_h$ to derive the convergence rate of the modified pressure equation as follows:

$$\begin{aligned} \beta_Q \|p_h - (p_i - \gamma_i \nabla \cdot \boldsymbol{u}_i)\| &\leq \sup_{\boldsymbol{v} \in \boldsymbol{X}_h \setminus \{0\}} \frac{(\nabla \cdot \boldsymbol{v}, p_h) - (\nabla \cdot \boldsymbol{v}, p_i) + \gamma_i (\nabla \cdot \boldsymbol{u}_i, \nabla \cdot \boldsymbol{v})}{\|\nabla \boldsymbol{v}\|} \\ &= \sup_{\boldsymbol{v} \in \boldsymbol{X}_h \setminus \{0\}} \frac{-\nu(\nabla \boldsymbol{e}_i, \nabla \boldsymbol{v})}{\|\nabla \boldsymbol{v}\|} \leq \nu \|\nabla \boldsymbol{e}_i\|. \end{aligned}$$

□

Remark 4.2.3. Since $\boldsymbol{w}_h \in \boldsymbol{X}_h \cap \boldsymbol{V}$, the error $\|\nabla(\boldsymbol{u} - \boldsymbol{u}_i)\|$ can be decomposed as follows

$$\begin{aligned}\|\nabla(\boldsymbol{u} - \boldsymbol{u}_i)\| &= \|\nabla(\boldsymbol{u} - \boldsymbol{w}_h + \boldsymbol{w}_h - \boldsymbol{u}_i)\| \\ &\leq \|\nabla(\boldsymbol{u} - \boldsymbol{w}_h)\| + \|\nabla \boldsymbol{e}_i\| \\ &\leq \inf_{\boldsymbol{v} \in \boldsymbol{V} \cap \boldsymbol{X}_h} \|\nabla(\boldsymbol{u} - \boldsymbol{v})\| + \frac{2}{\beta_Q^2 \gamma_i} \|\boldsymbol{f}\|_{*,h}.\end{aligned}$$

Since the pair $\boldsymbol{X}_h \times Q_h$ is inf-sup stable, we have by [15, Theorem 12.5.17] to get the estimate

$$\|\nabla(\boldsymbol{u} - \boldsymbol{u}_i)\| \leq \left(1 + \frac{C}{\beta_Q}\right) \inf_{\boldsymbol{v} \in \boldsymbol{X}_h} \|\nabla(\boldsymbol{u} - \boldsymbol{v})\| + \frac{2}{\beta_Q^2 \gamma_i} \|\boldsymbol{f}\|_{*,h}, \tag{69}$$

where $C > 0$ is a constant independent of h, β_Q and γ_i.

For comparison, the following estimate for grad-div stabilized finite element methods for the Stokes problem was derived in [38]:

$$\|\nabla(\boldsymbol{u} - \boldsymbol{u}_i)\|^2 \leq \inf_{\boldsymbol{v} \in \boldsymbol{V}_h} \left(4\|\nabla(\boldsymbol{u} - \boldsymbol{v})\|^2 + 2\frac{\gamma_i}{\nu}\|\nabla \cdot \boldsymbol{v}\|^2\right) + \frac{2}{\nu \gamma_i} \inf_{q_h \in Y_h} \|p_h - q_h\|^2, \tag{70}$$

Note that

$$\begin{aligned}\inf_{\boldsymbol{v} \in \boldsymbol{V}_h} \left(4\|\nabla(\boldsymbol{u} - \boldsymbol{v})\|^2 + 2\frac{\gamma_i}{\nu}\|\nabla \cdot \boldsymbol{v}\|^2\right) &\leq \inf_{\boldsymbol{v} \in \boldsymbol{X}_h \cap \boldsymbol{V}} \left(4\|\nabla(\boldsymbol{u} - \boldsymbol{v})\|^2 + 2\frac{\gamma_i}{\nu}\|\nabla \cdot \boldsymbol{v}\|^2\right) \\ &\leq \left(1 + \frac{C}{\beta_Q}\right) \inf_{\boldsymbol{v} \in \boldsymbol{X}_h} \|\nabla(\boldsymbol{u} - \boldsymbol{v})\|\end{aligned}$$

for a generally different constant $C > 0$. Thus, we see that the first term in the right-hand side of (70) is sharper than the analogous term in (69). On the other hand, unlike estimate (70), the bound (69) does not depend on ν. Thus, we conclude that the estimate (69) can be sharper than the estimate (70) for small values of ν.

4.3 Application I: Taylor–Hood Pairs

In this section, we apply Theorem 4.2.2 to the two–dimensional Taylor–Hood pair and show, under assumptions of the mesh and the polynomial degree, the Taylor–Hood finite element method with grad-div stabilization does not experience locking in the limit $\gamma \to \infty$. To proceed, we require some additional notation.

Denote by $\mathcal{T}_h$ a conforming, shape–regular, simplicial triangulation of $\Omega \subset \mathbb{R}^2$. For $\tau \in \mathcal{T}_h$, we denote by $h_\tau = \operatorname{diam}(\tau)$ and set $h = \max_{\tau \in \mathcal{T}_h} h_\tau$. Let $\mathcal{V}_h^I$ and $\mathcal{V}_h^B$ denote the sets of interior and boundary vertices of $\mathcal{T}_h$, respectively, and set $\mathcal{V}_h = \mathcal{V}_h^I \cup \mathcal{V}_h^B$.

Let $\mathcal{P}_k(S)$ denote the space of polynomials of degree $\leq k$ with domain S; the analogous vector-valued space is denoted by $\boldsymbol{\mathcal{P}}_k(S) := [\mathcal{P}_k(S)]^2$. We define the piecewise polynomials with respect to the mesh $\mathcal{T}_h$ as

$$\mathcal{P}_k(\mathcal{T}_h) := \prod_{\tau \in \mathcal{T}_h} \mathcal{P}_k(\tau).$$

For an integer $k \geq 2$, the Taylor–Hood pair is given as

$$\begin{aligned} \boldsymbol{X}_h^{TH} &= \boldsymbol{\mathcal{P}}_k(\mathcal{T}_h) \cap \boldsymbol{H}_0^1(\Omega), \\ Y_h^{TH} &= \mathcal{P}_{k-1}(\mathcal{T}_h) \cap H^1(\Omega) \cap L_0^2(\Omega). \end{aligned}$$

We also define the image of the divergence acting on the Taylor–Hood velocity space:

$$Q_h^{TH} := \nabla \cdot \boldsymbol{X}_h^{TH} = \{\nabla \cdot \boldsymbol{v} : \boldsymbol{v} \in \boldsymbol{X}_h^{TH}\}. \tag{71}$$

It is well known that the pair $\boldsymbol{X}^{TH} \times Y_h^{TH}$ is inf–sup stable provided that each $\tau \in \mathcal{T}_h$ has at most one boundary edge [10]. We assume this mild condition is satisfied throughout this section.

To apply Theorem 4.2.2 to the Taylor–Hood pair, we split the results into three cases, depending on the polynomial degree: $k \geq 4$, $k = 3$, and $k = 2$. The general theme is that additional mesh conditions are introduced for lower degree polynomial spaces.

4.3.1 High order pairs: $k \geq 4$

To apply Theorem 4.2.2 on the Taylor–Hood pair for $k \geq 4$, we need to establish the inf–sup stability of the pair $\boldsymbol{X}_h^{TH} \times Q_h^{TH}$. To do so, following the notation introduced in [37], we introduce the concept of a singular vertex and the vertex singularity of a mesh.

For $z \in \mathcal{V}_h$, let $\mathcal{T}_z \subset \mathcal{T}_h$ denote the set of triangles that have z as a vertex. We assume that $\mathcal{T}_z = \{\tau_1, \ldots, \tau_N\}$, enumerating such that τ_j and τ_{j+1} share an edge for $j = 1, \ldots, N-1$, and if z is an interior vertex, then τ_1 and τ_N share an edge. Letting θ_j denote the angle between the angle between the edges of τ_j originating from z, we define

$$\Theta_z := \begin{cases} \max\{|\sin(\theta_1 + \theta_2)|, \ldots, |\sin(\theta_{N-1} + \theta_N)|, |\sin(\theta_1 + \theta_N)|\} & \text{if } z \in \mathcal{V}_h^I, \\ \max\{|\sin(\theta_1 + \theta_2)|, \ldots, |\sin(\theta_{N-1} + \theta_N)|\} & \text{if } z \in \mathcal{V}_h^B. \end{cases}$$

Definition 4.3.1.

1. We say that a vertex z is *singular* if $\Theta_z = 0$; otherwise we say that z is *non–singular*.
2. The *measure of vertex singularity* of the mesh is given by the positive number

$$\Theta_* := \min_{\substack{z \in \mathcal{V}_h \\ \Theta_z \neq 0}} \Theta_z > 0.$$

Remark 4.3.2. An interior vertex is singular if and only if exactly two straight lines emanating from the vertex (and hence $N = 4$ in this case). A non–corner boundary vertex z is singular if exactly two triangles have z as a vertex. Finally, a corner (boundary) vertex z is singular if only one triangle in $\mathcal{T}_h$ has z as a vertex. Note that, because we assumed that each $\tau \in \mathcal{T}_h$ has at most one boundary edge, there exists no corner singular vertices.

The quantity Θ_z gives an indication on "how close" a non–singular vertex z is from being singular. Essentially, if Θ_* is small, then there exists a vertex in $\mathcal{T}_h$ that is a small perturbation of a singular vertex. Note that if the cardinality of $\mathcal{T}_z$ is greater than 4 for all $z \in \mathcal{V}_h^I$, and greater than 2 for all $z \in \mathcal{V}_h^B$, then Θ_* is uniformly bounded from below.

Let

$$\mathcal{S}_h = \{z \in \mathcal{V}_h : \ \Theta_z = 0\}$$

denote the set of singular vertices in the mesh $\mathcal{T}_h$. A characterization of the divergence operator acting on the Taylor–Hood velocity space is given in the next lemma for high–order pairs. Its proof is found in [37, 58].

Lemma 4.3.3. *Suppose that $k \geq 4$. Then there holds*

$$Y_h^{TH} \subset Q_h^{TH} := \nabla \cdot \boldsymbol{X}_h^{TH} = \{q \in \mathcal{P}_{k-1}(\mathcal{T}_h) \cap L_0^2(\Omega) : \ \sum_{\ell=1}^{N} (-1)^\ell q|_{\tau_\ell}(z) = 0 \ \forall z \in \mathcal{S}_h\}.$$

Moreover, $\boldsymbol{X}_h^{TH} \times Q_h^{TH}$ represents an inf-sup stable pair with inf-sup constant β_Q independent of size of the triangles in $\mathcal{T}_h$. Rather, $\beta_Q = C\Theta_*$ for some h-independent constant $C > 0$.

Combining Lemma 4.3.3 with Theorem 4.2.2 then yields the convergence of the (high–order) grad-div stabilized Taylor–Hood pair.

Theorem 4.3.4. *Let $\{\gamma_i\}_{i=1}^{\infty} \subset \mathbb{R}$ with $\gamma_i \to \infty$ and $(\boldsymbol{u}_i, p_i) \in \boldsymbol{X}_h^{TH} \times Y_h^{TH}$ be the solution of the grad-div stabilized Stokes problem (58) corresponding to γ_i using the Taylor–Hood pair with $k \geq 4$. Then $\boldsymbol{u}_i \to \boldsymbol{w}_h$ and $p_i - \gamma_i \nabla \cdot \boldsymbol{u}_i \to p_h$ as $i \to \infty$ for some $\boldsymbol{w}_h \in \boldsymbol{X}_h^{TH} \cap \boldsymbol{V}$ and $p_h \in Q_h^{TH}$ with $(\boldsymbol{w}_h, p_h)$ being the solution for (64) with $\boldsymbol{X}_h \times Q_h = \boldsymbol{X}_h^{TH} \times Q_h^{TH}$. In particular,*

$$\Theta_* \nu^{-1} \|p_h - (p_i - \gamma_i \nabla \cdot \boldsymbol{u}_i)\| \leq \|\nabla(\boldsymbol{w}_h - \boldsymbol{u}_i)\| \leq C\Theta_*^{-1} \min\{\Theta_*^{-1}\gamma_i^{-1}, (\nu\gamma_i)^{-1/2}\}, \tag{72}$$

where $C > 0$ is independent of h, ν, and Θ_*.

If $\boldsymbol{u} \in \boldsymbol{H}^s(\Omega)$ for some $s \geq 1$, then the divergence–free function $\boldsymbol{w}_h$ satisfies

$$\|\nabla(\boldsymbol{u} - \boldsymbol{w}_h)\| \leq Ch^{\ell-1} \|\boldsymbol{u}\|_{H^\ell(\Omega)}, \tag{73}$$

where $\ell = \min\{k+1, s\}$ and $C > 0$ is independent of h, γ, ν and Θ_*.

Remark 4.3.5. For fixed ν, Theorem 4.3.4 implies that the convergence for the sequence $\{(\boldsymbol{u}_i, p_i - \gamma_i \nabla \cdot \boldsymbol{u}_i)\}_{i=1}^{\infty}$ to $(\boldsymbol{w}_h, p_h)$ is $O(\gamma_i^{-1})$ provided $\gamma_i \gtrsim \Theta_*^{-2}\nu$. Otherwise, for smaller grad-div parameters the theorem predicts $O(\gamma_i^{-1/2})$ convergence.

Remark 4.3.6. Theorem 4.3.4 states that $\{\boldsymbol{u}_i\}_{i=1}^{\infty}$ converges to an exactly divergence–free solution with optimal order properties as $i \to \infty$; this is true on meshes with singular vertices or "nearly singular" vertices.

Proof. The convergence and convergence rates for the sequence $\{(\boldsymbol{u}_i, p_i - \gamma_i \nabla \cdot \boldsymbol{u}_i)\}_{i=1}^{\infty}$ directly follow from Lemma 4.3.3 with Theorem 4.2.2.

To prove (73), we first use the estimate (59):

$$\|\nabla(\boldsymbol{u} - \boldsymbol{w}_h)\| \leq \inf_{\boldsymbol{v} \in \boldsymbol{V} \cap \boldsymbol{X}_h} \|\nabla(\boldsymbol{u} - \boldsymbol{v})\|.$$

Following [25], we introduce the modified H^2-conforming Argyris (TUBA) finite element space [4]

$$\Sigma_h = \{s \in H_0^2(\Omega) \cap \mathcal{P}_{k+1}(\mathcal{T}_h) : \ s \text{ is } C^2 \text{ at all non-corner vertices of } \mathcal{T}_h\}.$$

We then have [25]

$$\nabla \times \Sigma_h := \{\nabla \times s : \ s \in \Sigma_h\} \subset \boldsymbol{V} \cap \boldsymbol{X}_h,$$

where $\nabla \times s = (\partial s/\partial x_2, -\partial s/\partial x_1)^\intercal$ is the two–dimensional curl operator. Therefore, by writing $\boldsymbol{u}$ in terms of its stream function $\boldsymbol{u} = \nabla \times \psi$ for some $\psi \in H_0^2(\Omega) \cap H^{s+1}(\Omega)$, we have

$$\begin{aligned}\inf_{\boldsymbol{v} \in \boldsymbol{V} \cap \boldsymbol{X}_h} \|\nabla(\boldsymbol{u} - \boldsymbol{v})\| &\leq \inf_{\boldsymbol{v} \in \nabla \times \Sigma_h} \|\nabla(\boldsymbol{u} - \boldsymbol{v})\| \\ &= \inf_{s \in \Sigma_h} \|D^2(\psi - s)\| \leq Ch^{\ell-1}\|\psi\|_{H^{\ell-1}(\Omega)} \leq Ch^{\ell-1}\|\boldsymbol{u}\|_{H^{\ell}(\Omega)}.\end{aligned}$$

□

4.3.2 The cubic–quadratic Taylor–Hood pair

To apply Theorem 4.2.2 to the cubic-quadratic Taylor–Hood pair, we incorporate the recent stability results of the cubic-quadratic Scott–Vogelius pair in [36]. In particular, a characterization of the space Q_h^{TH} (cf. (71)) was explicitly given and inf–sup stability results were shown. To explain these results further, we introduce the concept of an interpolating vertex.

Recall that for a vertex $z \in \mathcal{V}_h$, $\mathcal{T}_z = \{\tau_1, \ldots, \tau_N\}$ denotes the set of triangles that have z as vertex. Set

$$\boldsymbol{W}_z := \{\boldsymbol{a} \in \mathbb{R}^N : \sum_{j=1}^{N} (-1)^j a_j = 0\}.$$

Set

$$\Omega_z = \mathrm{int}\Big(\cup_{\tau \in \mathcal{T}_z} \bar{T}\Big),$$

and define

$$\begin{aligned}\boldsymbol{X}_z =& \{\boldsymbol{v} \in \boldsymbol{X}_h^{TH} : \ \mathrm{supp}\, \boldsymbol{v} \subset \Omega_z : \ \int_\tau \nabla \cdot \boldsymbol{v}\, dx = 0 \ \forall \tau \in \mathcal{T}_h, \ (\nabla \cdot \boldsymbol{v})(\sigma) = 0 \\ & \forall \sigma \in \mathcal{V}_h \backslash \{z\}\}.\end{aligned}$$

Definition 4.3.7. We say that $z \in \mathcal{V}_h$ is an *interpolating vertex* if, for all $\boldsymbol{a} \in \boldsymbol{W}_z$, there exists $\boldsymbol{v} \in \boldsymbol{X}_z$ such that $(\nabla \cdot \boldsymbol{v})|_{\tau_j}(z) = a_j$ for all $j \in \{1, 2, \ldots, N\}$. We denote the set of all interpolating vertices in $\mathcal{V}_h$ by $\mathcal{L}_h$.

Remark 4.3.8. examples are given in [36], where the local interpolating vertex property in Definition 4.3.7 is satisfied by all interior vertices. Examples include

1. Criss-crossed mesh
2. Every mesh $\mathcal{T}_h$ such that $|\mathcal{T}_z| = N$ is odd for all $z \in \mathcal{V}_h^I$.

It is also shown in [36] that not every interior vertex in a type–I triangulation (cf. Figure 1) is an interpolating vertex.

Now, we state the following lemma which gives a stability result of the cubic Scott-Vogelius pair. We refer to [36] for a detailed proof.

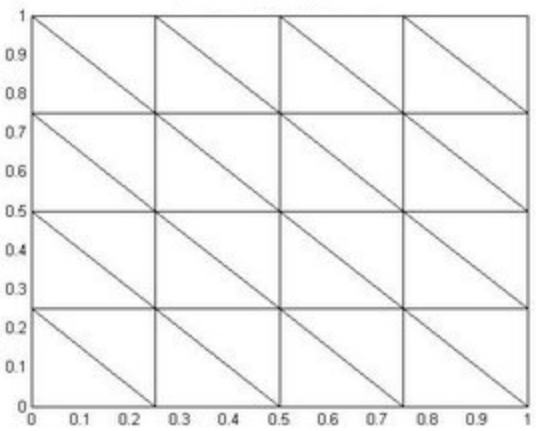

Figure 2: Type–I triangulation on $(0,1)^2$ on which each interior vertex is not an interpolating vertex.

Lemma 4.3.9. *Suppose that $k = 3$ and $\mathcal{V}_h^I \subset \mathcal{L}_h$. Then there holds*

$$Y_h^{TH} \subset Q_h^{TH} := \nabla \cdot \boldsymbol{X}_h^{TH} = \{q \in \mathcal{P}_{k-1}(\mathcal{T}_h) \cap L_0^2(\Omega) : \sum_{\ell=1}^{M} (-1)^\ell q|_{\tau_\ell}(z) = 0 \ \forall z \in \mathcal{S}_h\}.$$

Moreover, $\boldsymbol{X}_h^{TH} \times Q_h^{TH}$ represents an inf-sup stable pair with β_Q independent of size of the triangles in $\mathcal{T}_h$. Rather, $\beta_Q = C\Theta_*$ for some h-independent constant $C > 0$.

Combining Lemma 4.3.9 with Theorem 4.2.2 then yields the convergence of the grad-div stabilized Taylor–Hood pair.

Theorem 4.3.10. *Let $\{\gamma_i\}_{i=1}^{\infty} \subset \mathbb{R}$ with $\gamma_i \to \infty$ and $(\boldsymbol{u}_i, p_i) \in \boldsymbol{X}_h^{TH} \times Y_h^{TH}$ be the solution of the grad-div stabilized Stokes problem (58) corresponding to γ_i using the Taylor–Hood pair with $k = 3$. Assume $\mathcal{V}_h^I \subset \mathcal{L}_h$, i.e., all interior vertices in $\mathcal{T}_h$ are interpolating vertices. Then $\boldsymbol{u}_i \to \boldsymbol{w}_h$ and $p_i - \gamma_i \nabla \cdot \boldsymbol{u}_i \to p_h$ as $i \to \infty$ for some $\boldsymbol{w}_h \in \boldsymbol{X}_h^{TH} \cap \boldsymbol{V}$ and $p_h \in Q_h^{TH}$ with $(\boldsymbol{w}_h, p_h)$ being the solution for (64) with $\boldsymbol{X}_h \times Q_h = \boldsymbol{X}_h^{TH} \times Q_h^{TH}$. The rate of convergence of $(\boldsymbol{u}_i, p_i - \gamma_i \nabla \cdot \boldsymbol{u}_i)$ satisfies (72).*

4.3.3 The quadratic-linear Taylor–Hood pair on Clough-Tocher splits

The case quadratic–linear Taylor–Hood pair on Clough-Tocher splits was discussed and studied in detail in [16]; here, we state these results for completeness.

A Clough–Tocher split (or refinement) of a shape–regular triangulation $\mathcal{T}_h$ is obtained connecting the vertices of each triangle $\tau \in \mathcal{T}_h$ to its barycenter. Thus, each triangle is split into three sub-triangles. Denote by $\mathcal{T}_h^{CT}$ the Clough-Tocher split of $\mathcal{T}_h$, and, with an abuse of notation, define the quadratic–linear Taylor–Hood pair on $\mathcal{T}_h^{CT}$:

$$\boldsymbol{X}_h^{TH} = \boldsymbol{\mathcal{P}}_2(\mathcal{T}_h^{CT}) \cap \boldsymbol{H}_0^1(\Omega), \tag{74a}$$

$$Y_h^{TH} = \mathcal{P}_1(\mathcal{T}_h^{CT}) \cap H^1(\Omega) \cap L_0^2(\Omega). \tag{74b}$$

The following lemma gives a characterization of the divergence acting on $\boldsymbol{X}_h^{TH}$ and states that the quadratic-linear Scott–Vogelius pair is stable on Clough–Tocher splits. Its proof can be found in [5, 35].

Lemma 4.3.11. *Let $\boldsymbol{X}_h^{TH} \times Y_h^{TH}$ be defined by (74). Then there holds*

$$Y_h^{TH} \subset Q_h^{TH} := \nabla \cdot \boldsymbol{X}_h^{TH} = \mathcal{P}_1(\mathcal{T}_h^{CT}) \cap L_0^2(\Omega).$$

Moreover, $\boldsymbol{X}_h^{TH} \times Q_h^{TH}$ represents an inf-sup stable pair with inf-sup constant β_Q independent of size of the triangles in $\mathcal{T}_h$.

Combining Lemma 4.3.11 with Theorem 4.2.2 then yields the convergence of the (low–order) grad-div stabilized Taylor–Hood pair.

Theorem 4.3.12. *Let $\boldsymbol{X}_h^{TH} \times Y_h^{TH}$ be defined by (74), and let $\{\gamma_i\}_{i=1}^{\infty} \subset \mathbb{R}$ with $\gamma_i \to \infty$. Let $(\boldsymbol{u}_i, p_i) \in \boldsymbol{X}_h^{TH} \times Y_h^{TH}$ be the solution of the grad-div stabilized Stokes problem (58) corresponding to γ_i. Then $\boldsymbol{u}_i \to \boldsymbol{w}_h$ and $p_i - \gamma_i \nabla \cdot \boldsymbol{u}_i \to p_h$ as $i \to \infty$ with rate $O(\gamma_i^{-1})$ for some $\boldsymbol{w}_h \in \boldsymbol{X}_h^{TH} \cap \boldsymbol{V}$ and $p_h \in Q_h^{TH}$ with $(\boldsymbol{w}_h, p_h)$ being the solution to (64). If $\boldsymbol{u} \in \boldsymbol{H}^s(\Omega)$ for some $s \geq 1$, then the divergence–free function $\boldsymbol{w}_h$ satisfies*

$$\|\nabla(\boldsymbol{u} - \boldsymbol{w}_h)\| \leq C h^{\ell-1} \|\boldsymbol{u}\|_{H^\ell(\Omega)}, \tag{75}$$

where $\ell = \min\{3, s\}$ and $C > 0$ is independent of h, γ, ν and β_Q.

Proof. The convergence and convergence rates for the sequence $\{(\boldsymbol{u}_i, p_i - \gamma_i \nabla \cdot \boldsymbol{u}_i)\}_{i=1}^{\infty}$ directly follow from Lemma 4.3.3 with Theorem 4.2.2 (see also [16]).

To prove (75), and to show that the constant $C > 0$ is independent of β_Q, we first use the estimate (59):

$$\|\nabla(\boldsymbol{u} - \boldsymbol{w}_h)\| \leq \inf_{\boldsymbol{v} \in \boldsymbol{V} \cap \boldsymbol{X}_h} \|\nabla(\boldsymbol{u} - \boldsymbol{v})\|.$$

Following the ideas in Theorem 4.3.4, we introduce the modified H^2-conforming Hsieh–Clough–Tocher finite element space [39]

$$\Sigma_h^{CT} = H_0^2(\Omega) \cap \mathcal{P}_3(\mathcal{T}_h^{CT}).$$

We then have [39]

$$\nabla \times \Sigma_h^{CT} := \{\nabla \times s : \ s \in \Sigma_h^{CT}\} \subset \boldsymbol{V} \cap \boldsymbol{X}_h.$$

Writing $\boldsymbol{u} = \nabla \times \psi$ for some $\psi \in H_0^2(\Omega) \cap H^{s+1}(\Omega)$, we have

$$\begin{aligned} \inf_{\boldsymbol{v} \in \boldsymbol{V} \cap \boldsymbol{X}_h} \|\nabla(\boldsymbol{u} - \boldsymbol{v})\| &\leq \inf_{\boldsymbol{v} \in \nabla \times \Sigma_h^{CT}} \|\nabla(\boldsymbol{u} - \boldsymbol{v})\| \\ &= \inf_{s \in \Sigma_h^{CT}} \|D^2(\psi - s)\| \leq C h^{\ell-1} \|\psi\|_{H^{\ell-1}(\Omega)} \leq C h^{\ell-1} \|\boldsymbol{u}\|_{H^{\ell}(\Omega)}. \end{aligned}$$

□

4.4 Application II: The $\mathbf{P}_1 \times P_0$ Pair on Powell-Sabin Splits

In the previous section, we considered the Taylor–Hood pair with grad-div stabilization for various polynomial degrees. The general theme in the arguments is to use the stability of the Scott–Vogelius pair to prove convergence and the absence of locking in the limiting case $\gamma \to \infty$. In this section, we show that the grad-div connection discussed in the previous sections can be generalized to a low–order $\boldsymbol{\mathcal{P}}_1 \times \mathcal{P}_0$ pair defined on a Powell-Sabin split mesh by incorporating the recently developed divergence–free methods in [32, 17].

As before, we start with a shape–regular simplicial triangulation $\mathcal{T}_h$ of Ω. We then construct the Powell–Sabin split of $\mathcal{T}_h$ as follows [55, 42]. Let $\tau \in \mathcal{T}_h$ be a triangle with vertices z_1, z_2 and z_3 labelled counterclockwise, and let z_0 be the incenter of τ. Denote the

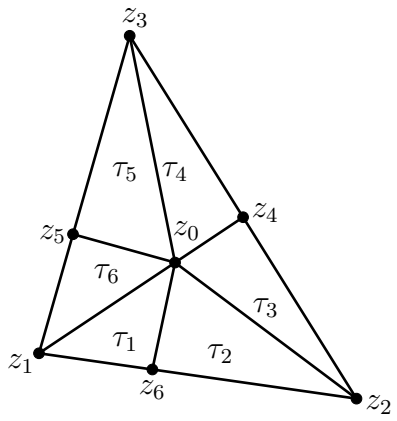

Figure 3: A Powell-Sabin local split of a triangle. Note that the vertices z_4, z_5, and z_6 are singular vertices in global mesh.

edges of τ by $\{e_i\}_{i=1}^3$, labelled such that z_i is not a vertex of e_i. Let z_{3+i} be the interior point of the edge of e_i that is the intersection of the line segment connecting the incenters of the triangles τ and its neighboring triangle that has e_i as an edge. We then construct the triangulation $\tau^{PS} = \{\tau_1, ..., \tau_6\}$ by connecting each z_i to z_0 for $1 \leq i \leq 6$; see Figures 3 and 4.

Let $\mathcal{T}_h^{PS} = \bigcup_{\kappa \in \mathcal{T}_h} \bigcup_{\tau \in \kappa^{PS}} \tau$ be the global triangulation of Ω, and $\mathcal{V}_h^{PS}$ be the set of vertices of $\mathcal{T}_h^{PS}$. Let $\mathcal{S}_h^{PS} \subset \mathcal{V}_h^{PS}$ be the set of all singular vertices in $\mathcal{T}_h^{PS}$. Let $\mathcal{S}_h^I = \{z \in \mathcal{S}_h^{PS} : z \notin \partial\Omega\}$ be the set of interior singular vertices, and $\mathcal{S}_h^B = \{z \in \mathcal{S}_h^{PS} : z \in \partial\Omega\}$ be the set of boundary singular vertices. Observe that each $z \in \mathcal{S}_h^I$ is attached to exactly four triangles, and each $z \in \mathcal{S}_h^B$ is attached to exactly two triangles. By construction, the cardinality of $\mathcal{S}_h^{PS}$ is exactly the number of edges in $\mathcal{T}_h$.

Definition 4.4.1. Let $p \in \mathcal{P}_0(\mathcal{T}_h^{PS}) = \{q \in L^2(\Omega) : q_{|\tau} \in P_0(\tau), \forall \tau \in \mathcal{T}_h^{PS}\}$. We say that p satisfies the *weak continuity property on* $\mathcal{T}_h^{PS}$ *if for any* $z \in \mathcal{S}_h^I$ *and* $\{\tau_1, ..., \tau_4\} = \mathcal{T}_z \subset \mathcal{T}_h^{PS}$ *we have that*

$$p_{|\tau_1} - p_{|\tau_2} + p_{|\tau_3} - p_{|\tau_4} = 0,$$

and for any $z \in \mathcal{S}_h^B$ *and* $\{\tau_1, \tau_2\} = \mathcal{T}_z \subset \mathcal{T}_h^{PS}$ *we have that*

$$p_{|\tau_1} = p_{|\tau_2}.$$

We introduce the finite element pair $\boldsymbol{X}_h^{PS} \times Q_h^{PS}$ defined on the Powell-Sabin triangulation $\mathcal{T}_h^{PS}$ proposed in [32]:

$$\boldsymbol{X}_h^{PS} = \boldsymbol{\mathcal{P}}_1(\mathcal{T}_h^{PS}) \cap \boldsymbol{H}_0^1(\Omega), \tag{76a}$$

$$Q_h^{PS} = \{q \in \mathcal{P}_0(\mathcal{T}_h^{PS}) \cap L_0^2(\Omega) : \ q \textit{ satisfies the weak continuity property}\}. \tag{76b}$$

Now, we state the following lemma concerning the image of the divergence operator acting on $\boldsymbol{X}_h^{PS}$ and the inf-sup stability of $\boldsymbol{X}_h^{PS} \times Q_h^{PS}$. We refer to [32] for a detailed proof.

Lemma 4.4.2. *There holds*

$$\nabla \cdot \boldsymbol{X}_h^{PS} = Q_h^{PS}$$

with bounded right-inverse. Therefore, $\boldsymbol{X}_h^{PS} \times Q_h^{PS}$ *is inf-sup stable, with inf-sup constant* β_Q *independent of* h.

We propose a smaller and simpler pressure space that conforms to the framework in the previous sections. To this end, we let

$$\mathcal{K}_h^{PS} = \{\bigcup_{\tau \in \mathcal{T}_z} \tau : z \in \mathcal{S}_h^{PS}\}$$

be the mesh obtained by taking the union of the triangles associated with each singular vertex. Thus, $\mathcal{K}_h^{PS}$ is a set consisting of quadrilaterals (in the case that z is an interior singular vertex) and triangles (in the case that z is a boundary singular vertex); see Figure 4.

We define the auxiliary pressure space

$$Y_h^{PS} = \{q \in L_0^2(\Omega) : q|_K \in P_0(K), \forall K \in \mathcal{K}_h^{PS}\}. \tag{77}$$

Remark 4.4.3. It was shown that the pair $\boldsymbol{X}_h^{PS} \times Q_h^{PS}$ is inf-sup stable when defined on the mesh $\mathcal{T}_h^{PS}$. Since $Y_h^{PS} \subset Q_h^{PS}$, the pair $\boldsymbol{X}_h^{PS} \times Y_h^{PS}$ is stable. Hence, we can incorporate Theorem 4.2.2 to conclude the following theorem.

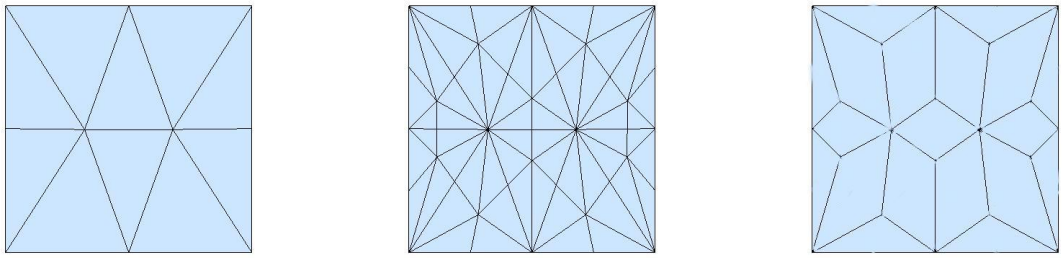

Figure 4: A triangulation $\mathcal{T}_h$ of the unit square (left), its Powell–Sabin refinement $\mathcal{T}_h^{PS}$ (middle), and the mesh $\mathcal{K}_h^{PS}$ (right).

Theorem 4.4.4. *Let $\{\gamma_i\}_{i=1}^{\infty} \subset \mathbb{R}$ with $\gamma_i \to \infty$ and $(\boldsymbol{u}_i, p_i) \in \boldsymbol{X}_h^{PS} \times Y_h^{PS}$ be the solution of the grad-div stabilized Stokes problem (58) correspondes to γ_i using the pair $\boldsymbol{X}_h^{PS} \times Y_h^{PS}$. Then $\boldsymbol{u}_i \to \boldsymbol{w}_h$ and $p_i - \gamma_i \nabla \cdot \boldsymbol{u}_i \to p_h$ as $i \to \infty$ with rate $O(\gamma_i^{-1})$ for some $\boldsymbol{w}_h \in \boldsymbol{X}_h^{PS} \cap \boldsymbol{V}$ and $p_h \in Q_h^{PS}$ with $(\boldsymbol{w}_h, p_h)$ being the solution for (64) with $\boldsymbol{X}_h \times Q_h = \boldsymbol{X}_h^{PS} \times Q_h^{PS}$.*

4.5 Numerical Examples

In this section, we perform some simple numerical experiments and compare the results with the theoretical ones given in the previous sections. In all tests, we take the domain to be the unit square $\Omega = (0,1)^2$, and choose the source function such that the exact velocity and pressure solutions are given respectively as

$$\boldsymbol{u} = \begin{pmatrix} \pi \sin^2(\pi x) \sin(2\pi y) \\ -\pi \sin^2(\pi y) \sin(2\pi x) \end{pmatrix}, \qquad p = \cos(\pi x) \cos(\pi y). \tag{78}$$

4.5.1 The $\mathbf{P}_1 \times P_0$ pair on Powell–Sabin splits

In this section, we report and discuss the numerical results for the $\boldsymbol{\mathcal{P}}_1 \times \mathcal{P}_0$ pair on Powell–Sabin splits.

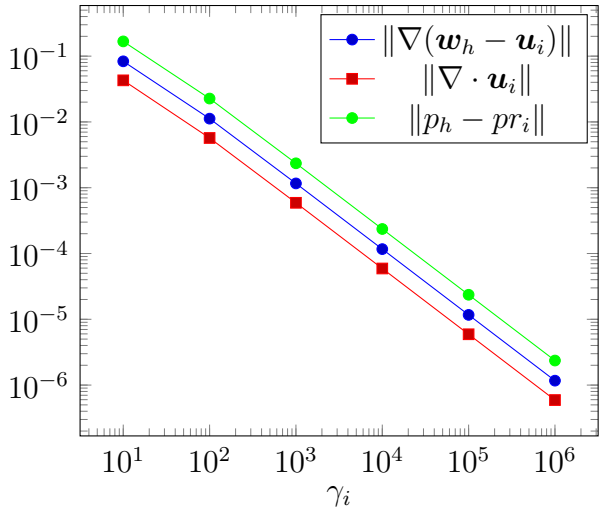

Figure 5: Numerical results on Powell-Sabin splits using the $\mathbf{P}_1 \times P_0$ pairs for fixed $h = 1/32$ and viscosity $\nu = 1$. The plot shows $O(\gamma_i^{-1})$ convergence for all three quantities.

Let $\mathcal{T}_h$ be a quasi–uniform Delaunay triangulation of Ω with $h = 1/32$, and let $\mathcal{T}_h^{PS}$ be the corresponding Powell-Sabin global triangulation (cf. Section 4.4). We compute problem (64) with $\boldsymbol{X}_h \times Q_h = \boldsymbol{X}_h^{PS} \times Q_h^{PS}$ defined by (76), and denote the solution pair by $(\boldsymbol{w}_h, p_h)$. We also compute problem (58) with $\boldsymbol{X}_h \times Y_h = \boldsymbol{X}_h^{PS} \times Y_h^{PS}$ (cf. (77)), and denote the solution pair corresponding to γ_i by $(\boldsymbol{u}_i, p_i)$. The grad-div parameters are taken to be $\gamma_i = 10^i$ for $i = 1, \ldots, 6$.

4.5.1.1 The $\mathbf{P}_1 \times P_0$ pair on Powell-Sabin splits with fixed viscosity $\nu = 1$

In Figure 5, we plot the quantities $\|\nabla(\boldsymbol{w}_h - \boldsymbol{u}_i)\|, \|\nabla \cdot \boldsymbol{u}_i\|$ and $\|p_h - pr_i\|$ versus γ_i for fixed $h = 1/32$ and fixed viscosity $\nu = 1$, where $pr_i = p_i - \gamma_i \nabla \cdot \boldsymbol{u}_i$. The plot clearly shows linear convergence with respect to γ_i^{-1} for all three quantities, which is in exact agreement with Theorem 4.4.4.

4.5.1.2 The $\mathbf{P}_1 \times P_0$ pair on Powell-Sabin splits with varying viscosity

In these series of tests, we compute the same problem as the previous section, but for different viscosity values: $\nu = 10^{-j}$ for $j = 1, 2, 3, 4$. We report the differences $\|\nabla(\boldsymbol{w}_h - \boldsymbol{u}_i)\|, \|\nabla \cdot \boldsymbol{u}_i\|$ and $\|p_h - pr_i\|$ versus the grad-div parameter in Figure 6.

Again, we observe that all three quantities converge with rate $O(\gamma_i^{-1})$ for each value of ν, at least for moderately sized values of γ_i. On the other hand, we see that, for small values of ν, the differences $\|p_h - pr_i\|_{L^2(\Omega)}$ and $\|\nabla(\boldsymbol{w}_h - \boldsymbol{u}_i)\|_{L^2(\Omega)}$ increase (with rate $= O(\gamma_i)$) as $\gamma_i \to \infty$. This behavior is due to round-off error as we now explain.

Observe that (67) reads

$$\nu(\nabla \boldsymbol{e}_i, \nabla \boldsymbol{v}) - (p_h - p_i, \nabla \cdot \boldsymbol{v}) + \gamma_i(\nabla \cdot \boldsymbol{e}_i, \nabla \cdot \boldsymbol{v}) = 0 \qquad \forall \boldsymbol{v} \in \boldsymbol{X}_h,$$

where $\boldsymbol{e}_i = \boldsymbol{w}_h - \boldsymbol{u}_i$. Consequently, by setting $\boldsymbol{v} = \boldsymbol{e}_i$ and using $\nabla \cdot \boldsymbol{w}_h = 0$, and dividing by ν and rearrange terms, we find

$$\|\nabla(\boldsymbol{w}_h - \boldsymbol{u}_i)\|^2_{L^2(\Omega)} = \|\nabla \boldsymbol{e}_i\|^2 = \frac{1}{\nu}(p_h - pr_i, \nabla \cdot \boldsymbol{u}_i).$$

We computed the term $(p_h - pr_i, \nabla \cdot \boldsymbol{u}_i)$, and we observed that as soon as this term is less than machine epsilon, both quantities $\|\nabla(\boldsymbol{w}_h - \boldsymbol{u}_i)\|$ and $\|p_h - pr_i\|$ grow as $\gamma_i \to \infty$.

4.5.2 Taylor–Hood finite elements

In this section we report and discuss the numerical results for Taylor–Hood finite element with polynomial degrees $k = 4, 3, 2$, and compare the results with the theoretical ones established in Section 4.3. We compute problem (64) with $\boldsymbol{X}_h \times Q_h = \boldsymbol{X}_h^{TH} \times Q_h^{TH}$, and we denote the solution pair by $(\boldsymbol{w}_h, p_h)$. Also, we consider the problem (58) with $\boldsymbol{X}_h \times Y_h = \boldsymbol{X}_h^{TH} \times Y_h^{TH}$ and we denote the solution pair by $(\boldsymbol{u}_i, p_i)$ that corresponding to γ_i.

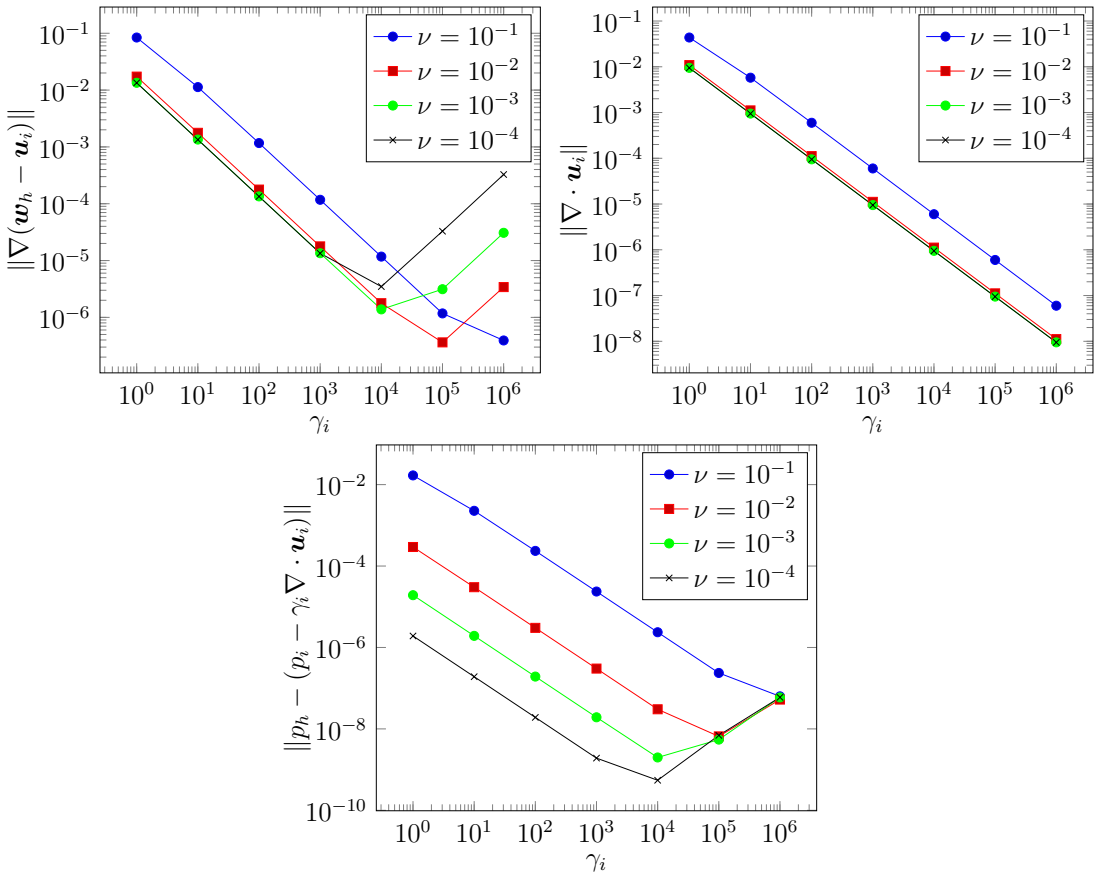

Figure 6: Numerical experiments using the $\mathbf{P}_1 \times P_0$ pairs on Powell–Sabin splits with fixed $h = 1/32$ and varying viscosity ν. The plot shows $O(\gamma_i^{-1})$ convergence for all three quantities. The increase in the first and third plots for large values of γ_i is due to round–off error.

4.5.2.1 Grad-div Taylor–Hood methods on perturbed criss–cross meshes with fixed viscosity

Recall from Lemmas 4.3.3 and 4.3.9 that the stability of Scott–Vogelius pair depends on the vertex singularity of the mesh Θ_* given in Definition 4.3.1. This in turn affects the convergence behavior of the grad-div solution $(\boldsymbol{u}_i, p_i)$ to the divergence–free solution $(\boldsymbol{w}_h, p_h)$; see Theorems 4.3.4 and 4.3.10. The purpose of the tests presented in this section is to gauge the affect of the vertex singularity of the mesh, and to compare the numerical results with the theoretical ones derived in Section 4.3.

To this end, we start by constructing criss–cross triangulation of Ω with $h = 1/20$ which has $O(h^{-2})$ singular vertices. Then for each singular vertex of the triangulation, we add its coordinates by $(r_1, r_2)h^{\alpha+1}$, where $r_i \in \{-2, -1, 1, 2\}$ is chosen randomly, and with exponent $\alpha \in \{0, 1, 2, 3\}$; see Figure 7. The resulting perturbed mesh has no singular vertices, but simple trigonometric arguments show the vertex singularity of the mesh is $\Theta_* \approx h^\alpha$.

We report the quantities quantities $\|\nabla \cdot \boldsymbol{u}_i\|$, $\|\nabla(\boldsymbol{w}_h - \boldsymbol{u}_i)\|$, and $\|p_h - (p_i - \gamma_i \nabla \cdot \boldsymbol{u}_i)\|$ using the $\boldsymbol{\mathcal{P}}_k \times \mathcal{P}_{k-1}$ $(k = 3, 4)$ Taylor–Hood and Scott–Vogelius elements with $\nu = 1$ in Figure 7. For comparison, the convergence estimate for the Taylor–Hood element stated in Theorems 4.3.4 and 4.3.10 read

$$h^\alpha \|p_h - (p_i - \gamma_i \nabla \cdot \boldsymbol{u}_i)\| \leq \|\nabla(\boldsymbol{w}_h - \boldsymbol{u}_i)\| \leq C h^{-\alpha} \min\{h^{-\alpha}\gamma_i^{-1}, \gamma_i^{-1/2}\},$$

which suggests a deterioration of the "errors" for large perturbation exponents α. Indeed, Figure 7 shows pre-asymptotic $O(\gamma_i^{-1/2})$ convergence rates for $\alpha = 0$ before achieving $O(\gamma_i^{-1})$ rates for large values of γ_i. On the other hand, for larger α-values (e.g., $\alpha = 2, 3$), we see pre-asymptotic convergence $(k = 4)$ or no convergence $(k = 3)$. The deterioration of the errors for large α-values is most evident for the modified pressure, where Figure 7 shows no convergence with respect to γ_i for $\alpha \in \{2, 3\}$. Therefore we conclude from these results that the quantity Θ_* stated in Theorem 4.3.4 does influence the convergence of the grad-div solution.

On the other hand, Figure 7 shows $\|\nabla \cdot \boldsymbol{u}_i\| = O(\gamma_i^{-1})$ for any value α. Consequently, the convergence estimate of this quantity stated in Theorem 4.3.4 may not be sharp for this quantity.

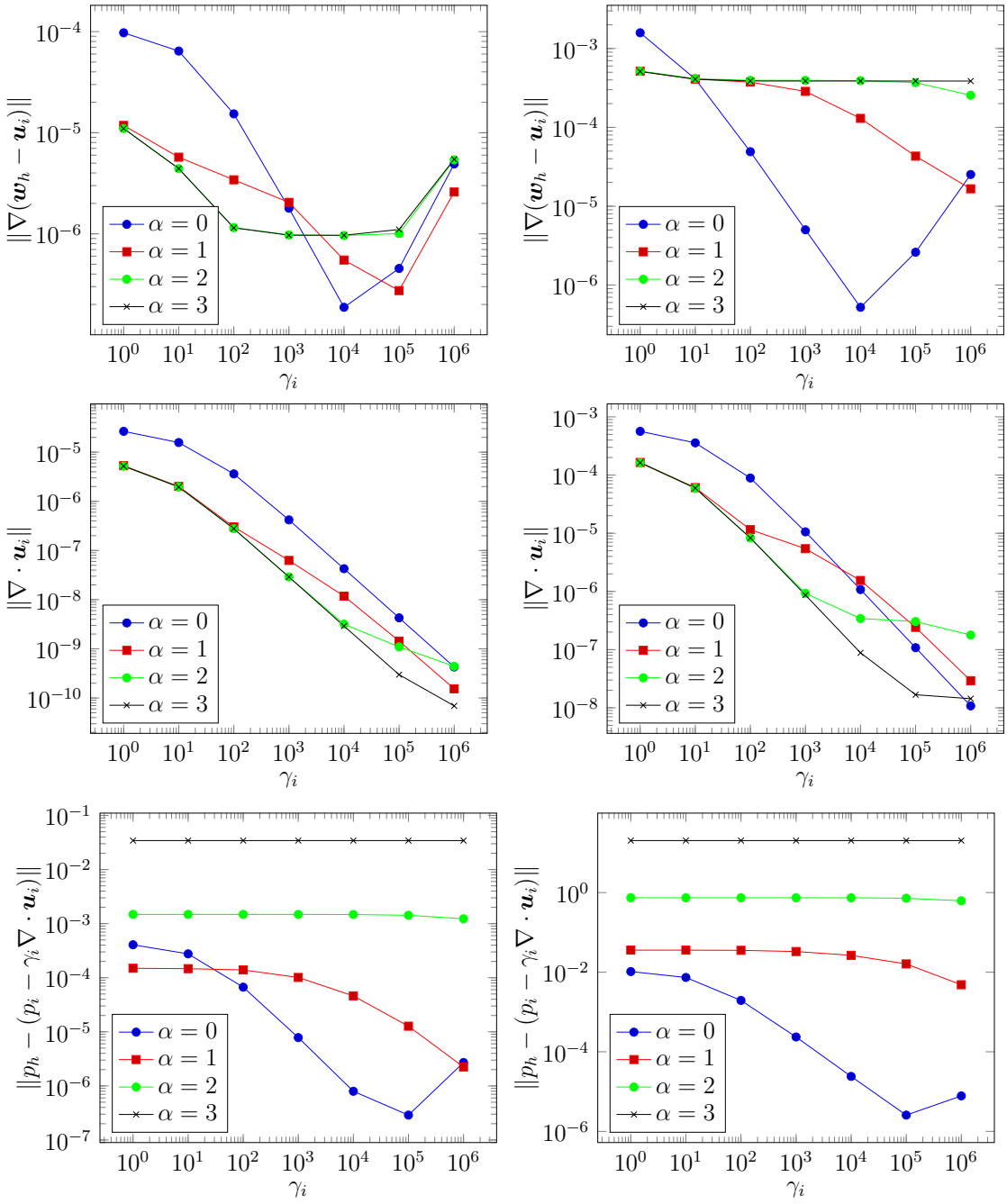

Figure 7: Results of the grad-div stabilized $\mathbf{P}_k \times P_{k-1}$ Taylor–Hood pair on $O(h^{\alpha+1})$ perturbed criss-cross meshes with $h = 1/20$ and $\nu = 1$. Left: $k = 4$. Right: $k = 3$.

4.5.2.2 Grad-div Taylor–Hood methods with varying viscosity

In this series of tests we compute the grad-div Taylor–Hood method with $k = 3, 4$ and vary the viscosity $\nu = 10^{-j}$ $j = 1, 2, 3, 4$ on a perturbed criss cross mesh with $h = 1/20$ and $\alpha = 0$. In this setting, vertex singularity of the mesh is $\Theta_* = O(1)$. The estimates stated in Theorems 4.3.4 and 4.3.10 read

$$\nu^{-1}\|p_h - pr_i\| \leq \|\nabla(\boldsymbol{w}_h - \boldsymbol{u}_i)\| \leq C \min\{\gamma_i^{-1}, (\nu\gamma_i)^{-1/2}\}.$$

We report the quantities $\|\nabla(\boldsymbol{w} - \boldsymbol{u}_i)\|$, $\|\nabla \cdot \boldsymbol{u}_i\|$ and $\|p_h - pr_i\|$ for $\gamma_i = 10^i$ and $k \in \{3, 4\}$ in Figure 8. We observe that the estimate $\|\nabla \cdot \boldsymbol{u}_i\|$ converges with rate $O(\gamma_i^{-1})$ regardless of the value of ν. The errors $\|p_h - pr_i\|$ and $\|\nabla(\boldsymbol{w}_h - \boldsymbol{u}_i)\|$ initially converge with rates $O(\gamma_i^{-1})$ but quickly increase for large γ_i-values with rate $O(\gamma_i)$ due to the round-off error (cf. Section 4.5.1.2).

4.5.3 Grad-div Taylor–Hood methods on type–I triangulations

In the final set of numerical experiments, we compute the grad-div Taylor–Hood pair on type–I triangulations with $h = 1/24$ (cf. Figure 2). Recall from Remark 4.3.8 that on this mesh, not all interior vertices are interpolating vertices, and therefore the cubic–quadratic Scott–Vogelius pair is not stable on this mesh.

Similar to the previous sections, we compute the grad-div stabilized finite element method using the $\boldsymbol{\mathcal{P}}_k \times \mathcal{P}_{k-1}$ pair with $k = 3, 4$ and fixed viscosity $\nu = 1$. As the Scott–Vogelius pair $(\boldsymbol{w}_h, p_h)$ is unavailable on this mesh, we instead compute the errors $\|\nabla(\boldsymbol{u} - \boldsymbol{u}_i)\|$, $\|\nabla \cdot \boldsymbol{u}_i\|$, and $\|p - pr_i\|$, where $(\boldsymbol{u}, p)$ are given by (84).

We report these quantities in Figure 9. We observe a clear convergence of the divergence of the computed solution with $\|\nabla \cdot \boldsymbol{u}_i\| = O(\gamma_i^{-1})$ (asymptotically) in both cases $k = 3, 4$. On the other hand, the errors for the quartic–cubic pair perform much better for large values of the grad-div parameter γ_i. Indeed, in this case the errors stabilize relatively quickly at $\gamma_i = 10^2$. On the other hand, for the cubic-quadratic case, we see that the errors $\|\nabla(\boldsymbol{u} - \boldsymbol{u}_i)\|$ and especially $\|p - pr_i\|$ increase for large γ_i-values. This behavior may be due to the

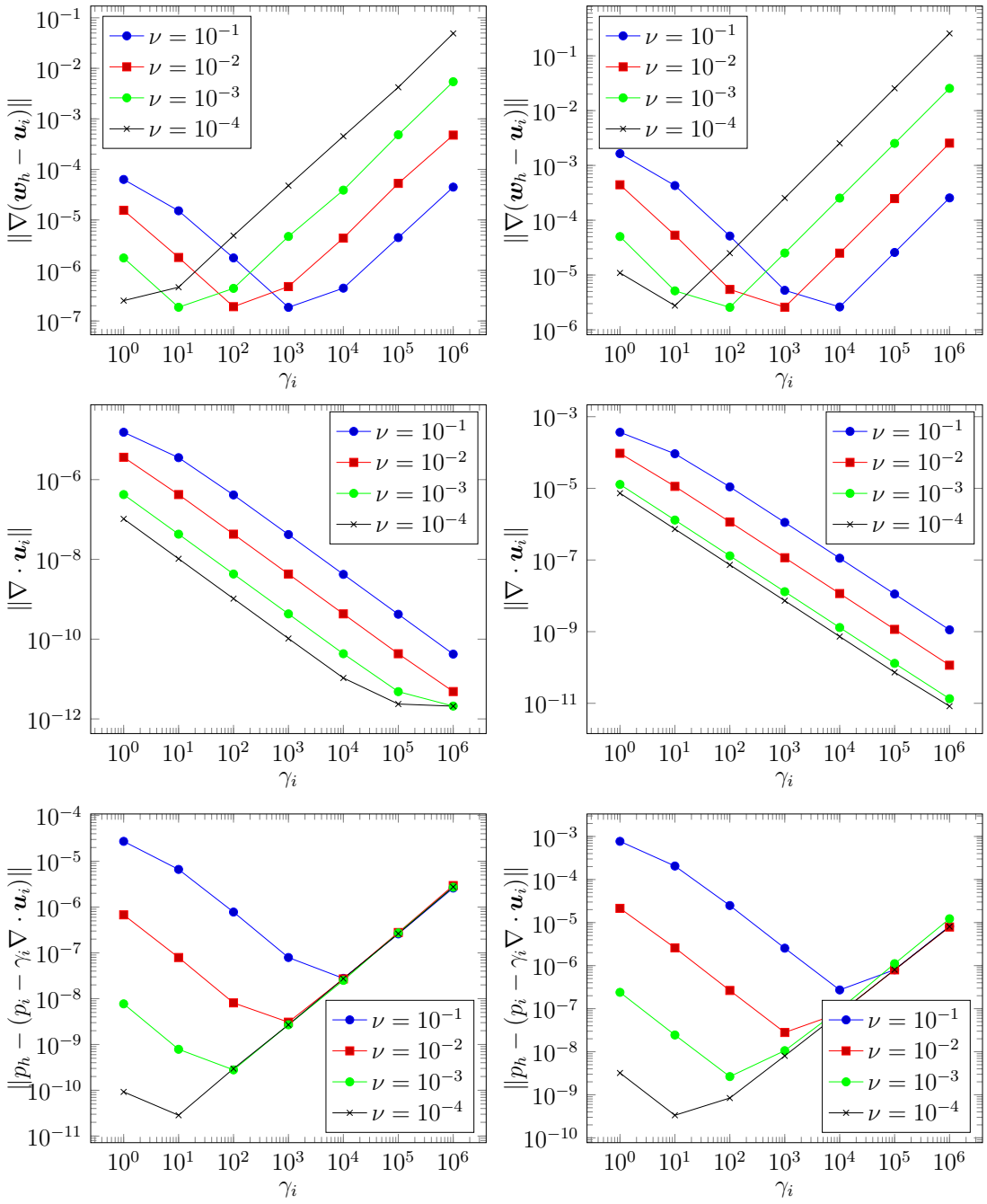

Figure 8: $\mathbf{P}_k \times P_{k-1}$ grad-div sequences errors for $O(h)$ perturbed mesh with different viscosities. Left: $k = 4$. Right: $k = 3$.

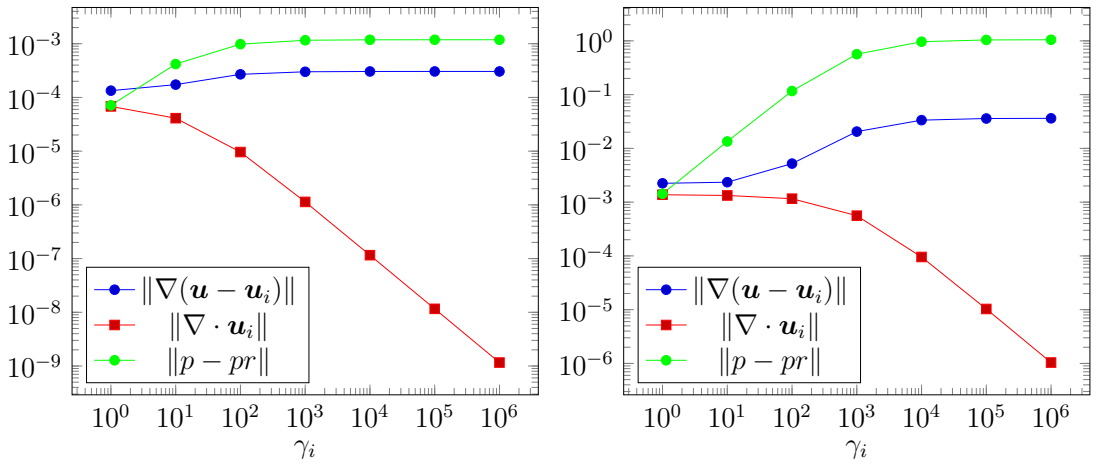

Figure 9: Errors of grad-div finite element method using the Taylor-Hood pair $\mathbf{P}_k \times P_{k-1}$ on type–I triangulation with $k = 4$ (left) and $k = 3$ (right).

instability of the Scott-Vogelius pair and the lack of a discrete divergence–free subspace with optimal approximation properties.

5.0 LOW-ORDER DIVERGENCE-FREE APPROXIMATIONS FOR THE STOKES PROBLEM ON WORSEY-FARIN AND POWELL SABIN SPLITS

In this chapter we derive low-order, inf-sup stable and divergence-free finite element approximations for the Stokes problem using Worsey-Farin splits in three dimensions and Powell-Sabin splits in two dimensions. The velocity space simply consists of continuous, piecewise linear polynomials, where as the pressure space is a subspace of piecewise constants with weak continuity properties at singular edges (3D) and singular vertices (2D). We discuss implementation aspects that arise when coding the pressure space, and in particular, show that the pressure constraints can be enforced at an algebraic level.

5.1 Introduction

The 4^{th}-order SV finite element pair introduced in [59] was the first known finite element pair to yield a divergence-free solutions for incompressible flow models on simplicial triangulations. Afterward, several articles study the stability of lower order finite element pairs that yield divergence-free approximations [56, 57, 5, 62, 63, 64, 34, 35, 65]. The main scheme in these articles is that the stability of lower order finite element pairs can be achieved on certain refinements of simplicial meshes.

In this chapter, we show that the lowest (possible) polynomial order velocity space can be defined for the Stokes problem is inf-sup stable and yields divergence free solutions provided that it is coupled with a piecewise constant pressure space that satisfies a certain weak continuity property, and a certain mesh refinement is used; in particular, Worsey-Farin splits for (3D) domains, and Powell-Sabin splits for (2D) domains.

Although the discrete pressure space we use is not available on computational software packages due to its weak continuity property, we still can use the saddle-point approach to find the approximated solutions by enforcing the weak continuity property at the algebraic level. We provide Algorithms that show how to implement this method on standard finite

element software packages (e.g., FEniCS).

Also, we provide numerical experiments that support our theoretical results.

The chapter is organized as follows. In the next section we give notation that will be used in the rest of the chapter. In Section 5.3 we prove stability of the analogous three-dimensional pair on Worsey-Farin splits. In Section 5.4 we discuss implementation aspects on Powell-Sabin splits and in Section 5.5 we do the same for Worsey-Farin splits. Finally, in Section 5.6 we provide numerical experiments.

5.2 Preliminaries

In this section we develop basic notation that we use throughout the chapter. We provide this in the following list:

- $\mathcal{T}_h$ is a shape-regular, simplicial triangulation of a contractible polytope $\Omega \subset \mathbb{R}^d$ ($d = 2, 3$).
- $h_\tau = \operatorname{diam}(\tau)$ for all $\tau \in \mathcal{T}_h$ and $h = \max_{\tau \in \mathcal{T}_h} h_\tau$.
- For an n-dimensional simplex S ($n \leq d$) and $m \in \{0, \dots n\}$, denote by $\Delta_m(S)$ the set of m-dimensional simplices of S.
- For a simplicial triangulation $\mathcal{Q}_h$ of Ω we define the spaces of piecewise polynomials

$$\mathcal{P}_k(\mathcal{Q}_h) = \prod_{\tau \in \mathcal{Q}_h} \mathcal{P}_k(\tau), \qquad \boldsymbol{\mathcal{P}}_k(\mathcal{Q}_h) = \prod_{K \in \mathcal{Q}_h} \boldsymbol{\mathcal{P}}_k(\tau),$$
$$\mathring{\mathcal{P}}_k(\mathcal{Q}_h) = \mathcal{P}_k(\mathcal{Q}_h) \cap L^2_0(\Omega), \qquad \mathring{\boldsymbol{\mathcal{P}}}^c_k(\mathcal{Q}_h) = \boldsymbol{\mathcal{P}}_k(\mathcal{Q}_h) \cap \boldsymbol{H}^1_0(\Omega).$$

  Thus $\mathring{\mathcal{P}}_k(\mathcal{Q}_h)$ consists of piecewise polynomials of degree $\leq k$ with respect to the triangulation $\mathcal{Q}_h$ with mean zero, and $\mathring{\boldsymbol{\mathcal{P}}}^c_k(\mathcal{Q}_h)$ is the space of continuous, piecewise polynomials of degree $\leq k$ with vanishing trace (i.e., the kth degree vector-valued Lagrange finite element space).
- The constant C denotes a generic positive constant, independent of the mesh parameter h.

5.3 Inf-sup Stability on Worsey-Farin Splits

Let $\mathcal{T}_h$ be a simplicial triangulation of a polyhedral domain $\Omega \subset \mathbb{R}^3$. The Worsey-Farin triangulation $\mathcal{T}_h^{\mathrm{WF}}$ is obtained by splitting each tetrahedron into twelve sub-tetrahedra by the following procedure. Similar to the Powell–Sabin case, for each $\tau \in \mathcal{T}_h$, we connect the incenter of τ to its vertices. Next, the incenters of neighboring pairs of tetrahedra are connected with an edge. This creates a face split point (a vertex) on each face of τ. If τ has a boundary face, then we connect the incenter of τ to the barycenter of the face by a line. Finally, the face split points are connected to the vertices of the face. For each $\tau \in \mathcal{T}_h$, we denote by τ^{WF} the triangulation resulting from local Worsey-Farin refinement of τ, i.e.,

$$\tau^{\mathrm{WF}} = \{\kappa \in \mathcal{T}_h^{\mathrm{WF}} : \ \kappa \subset \bar{\tau}\}.$$

Definition 5.3.1. An edge in a 3D simplicial triangulation is called *singular* if the faces meeting at the edge fall on exactly two planes.

By construction, the Worsey-Farin triangulation contains many singular edges; for each face in the unrefined triangulation $\mathcal{T}_h$, there are three associated singular edges in $\mathcal{T}_h^{\mathrm{WF}}$.

Let $\mathcal{E}_h^{\mathcal{S}}$ denote the set of singular edges in $\mathcal{T}_h^{\mathrm{WF}}$, and let $\mathcal{E}_h^{\mathcal{S},I}$ and $\mathcal{E}_h^{\mathcal{S},B}$ denote the sets of interior and boundary singular edges, respectively. For each $e \in \mathcal{E}_h^{\mathcal{S}}$, let $\mathcal{T}_e = \{\tau_e^{(1)}, \ldots, \tau_e^{(n_e)}\}$ denote the set of tetrahedra that have e as an edge. Here, $n_e = 4$ if e is an interior edge, and $n_e = 2$ if e is a boundary edge. We assume the tetrahedra are labeled such that $\tau_e^{(j)}$ and $\tau_e^{(j+1)}$ share a common face.

5.3.1 Finite element spaces on Worsey–Farin triangulations

Similar to the two-dimensional case, the divergence operator acting on the Lagrange finite element space has weak continuity properties on singular edges (cf. [33]).

Lemma 5.3.2. *For $e \in \mathcal{E}_h^{\mathcal{S}}$, and a piecewise smooth function q, define*

$$\theta_e(q) = \begin{cases} q_e^{(1)}|_e - q_e^{(2)}|_e + q_e^{(3)}|_e - q_e^{(4)}|_e & e \in \mathcal{E}_h^{\mathcal{S},I}, \\ q_e^{(1)}|_e - q_e^{(2)}|_e & e \in \mathcal{E}_h^{\mathcal{S},B}, \end{cases}$$

where $q_e^{(j)} = q|_{\tau_e^{(j)}}$. Then there holds $\theta_e(\mathrm{div}\boldsymbol{v}) = 0$ for all $\boldsymbol{v} \in \mathring{\boldsymbol{\mathcal{P}}}_k^c(\mathcal{T}_h^{\mathrm{WF}})$.

Analogous to the Powell–Sabin case, we define the finite element spaces to discretize the Stokes problem on Worsey-Farin splits. We first define the spaces without boundary conditions

$$\begin{aligned}\boldsymbol{V}_h^{\mathrm{WF}} &= \boldsymbol{\mathcal{P}}_1^c(\mathcal{T}_h^{\mathrm{WF}}),\\ Y_h^{\mathrm{WF}} &= \{q \in \mathring{\mathcal{P}}_0(\mathcal{T}_h^{\mathrm{WF}}) :\ \theta_e(q) = 0\ \forall e \in \mathcal{E}_h^{\mathcal{S},I}\}.\end{aligned}$$

Then, we define an intermediate pressure space

$$\hat{Y}_h^{\mathrm{WF}} = \{q \in \mathring{\mathcal{P}}_0(\mathcal{T}_h^{\mathrm{WF}}) :\ \theta_e(q) = 0\ \forall e \in \mathcal{E}_h^{\mathcal{S}}\}.$$

We now define the spaces with boundary conditions

$$\begin{aligned}\mathring{\boldsymbol{V}}_h^{\mathrm{WF}} &= \boldsymbol{V}_h^{\mathrm{WF}} \cap \boldsymbol{H}_0^1(\Omega),\\ \mathring{Y}_h^{\mathrm{WF}} &= \hat{Y}_h^{\mathrm{WF}} \cap L_0^2(\Omega).\end{aligned}$$

5.3.2 Stability of $\mathring{\boldsymbol{V}}_h^{\mathrm{WF}} \times \mathring{Y}_h^{\mathrm{WF}}$

In this section, we show that the pair $\mathring{\boldsymbol{V}}_h^{\mathrm{WF}} \times \mathring{Y}_h^{\mathrm{WF}}$ is inf-sup stable. First we introduce some notation.

Let $\tau \in \mathcal{T}_h$, and let τ^{A} denote the local triangulation of τ consisting of four tetrahedra, obtained by connecting the vertices of τ with its incenter, i.e., τ^{A} denotes the Alfeld split of τ. For a face $F \subset \tau$, denote by F^{CT} the set of three triangles formed from F by the Worsey-Farin refinement, i.e., F^{CT} is the Clough-Tocher refinement of F. We denote by $\Delta_1^I(F^{\mathrm{CT}})$ the set of three interior edges in F^{CT}, and let $e_F \in \Delta_1^I(F^{\mathrm{CT}})$ denote an arbitrary, fixed interior edge of F^{CT}.

Definition 5.3.3. Consider the triangulation F^{CT} of a face $F \in \Delta_2(\tau)$, and let the three triangles of F^{CT} be labeled Q_1, Q_2, Q_3. Let $e = \partial Q_1 \cap \partial Q_2$ be an internal edge, let $\boldsymbol{t}$ be the unit vector tangent to e pointing away from the split point m_F, and let $\boldsymbol{s}$ be the unit vector orthogonal to $\boldsymbol{t}$ such that $\boldsymbol{s} \times \boldsymbol{n}_F = \boldsymbol{t}$. Then the jump of a piecewise smooth function p across e is defined as

$$[\![p]\!]_e = \big(p|_{Q_1} - p|_{Q_2}\big)\boldsymbol{s}.$$

We now state the degrees of freedom for the spaces $\mathring{\boldsymbol{V}}_h^{\mathrm{WF}}$ and $\mathring{Y}_h^{\mathrm{WF}}$. The proofs of the following two lemmas are given in [33, Lemmas 5.11–5.12].

Lemma 5.3.4. *A function $\boldsymbol{v} \in \boldsymbol{V}_h^{\mathrm{WF}}$ is uniquely determined by the values*

$$\begin{aligned}
&\boldsymbol{v}(a) && \forall a \in \Delta_0(\tau),\\
&\int_F (\boldsymbol{v}\cdot\boldsymbol{n}_F) && \forall F \in \Delta_2(\tau),\\
&\int_e [\![\mathrm{div}\boldsymbol{v}]\!]_e && \forall e \in \Delta_1^I(F^{\mathrm{CT}})\backslash\{e_F\},\ \forall F \in \Delta_2(\tau),\\
&\int_\tau (\mathrm{div}\boldsymbol{v})p && \forall p \in \mathring{\mathcal{V}}_0(\tau) := \mathcal{P}_0(\tau^{\mathrm{A}}) \cap L_0^2(\tau).
\end{aligned}$$

for each $T \in \mathcal{T}_h$.

Lemma 5.3.5. *A function $q \in Y_h^{\mathrm{WF}}$ is uniquely determined by*

$$\begin{aligned}
&\int_e [\![q]\!]_e && \forall e \in \Delta_1^I(F^{\mathrm{CT}})\backslash\{e_F\},\ \forall F \in \Delta_2(\tau),\\
&\int_\tau qp && \forall p \in \mathcal{P}_0(\tau^{\mathrm{A}}).
\end{aligned}$$

for all $\tau \in \mathcal{T}_h$.

If we restrict ourselves to $\hat{Y}_h^{\mathrm{WF}}$ then we only take interior faces F in the first set of degrees of freedom.

Proposition 5.3.6. *Let $\boldsymbol{v} \in \boldsymbol{V}_h^{\mathrm{WF}}$ and $\tau \in \mathcal{T}_h$. For $m = 0, 1$, there holds*

$$|\boldsymbol{v}|_{H^m(\tau)} \le C h_\tau^{-1-2m}\Big(h_\tau^4 \sum_{a\in\Delta_0(\tau)} |\boldsymbol{v}(a)|^2 + \sum_{F\in\Delta_2(\tau)} \Big|\int_F \boldsymbol{v}\cdot\boldsymbol{n}_F\Big|^2 + h_\tau^3 \|\mathrm{div}\boldsymbol{v}\|_{L^2(\tau)}^2\Big).$$

Proof. Let $\hat{\tau}$ be the reference tetrahedron, and let $F_\tau : \hat{\tau} \to \tau$ be an affine bijection with $F_\tau(\hat{x}) = A_\tau \hat{x} + b_\tau$ with $A_\tau \in \mathbb{R}^{3\times 3}$ and $b_\tau \in \mathbb{R}^3$. We define $\hat{\boldsymbol{v}} : \hat{\tau} \to \mathbb{R}^3$ via the Piola transform

$$\boldsymbol{v}(x) = \frac{A_\tau \hat{\boldsymbol{v}}(\hat{x})}{\det(A_\tau)}, \qquad x = F_\tau(\hat{x}).$$

Let $\hat{\tau}^{\mathrm{WF}}$ be the split of $\hat{\tau}$ induced by τ^{WF} and the mapping F_τ^{-1}, i.e.,

$$\hat{\tau}^{\mathrm{WF}} = \{F_\tau^{-1}(K) :\ K \in \tau^{\mathrm{WF}}\}.$$

Then $\hat{\boldsymbol{v}}$ is a continuous piecewise linear polynomial with respect to $\hat{\tau}^{\mathrm{WF}}$, and therefore by equivalence of norms, and Lemma 5.3.4,

$$|\hat{\boldsymbol{v}}|^2_{H^m(\hat{\tau})} \le C\Big(\sum_{\hat{a}\in\Delta_0(\hat{\tau})} |\hat{\boldsymbol{v}}(\hat{a})|^2 + \sum_{\hat{F}\in\Delta_2(\hat{\tau})} \Big| \int_{\hat{F}} \hat{\boldsymbol{v}}\cdot\hat{\boldsymbol{n}}_{\hat{F}} \Big|^2 + \sum_{\hat{F}\in\Delta_2(\hat{\tau})} \sum_{\hat{e}\in\Delta_1^I(\hat{F}^{\mathrm{CT}})\setminus\{\hat{e}_{\hat{F}}\}} \Big| \int_{\hat{e}} \Big[\Big[\widehat{\mathrm{div}}\hat{\boldsymbol{v}}\Big]\Big]_{\hat{e}} \Big|^2 + \sup_{\substack{\hat{p}\in\mathring{\mathcal{V}}_0(\hat{\tau}) \\ \|\hat{p}\|_{L^2(\hat{\tau})}=1}} \Big| \int_{\hat{\tau}} (\widehat{\mathrm{div}}\hat{\boldsymbol{v}})\hat{p} \Big|^2 \Big).$$

By well-known properties of the Piola transform, we have

$$\mathrm{div}\boldsymbol{v}(x) = \frac{1}{\det(A_\tau)}\widehat{\mathrm{div}}\hat{\boldsymbol{v}}(\hat{x}), \qquad \int_F \boldsymbol{v}\cdot\boldsymbol{n}_F = \int_{\hat{F}} \hat{\boldsymbol{v}}\cdot\hat{\boldsymbol{n}}_{\hat{F}}.$$

Thus, we have

$$|\hat{\boldsymbol{v}}|^2_{H^m(\hat{\tau})} \le C\Big(\sum_{a\in\Delta_0(\tau)} |\det(A_\tau)A_\tau^{-1}\boldsymbol{v}(a)|^2 + \sum_{F\in\Delta_2(\tau)} \Big| \int_F \boldsymbol{v}\cdot\boldsymbol{n}_F \Big|^2 + |\det(A_\tau)|^2 \sum_{F\in\Delta_2(\tau)} \sum_{e\in\Delta_1(F)\setminus\{e_F\}} \Big| \frac{|\hat{e}|}{|e|} \int_e [\![\mathrm{div}\boldsymbol{v}]\!]_e \Big|^2 + \sup_{\substack{\hat{p}\in\mathring{\mathcal{V}}_0(\hat{\tau}) \\ \|\hat{p}\|_{L^2(\hat{\tau})}=1}} \Big| \int_{\hat{\tau}} (\widehat{\mathrm{div}}\hat{\boldsymbol{v}})\hat{p} \Big|^2 \Big).$$

Next, for $\hat{p} \in \mathring{\mathcal{V}}_0(\hat{\tau})$ with $\|\hat{p}\|_{L^2(\hat{\tau})} = 1$, let $p : \tau \to \mathbb{R}$ be given by $p(x) = \hat{p}(\hat{x})$. Then $p \in \mathring{\mathcal{V}}_0(\tau)$, $\|p\|_{L^2(\tau)} = \sqrt{6|\tau|}$, and

$$\int_{\hat{\tau}} (\widehat{\mathrm{div}}\hat{\boldsymbol{v}})\hat{p} = \int_\tau (\mathrm{div}\boldsymbol{v})p.$$

We conclude

$$\sup_{\substack{\hat{p}\in\mathring{\mathcal{V}}_0(\hat{\tau}) \\ \|\hat{p}\|_{L^2(\hat{\tau})}=1}} \Big| \int_{\hat{\tau}} (\widehat{\mathrm{div}}\hat{\boldsymbol{v}})\hat{p} \Big|^2 \le \sup_{\substack{p\in\mathring{\mathcal{V}}_0(\tau) \\ \|p\|_{L^2(\tau)}=\sqrt{6|\tau|}}} \Big| \int_\tau (\mathrm{div}\boldsymbol{v})p \Big|^2 \le Ch_\tau^3 \|\mathrm{div}\boldsymbol{v}\|^2_{L^2(\tau)}.$$

Finally, we use $\|A_\tau^{-1}\| \le Ch_\tau^{-1}$ and $|\det(A_\tau)| = 6|\tau| \le Ch_\tau^3$ to get

$$|\hat{\boldsymbol{v}}|^2_{H^m(\hat{\tau})} \le C\Big(h_\tau^4 \sum_{a\in\Delta_0(\tau)} |\boldsymbol{v}(a)|^2 + \sum_{F\in\Delta_2(\tau)} \Big| \int_F \boldsymbol{v}\cdot\boldsymbol{n}_F \Big|^2 + h_\tau^4 \sum_{F\in\Delta_2(\tau)} \sum_{e\in\Delta_1^I(F^{\mathrm{CT}})\setminus\{e_F\}} \Big| \int_e [\![\mathrm{div}\boldsymbol{v}]\!]_e \Big|^2 + h_\tau^3 \|\mathrm{div}\boldsymbol{v}\|^2_{L^2(\tau)} \Big),$$

and therefore

$$
\begin{aligned}
|\boldsymbol{v}|^2_{H^m(\hat{\tau})} \le Ch_\tau^{-1-2m}|\hat{\boldsymbol{v}}|^2_{H^m(\hat{\tau})} \le Ch_\tau^{-1-2m}\Big(&h_\tau^4 \sum_{a\in\Delta_0(\tau)} |\boldsymbol{v}(a)|^2 + \sum_{F\in\Delta_2(\tau)} \Big| \int_F \boldsymbol{v}\cdot\boldsymbol{n}_F \Big|^2 \\
&+ h_\tau^4 \sum_{F\in\Delta_2(\tau)} \sum_{e\in\Delta_1(F)\backslash\{e_F\}} \Big| \int_e [\![\mathrm{div}\boldsymbol{v}]\!]_e \Big|^2 \\
&+ h_\tau^3 \|\mathrm{div}\boldsymbol{v}\|^2_{L^2(\tau)}\Big) \\
\le Ch_\tau^{-1-2m}\Big(&h_\tau^4 \sum_{a\in\Delta_0(\tau)} |\boldsymbol{v}(a)|^2 \\
&+ \sum_{F\in\Delta_2(\tau)} \Big| \int_F \boldsymbol{v}\cdot\boldsymbol{n}_F \Big|^2 + h_\tau^3 \|\mathrm{div}\boldsymbol{v}\|^2_{L^2(\tau)}\Big),
\end{aligned}
$$

where the last inequality comes from standard trace and inverse inequalities. □

Theorem 5.3.7. *The pair* $\mathring{\boldsymbol{V}}_h^{\mathrm{WF}} \times \mathring{Y}_h^{\mathrm{WF}}$ *is inf-sup stable.*

Proof. Fix a $q \in \mathring{Y}_h^{\mathrm{WF}}$, and let $\boldsymbol{w} \in \boldsymbol{H}_0^1(\Omega)$ satisfy $\mathrm{div}\boldsymbol{w} = q$ and $\|\nabla \boldsymbol{w}\|_{L^2(\Omega)} \le C\|q\|_{L^2(\Omega)}$. Let $\boldsymbol{w}_h \in \mathring{\boldsymbol{\mathcal{P}}}_1(\mathcal{T}_h)$ be the Scott-Zhang interpolant of $\boldsymbol{w}$ with respect to $\mathcal{T}_h$. Define $\boldsymbol{v} \in \mathring{\boldsymbol{\mathcal{P}}}_1(\mathcal{T}_h^{\mathrm{WF}})$ such that

$$
\begin{aligned}
&\boldsymbol{v}(a) = \boldsymbol{w}_h(a) && \forall a \in \Delta_0(\tau), \\
&\int_F (\boldsymbol{v}\cdot\boldsymbol{n}_F) = \int_F (\boldsymbol{w}\cdot\boldsymbol{n}_F) && \forall F \in \Delta_2(\tau), \\
&\int_e [\![\mathrm{div}\boldsymbol{v}]\!]_e = \int_e [\![q]\!]_e && \forall e \in \Delta_1^I(F^{\mathrm{CT}})\backslash\{e_F\},\ \forall F \in \Delta_2(\tau), \\
&\int_\tau (\mathrm{div}\boldsymbol{v})p = \int_\tau qp && \forall p \in \mathring{\mathcal{V}}_0(\tau).
\end{aligned}
$$

Noting $(\mathrm{div}\boldsymbol{v} - q) \in \boldsymbol{Y}_h^{\mathrm{WF}}$, and

$$
\begin{aligned}
&\int_e [\![\mathrm{div}\boldsymbol{v} - q]\!]_e = 0 && \forall e \in \Delta_1^I(F^{\mathrm{CT}})\backslash\{e_F\},\ \forall F \in \Delta_2(\tau), \\
&\int_\tau (\mathrm{div}\boldsymbol{v} - q)p && \forall p \in \mathcal{P}_0(\tau^{\mathrm{A}})
\end{aligned}
$$

for all $\tau \in \mathcal{T}_h$ (by the divergence theorem), we conclude $\mathrm{div}\boldsymbol{v} = q$ by Lemma 5.3.5.

We apply Proposition 5.3.6 to $(\boldsymbol{v}-\boldsymbol{w}_h)$ with $m=1$:

$$\begin{aligned}\|\nabla(\boldsymbol{v}-\boldsymbol{w}_h)\|^2_{L^2(\tau)} &\le Ch_\tau^{-3}\Big(h_\tau^4\sum_{a\in\Delta_0(\tau)}|(\boldsymbol{v}-\boldsymbol{w}_h)(a)|^2+\sum_{F\in\Delta_2(\tau)}\Big|\int_F(\boldsymbol{v}-\boldsymbol{w}_h)\cdot\boldsymbol{n}_F\Big|^2\\ &\qquad +h_\tau^3\|\mathrm{div}(\boldsymbol{v}-\boldsymbol{w}_h)\|^2_{L^2(\tau)}\Big)\\ &= Ch_\tau^{-3}\Big(\sum_{F\in\Delta_2(\tau)}\Big|\int_F(\boldsymbol{w}-\boldsymbol{w}_h)\cdot\boldsymbol{n}_F\Big|^2+h_\tau^3\|q-\mathrm{div}\boldsymbol{w}_h\|^2_{L^2(\tau)}\Big)\\ &\le Ch_\tau^{-3}\Big(h_\tau^2\sum_{F\in\Delta_2(\tau)}\|\boldsymbol{w}-\boldsymbol{w}_h\|^2_{L^2(F)}+h_\tau^3\|q-\mathrm{div}\boldsymbol{w}_h\|^2_{L^2(\tau)}\Big)\\ &\le C\Big(\|q\|^2_{L^2(\tau)}+h_\tau^{-2}\|\boldsymbol{w}-\boldsymbol{w}_h\|^2_{L^2(\tau)}+\|\nabla(\boldsymbol{w}-\boldsymbol{w}_h)\|^2_{L^2(\tau)}+\|\nabla\boldsymbol{w}_h\|^2_{L^2(\tau)}\Big).\end{aligned}$$

We then sum over $\tau\in\mathcal{T}_h$ and apply stability and approximation properties of the Scott-Zhang interpolant to conclude $\|\nabla\boldsymbol{v}\|_{L^2(\Omega)}\le C\|q\|_{L^2(\Omega)}$.

□

5.4 Implementation Aspects for Powell-Sabin Splits

The only tricky part to implement these finite elements is the pressure spaces since they have non-standard constraints in their definitions. In this section and the subsequent one, we give details to form the algebraic system for the Stokes problem.

5.4.1 A basis for the weak continuity pressure space and the construction of the algebraic system

Recall the pair $\boldsymbol{X}_h^{PS}\times Q_h^{PS}$ defined on the Powell-Sabin triangulation $\mathcal{T}_h^{PS}$ in equation (76).

Clearly, the space Q_h^{PS} is a non-standard space, and in particular the space is not explicitly found in current finite element software packages. Nonetheless, in this section, we identify a basis of the space Q_h^{PS}, and as a byproduct show that the weak continuity property $\theta_z(q)=0$ can be imposed purely at the algebraic level.

To be consistent with the notation introduced in section 5.2, let $\mathring{\boldsymbol{V}}_h^{\mathrm{PS}}\times\mathring{Y}_h^{\mathrm{PS}}=\boldsymbol{X}_h^{PS}\times Q_h^{PS}$.

As a first step, we note that, by definition of the Powell–Sabin triangulation,

$$\mathcal{T}_h^{\mathrm{PS}} = \{K_z^{(j)} : \ K_z^{(j)} \in \mathcal{T}_z, \ z \in \mathcal{S}_h\}.$$

With this (implicit) labeling of the triangles in $\mathcal{T}_h^{\mathrm{PS}}$, we can write the canonical basis of $\mathcal{P}_0(\mathcal{T}_h^{\mathrm{PS}})$ as the set $\{\varphi_z^{(j)}\} \subset \mathcal{P}_0(\mathcal{T}_h^{\mathrm{PS}})$ with

$$\varphi_z^{(j)}|_{K_v^{(i)}} = \delta_{v,z}\delta_{i,j} \qquad \forall z, v \in \mathcal{S}_h, \ i = 1, \ldots, n_v, \ j = 1, \ldots, n_z.$$

The next proposition shows that a basis of $\mathring{Y}_h^{\mathrm{PS}}$ is easily extracted from the basis of $\mathcal{P}_0(\mathcal{T}_h^{\mathrm{PS}})$ (see Figure 10).

Proposition 5.4.1. *For each $z \in \mathcal{S}_h$ and $j \in \{2, \ldots, n_z\}$, define*

$$\psi_z^{(j)} = \varphi_z^{(j)} + (-1)^j \varphi_z^{(1)}.$$

Then $\{\psi_z^{(j)} : \ z \in \mathcal{S}_h, \ j = 2, \ldots, n_z\}$ forms a basis of $\hat{Y}_h^{\mathrm{PS}}$.

Proof. Note that the number of functions $\{\psi_z^{(j)}\}$ given is $\sum_{z \in \mathcal{S}_h}(n_z - 1)$, and

$$\dim Y_h^{PS} = \dim \mathcal{P}_0(\mathcal{T}_h^{\mathrm{PS}}) - |\mathcal{S}_h| = \sum_{z \in \mathcal{S}_h} n_z - |\mathcal{S}_h| = \sum_{z \in \mathcal{S}_h} (n_z - 1).$$

Because $\psi_z^{(j)} \in \mathring{Y}_h^{\mathrm{PS}}$, and they are clearly linear independent, we conclude that $\{\psi_z^{(j)}\}$ form a basis of $\mathring{Y}_h^{\mathrm{PS}}$. □

We now explain how Proposition 5.4.1 provides a simple way to construct the stiffness matrix for the Stokes problem using the $\mathring{\boldsymbol{V}}_h^{\mathrm{PS}} \times \mathring{Y}_h^{\mathrm{PS}}$ pair. To explain the procedure, we require some notation.

Let A be the matrix associated with the bilinear form

$$(\boldsymbol{v}, \boldsymbol{w}) \to \int_\Omega \nu \nabla \boldsymbol{v} : \nabla \boldsymbol{w} \, dx \quad \text{over } \boldsymbol{v}, \boldsymbol{w} \in \mathring{\boldsymbol{V}}_h^{\mathrm{PS}},$$

and let $\tilde{B}$ is the matrix associated with the bilinear form

$$(\boldsymbol{v}, q) \to -\int_\Omega (\mathrm{div} \boldsymbol{v}) q \, dx \quad \text{over } \boldsymbol{v} \in \mathring{\boldsymbol{V}}_h^{\mathrm{PS}}, \ q \in \mathcal{P}_0(\mathcal{T}_h^{\mathrm{PS}}).$$

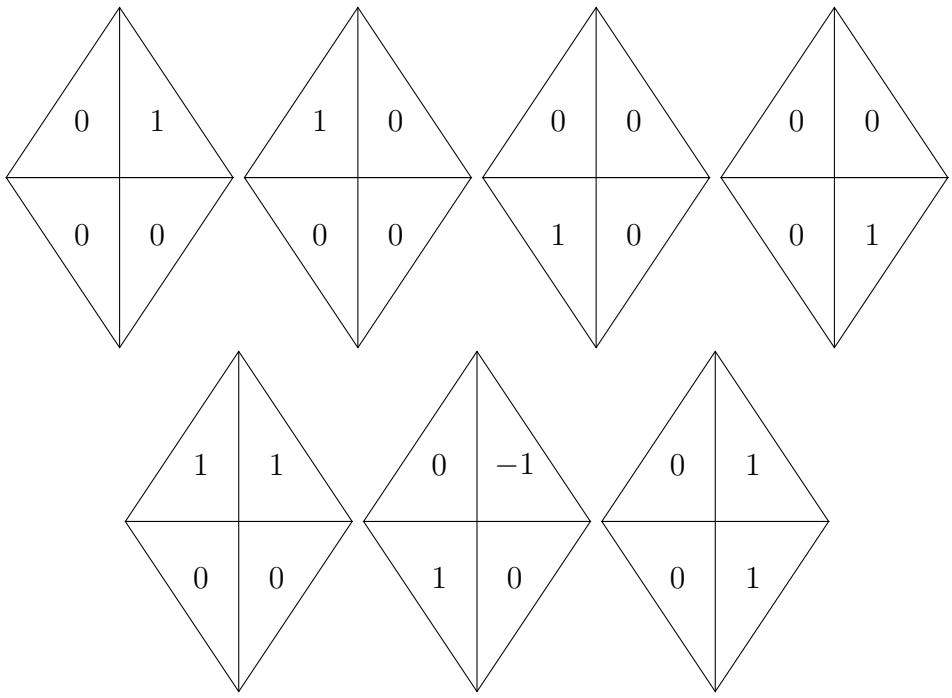

Figure 10: Local mesh $\mathcal{T}_z$ with $z \in \mathcal{S}_h^I$. Top row: Values of canonical basis functions of piecewise constants $\{\varphi_z^{(j)}\}_{j=1}^{n_z}$. Bottom row: Values of basis functions of piecewise constants with weak continuity constraint $\{\psi_z^{(j)}\}_{j=2}^{n_z}$.

The stiffness matrix for the Stokes problem based on the (unstable) $\mathring{\boldsymbol{V}}_h^{\mathrm{PS}} \times \mathcal{P}_0(\mathcal{T}_h^{\mathrm{PS}})$ pair is given by

$$\begin{pmatrix} A & \tilde{B} \\ \tilde{B}^{\intercal} & 0 \end{pmatrix}.$$

We emphasize that this system can be easily constructed using standard finite element software packages.

Let $\{\boldsymbol{\phi}^{(i)}\}_{k=1}^{N}$ denote a basis of $\mathring{\boldsymbol{V}}_h^{\mathrm{PS}}$ with $N = \dim \mathring{\boldsymbol{V}}_h^{\mathrm{PS}}$ so that

$$A_{i,j} = \nu \int_\Omega \nabla \boldsymbol{\phi}^{(j)} : \nabla \boldsymbol{\phi}^{(i)}\, dx.$$

Let $M = \dim \mathcal{P}_0(\mathcal{T}_h^{\mathrm{PS}})$, the number of triangles in $\mathcal{T}_h^{\mathrm{PS}}$, and introduce the local-to-global label mapping $\sigma : \mathcal{S} \times \{1, \dots, n_z\} \to \{1, 2, \dots, M\}$ such that

$$\tilde{B}_{i,\sigma(z,j)} = -\int_\Omega (\mathrm{div}\boldsymbol{\phi}^{(i)}) \varphi_z^{(j)}\, dx.$$

Then by Proposition 5.4.1, we have for $z \in \mathcal{S}_h$ and $j = 2, \dots, n_z$,

$$\begin{aligned} -\int_\Omega (\mathrm{div}\boldsymbol{\phi}^{(i)}) \psi_z^{(j)}\, dx &= -\int_\Omega (\mathrm{div}\boldsymbol{\phi}^{(i)}) \varphi_z^{(j)}\, dx - (-1)^j \int_\Omega (\mathrm{div}\boldsymbol{\phi}^{(i)}) \varphi_z^{(1)}\, dx \\ &= \tilde{B}_{i,\sigma(z,j)} + (-1)^j \tilde{B}_{i,\sigma(z,1)}. \end{aligned}$$

This identity leads to the following algorithm.

1. Construct Powell–Sabin triangulation $\mathcal{T}_h^{\mathrm{PS}}$
2. Construct $\tilde{B} \in \mathbb{R}^{N \times M}$ based on the $\mathring{\boldsymbol{V}}_h^{\mathrm{PS}} \times \mathcal{P}_0(\mathcal{T}_h^{\mathrm{PS}})$ pair.
3. Set $B = \tilde{B}$.
4. For each $z \in \mathcal{S}_h$ and for each $j \in \{2, \dots, n_z\}$, do the elementary column operation

$$B_{:,\sigma(z,j)} = B_{:,\sigma(z,j)} + (-1)^j B_{:,\sigma(z,1)}.$$

5. Delete column $B_{:,\sigma(z,1)}$ for each $z \in \mathcal{S}_h$.

The stiffness matrix for the Stokes problem based on the $\mathring{\boldsymbol{V}}_h^{\mathrm{PS}} \times \hat{Y}_h^{\mathrm{PS}}$ pair is then given by

$$\begin{pmatrix} A & B \\ B^{\intercal} & 0 \end{pmatrix}. \tag{79}$$

5.5 Implemenation Aspects for Worsey Farin Splits

5.5.1 A basis for $\hat{Y}_h^{\mathrm{WF}}$ and the construction of the algebraic system

Notice that the collection of local triangulations $\mathcal{T}_e$ (with $e \in \mathcal{E}_h^{\mathcal{S}}$) do not form a disjoint partition of the global triangulation $\mathcal{T}_h^{\mathrm{WF}}$. In particular, there exists $K \in \mathcal{T}_h^{\mathrm{WF}}$ such that $K \in \mathcal{T}_e$ and $K \in \mathcal{T}_s$ with $e, s \in \mathcal{E}_h^{\mathcal{S}}$ and $e \neq s$. As a result, the methodology used in the previous section for Powell–Sabin meshes is not directly applicable.

Instead, we consider a geometric decomposition of the mesh based on the face split points in $\mathcal{T}_h^{\mathrm{WF}}$. To this end, we denote by $\mathcal{S}_h^I$ and $\mathcal{S}_h^B$ the sets of interior and boundary face split points, respectively, and set $\mathcal{S}_h = \mathcal{S}_h^I \cup \mathcal{S}_h^B$. For $z \in \mathcal{S}_h$, let $\mathcal{T}_z := \{K_z^{(1)}, \dots, K_z^{(n_z)}\}$ denote the set of tetrahedra in $\mathcal{T}_h^{\mathrm{WF}}$ that have z as a vertex. Here, $n_z = 6$ if z is an interior vertex, and $n_z = 3$ if z is a boundary vertex. For an interior face split point z, we assume the simplices in $\mathcal{T}_z$ are labeled such that

$$K_z^{(1)}, K_z^{(2)}, K_z^{(3)} \subset \tau^{(1)}, \qquad K_z^{(4)}, K_z^{(5)}, K_z^{(6)} \subset \tau^{(2)}$$

for some $\tau^{(1)}, \tau^{(2)} \in \mathcal{T}_h$, and that $K_z^{(j)}$ and $K_z^{(j+3)}$ share a common face for $j \in \{1, 2, 3\}$. For a boundary split point z, the set $\mathcal{T}_z = \{K_z^{(1)}, K_z^{(2)}, K_z^{(3)}\}$ is labeled arbitrarily.

We clearly have

$$\mathcal{T}_h^{\mathrm{WF}} = \{K_z^{(j)} : \ z \in \mathcal{S}_h, j = 1, \dots, n_z\}, \tag{80}$$

and the map $(z, j) \to K_z^{(j)}$ is injective. Furthermore, each local partition $\mathcal{T}_z$ contains three singular edges.

Proposition 5.5.1. *There holds*

$$\dim \hat{Y}_h^{\mathrm{WF}} = 4|\mathcal{S}_h^I| + |\mathcal{S}_h^B|.$$

Proof. By Proposition 5.3.5, we have

$$\dim \hat{Y}_h^{\mathrm{WF}} = 4|\mathcal{T}_h| + 2|\mathcal{F}_h^I|,$$

where $|\mathcal{F}_h^I|$ is the number of interior faces in $\mathcal{T}_h$. From (80), we have

$$12|\mathcal{T}_h| = |\mathcal{T}_h^{\mathrm{WF}}| = 6|\mathcal{S}_h^I| + 3|\mathcal{S}_h^B|,$$

and by construction of the Worsey-Farin split, there holds

$$|\mathcal{F}_h| = |\mathcal{S}_h^I|.$$

Therefore,

$$\dim \hat{Y}_h^{\mathrm{WF}} = 4|\mathcal{T}_h| + 2|\mathcal{F}_h^I| = \frac{1}{3}\big(6|\mathcal{S}_h^I| + 3|\mathcal{S}_h^B|\big) + 2|\mathcal{S}_h^I| = 4|\mathcal{S}_h^I| + |\mathcal{S}_h^B|.$$

□

For an interior split point z, and for a piecewise constant function q on $\mathcal{T}_z$, the three constraints $\theta_e(q) = 0$ read

$$\begin{aligned} q_1 - q_2 + q_5 - q_4 &= 0, \\ q_2 - q_3 + q_6 - q_5 &= 0, \\ q_3 - q_1 + q_4 - q_6 &= 0, \end{aligned}$$

where $q_j = q|_{K_z^{(j)}}$

We write this as a 3×6 linear system

$$C\vec{q} := \begin{pmatrix} 1 & -1 & 0 & -1 & 1 & 0 \\ 0 & 1 & -1 & 0 & -1 & 1 \\ -1 & 0 & 1 & 1 & 0 & -1 \end{pmatrix} \begin{pmatrix} q_1 \\ q_2 \\ q_3 \\ q_4 \\ q_5 \\ q_6 \end{pmatrix} = 0.$$

We clearly see that this matrix has rank 2 (e.g., adding the first and third rows gets the negation of the second row). We find that the nullspace of C is given by

$$\mathrm{null}(C) = \mathrm{span}\left\{ \begin{pmatrix} 1 \\ 1 \\ 1 \\ 0 \\ 0 \\ 0 \end{pmatrix}, \begin{pmatrix} 1 \\ 0 \\ 0 \\ 1 \\ 0 \\ 0 \end{pmatrix}, \begin{pmatrix} 0 \\ 1 \\ 0 \\ 0 \\ 1 \\ 0 \end{pmatrix}, \begin{pmatrix} -1 \\ -1 \\ 0 \\ 0 \\ 0 \\ 1 \end{pmatrix} \right\}.$$

These four vectors implicitly give us a basis for $\hat{Y}_h^{\mathrm{WF}}$. In particular, we have

Proposition 5.5.2. *For $z \in \mathcal{S}_h$ and $j \in \{1, 2, \dots, n_z\}$, let $\varphi_z^{(j)}$ be the piecewise constant function*

$$\varphi_z^{(j)}|_{K_v^{(i)}} = \delta_{v,z}\delta_{i,j} \qquad \forall v, z \in \mathcal{S}_h,\ i = 1, \dots, n_v,\ j = 1, \dots, n_z.$$

For an interior face split point z, define

$$\begin{aligned}
\psi_z^{(3)} &= \varphi_z^{(3)} + \varphi_z^{(1)} + \varphi_z^{(2)}, \\
\psi_z^{(4)} &= \varphi_z^{(4)} + \varphi_z^{(1)}, \\
\psi_z^{(5)} &= \varphi_z^{(5)} + \varphi_z^{(2)}, \\
\psi_z^{(6)} &= \varphi_z^{(6)} - \varphi_z^{(1)} - \varphi_z^{(2)}.
\end{aligned}$$

For a boundary face split point z, define

$$\psi_z^{(3)} = \varphi_z^{(3)} + \varphi_z^{(1)} + \varphi_z^{(2)}.$$

Then $\{\psi_z^{(j)}\}$ is a basis of $\hat{Y}_h^{\mathrm{WF}}$.

Proof. The proof essentially follows from the same arguments as Proposition 5.4.1, noting that the number of given $\psi_z^{(j)}$ is

$$4|\mathcal{S}_h^I| + |\mathcal{S}_h^B| = \dim \hat{Y}_h^{\mathrm{WF}}$$

by Proposition 5.5.1. □

As in the two-dimensional case, Proposition 5.5.2 give an algorithm to construct the stiffness matrix for the Stokes problem using the $\mathring{\boldsymbol{V}}_h^{\mathrm{WF}} \times \hat{Y}_h^{\mathrm{WF}}$ pair. First, we construct the stiffness matrix based on the $\mathring{\boldsymbol{V}}_h^{\mathrm{WF}} \times \mathcal{P}_0(\mathcal{T}_h^{\mathrm{WF}})$ pair:

$$\begin{pmatrix} A & \tilde{B} \\ \tilde{B}^{\intercal} & 0 \end{pmatrix},$$

and then perform elementary column operations on the $\tilde{B}$.

Let $\{\boldsymbol{\phi}^{(k)}\}_{k=1}^N$ denote a basis of $\mathring{\boldsymbol{V}}_h^{\mathrm{WF}}$ with $N = \dim \mathring{\boldsymbol{V}}_h^{\mathrm{WF}}$ and let $M = \dim \mathcal{P}_0(\mathcal{T}_h^{\mathrm{WF}})$ be the number of tetrahedra in $\mathcal{T}_h^{\mathrm{WF}}$, and introduce the local-to-global label mapping $\sigma : \mathcal{S}_h \times \{1, \dots, n_z\} \to \{1, 2, \dots, M\}$ such that

$$\tilde{B}_{k,\sigma(z,j)} = -\int_\Omega (\mathrm{div}\boldsymbol{\phi}^{(k)})\varphi_z^{(j)}.$$

Proposition 5.5.2 leads to the following algorithm.

1. Construct Worsey-Farin triangulation $\mathcal{T}_h^{\mathrm{WF}}$
2. Construct $\tilde{B} \in \mathbb{R}^{N\times M}$ based on the $\mathring{\boldsymbol{V}}_h^{\mathrm{WF}} \times \mathcal{P}_0(\mathcal{T}_h^{\mathrm{WF}})$ pair.
3. Set $B = \tilde{B}$.
4. For each interior face split point $z \in \mathcal{S}_h$ do the elementary column operations

$$\begin{aligned}
B_{:,\sigma(z,3)} &= B_{:,\sigma(z,3)} + B_{:,\sigma(z,1)} + B_{:,\sigma(z,2)},\\
B_{:,\sigma(z,4)} &= B_{:,\sigma(z,4)} + B_{:,\sigma(z,1)},\\
B_{:,\sigma(z,5)} &= B_{:,\sigma(z,5)} + B_{:,\sigma(z,2)},\\
B_{:,\sigma(z,6)} &= B_{:,\sigma(z,6)} - B_{:,\sigma(z,1)} - B_{:,\sigma(z,2)}.
\end{aligned}$$

5. For each boundary face split point $z \in \mathcal{S}_h$ do the elementary column operation

$$B_{:,\sigma(z,3)} = B_{:,\sigma(z,3)} + B_{:,\sigma(z,1)} + B_{:,\sigma(z,2)}.$$

6. Delete columns $B_{:,\sigma(z,1)}$ and $B_{:,\sigma(z,2)}$ for each $z \in \mathcal{S}_h$.

The stiffness matrix for the Stokes problem based on the $\mathring{\boldsymbol{V}}_h^{\mathrm{WF}} \times \hat{Y}_h^{\mathrm{WF}}$ pair is then given by

$$\begin{pmatrix} A & B \\ B^{\intercal} & 0 \end{pmatrix}. \tag{81}$$

5.6 Numerical Experiments

In this section, we perform some simple numerical experiments for the Stokes problem on Powell–Sabin and Worsey–Farin splits. We note standard theory shows that the velocity and pressure errors satisfy

$$|\boldsymbol{u} - \boldsymbol{u}_h|_{H^1(\Omega)} \leq (1+\beta^{-1}) \inf_{\boldsymbol{v}_h \in \boldsymbol{V}_h} |\boldsymbol{v}_h - \boldsymbol{u}|_{H^1(\Omega)}, \tag{82}$$

$$\|p - p_h\|_{L^2(\Omega)} \leq \inf_{q\in Y_h} \|p - q\|_{L^2(\Omega)} + \frac{\nu}{\beta}|\boldsymbol{u} - \boldsymbol{u}_h|_{H^1(\Omega)}, \tag{83}$$

where either $\boldsymbol{V}_h \times Y_h = \boldsymbol{V}_h^{\mathrm{PS}} \times \mathring{Y}_h^{\mathrm{PS}}$ or $\boldsymbol{V}_h \times Y_h = \mathring{\boldsymbol{V}}_h^{\mathrm{WF}} \times \mathring{Y}_h^{\mathrm{WF}}$, $\nu > 0$ is the viscosity, and β is the inf-sup constant for the finite element pair $\boldsymbol{V}_h \times Y_h$.

Table 3: Errors and rates of convergence for example (84) with $\nu = 1$.

h	$\|\boldsymbol{u} - \boldsymbol{u}_h\|_{L^2(\Omega)}$	rate	$\|p - p_h\|_{L^2(\Omega)}$	rate	$\|\nabla \cdot \boldsymbol{u}_h\|_{L^2(\Omega)}$	β
2^{-2}	1.70E-01	–	5.26E 00	–	2.70E-14	1.56E-01
2^{-3}	5.66E-02	1.587	3.77E 00	0.480	6.65E-14	1.38E-01
2^{-4}	1.35E-02	2.068	1.68E 00	1.166	2.38E-13	1.07E-01
2^{-5}	3.35E-03	2.011	8.28E-01	1.021	8.38E-12	1.06E-01
2^{-6}	8.77E-04	1.934	4.25E-01	0.962	4.05E-10	9.34E-02

5.6.1 The Stokes pair on Powell-Sabin splits

We consider the example such that the data is taken to be $\Omega = (0,1)^2$, and the source function is chosen such that the exact velocity and pressure solutions for (54) are given respectively as

$$\boldsymbol{u} = \begin{pmatrix} \pi \sin^2(\pi x_1)\sin(2\pi x_2) \\ -\pi \sin^2(\pi x_2)\sin(2\pi x_1) \end{pmatrix}, \quad p = \cos(\pi x_1)\cos(\pi x_2). \tag{84}$$

Let $\mathcal{T}_h$ be a Delaunay triangulation of Ω and $\mathcal{T}_h^{PS}$ the corresponding Powell-Sabin global triangulation.

The resulting errors, rates of convergence, and inf-sup constants are listed in Tables 3 and 4 for viscosities $\nu = 1$ and $\nu = 10^{-2}$, respectively. The results show that the L^2 pressure error and the H^1 velocity error converge with linear rate, the discrete velocity solution (and error) are independent of the viscosity ν, and the pressure error improves for small viscosity. The experiments also show that the inf-sup constant does not deteriorate as the mesh is refined with $\beta \approx 0.1$. These results are in agreement with the theoretical estimates (82)–(83)

In Tables 5 and 6, we compute the right-hand side of (83) and (82), respectively, and compare the data with the computed errors $\|p - p_h\|_{L^2(\Omega)}$ and $|\boldsymbol{u} - \boldsymbol{u}_h|_{H^1(\Omega)}$. Again, the results are consistent with (82)–(83), and they suggest that the term $|\boldsymbol{u} - \boldsymbol{u}_h|_{H^1(\Omega)}$ is the dominant term in the pressure error (83).

Table 4: Errors and rates of convergence for example (84) with $\nu = 10^{-2}$.

h	$\|\boldsymbol{u} - \boldsymbol{u}_h\|_{L^2(\Omega)}$	rate	$\|p - p_h\|_{L^2(\Omega)}$	rate	$\|\nabla \cdot \boldsymbol{u}_h\|_{L^2(\Omega)}$
2^{-2}	1.70E-01	–	1.02E-01	–	2.43E-14
2^{-3}	5.66E-02	1.587	5.79E-02	0.816	5.88E-14
2^{-4}	1.35E-02	2.068	2.76E-02	1.069	2.36E-13
2^{-5}	3.35E-03	2.011	1.37E-02	1.010	8.39E-12
2^{-6}	8.77E-04	1.934	6.96E-03	0.977	4.05E-10

Table 5: Errors for example (84) with $\nu = 10^{-2}$ and the RHS of (83) .

h	$\|p - p_h\|_{L^2(\Omega)}$	$\|\boldsymbol{u} - \boldsymbol{u}_h\|_{H^1(\Omega)}$	β_h	$\inf_{q \in \mathring{Y}_h^{\mathrm{PS}}} \|p - q\|_{L^2(\Omega)}$	RHS of (83)
2^{-2}	1.02E-01	3.77E 00	1.56E-01	6.08E-02	3.02E-01
2^{-3}	5.79E-02	2.17E 00	1.38E-01	2.77E-02	1.84E-01
2^{-4}	2.76E-02	1.07E 00	1.07E-01	1.35E-02	1.13E-01
2^{-5}	1.37E-02	5.32E-01	1.06E-01	6.61E-03	5.67E-02
2^{-6}	6.96E-03	2.72E-01	9.34E-02	3.28E-03	3.24E-02

Table 6: Errors for example (84) with $\nu = 10^{-2}$ and the RHS of (82) .

h	$\|\boldsymbol{u} - \boldsymbol{u}_h\|_{H^1(\Omega)}$	β_h	$\inf_{\boldsymbol{v}_h \in \boldsymbol{V}_h^{\mathrm{PS}}} \|\boldsymbol{v}_h - \boldsymbol{u}\|_{H^1(\Omega)}$	RHS of (82)
2^{-2}	3.77E 00	1.56E-01	3.08E 00	2.28E+01
2^{-3}	2.17E 00	1.38E-01	1.63E 00	1.34E+01
2^{-4}	1.07E 00	1.07E-01	8.04E-01	8.31E 00
2^{-5}	5.32E-01	1.06E-01	4.06E-01	4.23E 00
2^{-6}	2.72E-01	9.34E-02	2.05E-01	2.39E 00

5.6.2 The Stokes pair on Worsey-Farin splits

We consider the example such that the data is taken to be $\Omega = (0,1)^3$, and the source function is chosen such that the exact velocity and pressure solutions for (54) are given respectively as

$$\boldsymbol{u} = \begin{pmatrix} \pi \sin^2(\pi x_1)\sin(2\pi x_2) \\ -\pi \sin^2(\pi x_2)\sin(2\pi x_1) \\ 0 \end{pmatrix}, \quad p = \cos(\pi x_1)\cos(\pi x_2)\cos(\pi x_3). \tag{85}$$

Let $\mathcal{T}_h$ be a Delaunay triangulation of Ω and $\mathcal{T}_h^{WF}$ be the corresponding Worsey-Farin global triangulation.

The resulting rates of convergence of the numerical experiments for viscosities $\nu = 1$ and $\nu = 10^{-3}$ are listed in Tables 7 and 8, respectively. We also state the computed inf-sup constant on these meshes, and the results show that that it stays uniformly bounded from below with $\beta \approx 0.13$ on all meshes. The stated errors, especially those in Table 7, indicate that the rates of convergence are still in the preasymptotic regime. On the other hand, for small viscosity value $\nu = 10^{-3}$, Table 8 shows that the pressure error converges with linear rate. This behavior suggests that the velocity error is the dominating term in (83).

To verify this claim, we explicitly compute the right-hand side of (83) and (82) and report the results in Tables 9 and 10, respectively. The results show that indeed $|\boldsymbol{u} - \boldsymbol{u}_h|_{H^1(\Omega)}$ is the dominating term in the pressure error (83).

5.6.3 Iterated penalty method for $(\mathbf{P_1}, \mathbf{P_0})$ pair on Worsey-Farin splits

We consider the example such that the data is taken to be $\Omega = (0,1)^3$, and the source function is chosen such that the exact velocity and pressure solutions for (54) are given respectively as

$$\boldsymbol{u}(x,y,z) = \nabla \times \begin{pmatrix} 0 \\ g \\ g \end{pmatrix}, \quad p = \frac{1}{9}\frac{\partial^2 g}{\partial x \partial y}, \tag{86}$$

Table 7: Errors and rates of convergence for example (85) with $\nu = 1$.

h	$\|\boldsymbol{u} - \boldsymbol{u}_h\|_{L^2(\Omega)}$	rate	$\|p - p_h\|_{L^2(\Omega)}$	rate	$\|\nabla \cdot \boldsymbol{u}_h\|_{L^2(\Omega)}$	β
1/2	1.29E 00	–	9.81E 00	–	5.07E-14	1.31E-01
1/4	8.58E-01	0.588	19.4E 00	-0.98	5.20E-13	1.31E-01
1/8	3.93E-01	1.286	16.6E 00	0.414	2.68E-12	1.32E-01
1/16	1.32E-01	1.573	10.5E 00	0.667	4.10E-12	1.32E-01
1/32	3.69E-02	1.839	5.75E 00	0.872	4.32E-12	1.32E-01
1/48	1.68E-02	1.941	3.93E 00	0.936	6.07E-12	1.32E-01

Table 8: Errors and rates of convergence for example (85) with $\nu = 10^{-3}$.

h	$\|\boldsymbol{u} - \boldsymbol{u}_h\|_{L^2(\Omega)}$	rate	$\|p - p_h\|_{L^2(\Omega)}$	rate	$\|\nabla \cdot \boldsymbol{u}_h\|_{L^2(\Omega)}$
1/2	1.29E 00	–	1.33E-01	–	1.28E-15
1/4	8.58E-01	0.588	6.97E-02	0.932	3.43E-14
1/8	3.93E-01	1.286	3.70E-02	0.911	3.22E-13
1/16	1.32E-01	1.574	1.91E-02	0.953	6.40E-13
1/32	3.69E-02	1.838	9.68E-03	0.980	9.52E-13
1/48	9.63E-03	1.940	4.89E-03	0.983	1.03E-12

Table 9: Errors for example (85) with $\nu = 10^{-3}$ and the RHS of (83) .

h	$\|p - p_h\|_{L^2(\Omega)}$	$\|\boldsymbol{u} - \boldsymbol{u}_h\|_{H^1(\Omega)}$	β_h	$\inf_{q \in \mathring{Y}_h^{\mathrm{WF}}} \|p - q\|_{L^2(\Omega)}$	RHS of (83)
1/2	1.33E-01	1.07E+01	1.31E-01	5.00E-01	5.81E-01
1/4	6.97E-02	8.50E 00	1.31E-01	6.70E-02	1.31E-01
1/6	4.81E-02	6.82E 00	1.32E-01	4.43E-02	9.59E-02
1/8	3.70E-02	5.60E 00	1.32E-01	3.30E-02	7.54E-02
1/10	3.02E-02	4.71E 00	1.32E-01	2.63E-02	6.19E-02
1/12	2.55E-02	4.06E 00	1.32E-01	2.19E-02	5.26E-02

Table 10: Errors for example (85) with $\nu = 10^{-3}$ and the RHS of (82) .

h	$\|\boldsymbol{u} - \boldsymbol{u}_h\|_{H^1(\Omega)}$	β_h	$\inf_{\boldsymbol{v}_h \in \mathring{\boldsymbol{V}}_h^{\mathrm{WF}}} \|\boldsymbol{v}_h - \boldsymbol{u}\|_{H^1(\Omega)}$	RHS of (82)
1/2	1.07E+01	1.31E-01	9.99E 00	8.62E+01
1/4	8.50E 00	1.31E-01	5.85E 00	5.05E+01
1/6	6.82E 00	1.32E-01	4.08E 00	3.49E+01
1/8	5.60E 00	1.32E-01	3.10E 00	2.65E+01
1/10	4.71E 00	1.32E-01	2.49E 00	2.13E+01
1/12	4.06E 00	1.32E-01	2.08E 00	1.78E+01

Table 11: Errors and rates of convergence for example (86) with $\nu = 1$.

h	$\|\boldsymbol{u} - \boldsymbol{u}_h^n\|_{L^2(\Omega)}$	rate	$\|\boldsymbol{u} - \boldsymbol{u}_h^n\|_{H^1(\Omega)}$	rate	$\|p - p_h^n\|_{L^2(\Omega)}$	rate
2^{-2}	1.11768	-	11.55063	-	25.32256	-
2^{-3}	0.48896	1.19273	7.53829	0.61566	22.35349	0.17992
2^{-4}	0.15482	1.65908	4.15598	0.85905	13.67635	0.70882
2^{-5}	0.04176	1.89040	2.13224	0.96282	7.24129	0.91736
1/48	0.01881	1.96680	1.42643	0.99145	4.88909	0.96875

where

$$g = g(x, y, z) = 2^{12}(x - x^2)^2(y - y^2)^2(z - z^2)^2.$$

Similar to the previous section, we let $\mathcal{T}_h$ be a delaunay triangulation of Ω and $\mathcal{T}_h^{\mathrm{WF}}$ be the corresponding Worsey-Farin global triangulation.

The iterated penalty method [15] applied to the Stokes equations with $\mathring{\boldsymbol{V}}_h = \mathring{\boldsymbol{V}}_h^{\mathrm{WF}}$ reads: Let $\boldsymbol{u}_h^0 = \boldsymbol{0}$ and $\rho, \gamma > 0$ be parameters. For $n \geq 1$, $\boldsymbol{u}_h^n$ is recursively defined to be the solution to the variational formulation

$$\nu(\nabla \boldsymbol{u}_h^n, \nabla \boldsymbol{v}) + \gamma(\nabla \cdot \boldsymbol{v}, \nabla \cdot \boldsymbol{u}_h^n) = (\boldsymbol{f}, \boldsymbol{v}) - (\sum_{i=0}^{n-1} \rho \nabla \cdot \boldsymbol{u}_h^i, \nabla \cdot \boldsymbol{v}), \quad \forall \boldsymbol{v} \in \mathring{\boldsymbol{V}}_h^{WF}. \tag{87}$$

It was shown in [15] that $\lim_{n\to\infty} \boldsymbol{u}_h^n = \boldsymbol{u}_h$ and $\lim_{n\to\infty} \sum_{i=0}^n \rho \nabla \cdot \boldsymbol{u}_h^i = p_h$. Also, [15] suggests to use $\|\nabla \cdot \boldsymbol{u}_h^n\|_{L^2(\Omega)}$ as a stopping criterion since the difference error between $\boldsymbol{u}_h^n, \boldsymbol{u}_h$ is given by

$$\|\boldsymbol{u}_h^n - \boldsymbol{u}_h\|_{L^2(\Omega)} \leq C \|\nabla \cdot \boldsymbol{u}_h^n\|_{L^2(\Omega)}.$$

The resulting rates of convergence of the numerical experiment are listed in Tables 11. The errors $\|\boldsymbol{u} - \boldsymbol{u}_h^n\|_{L^2(\Omega)}$ and $\|p - p_h^n\|_{L^2(\Omega)}$ are computed with $\|\nabla \cdot \boldsymbol{u}_h^n\|_{L^2(\Omega)} \leq 10^{-7}$ and $\gamma = \rho = 100$.

6.0 CONCLUSIONS

In this chapter, we make some conclusions regarding the work introduced in the previous chapters and future plans.

While we were successful proving the stability for the lowest order RT finite element pair for the axisymmetric Darcy problem, we still have to investigate other Darcy finite element pairs like lowest order BDM.

It was shown in [43] that the TH finite element pairs is stable under the axisymmetric variational formulation. We tried to prove the stability of Stokes div-free finite element pairs (e.g. SV), but the analysis was vague. We ran some numerical experiments and the results were hinting towards the stability of such elements.

While the theoretical results in chapter 4 suggest that the approximated solution of the grad-div stabilized variational formulation converges to the divergence-free solution of the non grad-div stabilized variational formulation as $\gamma \to \infty$, the numerical experiments show that the error increases as $\gamma \to \infty$ due to round-off error. We still have to investigate the optimal γ to use in numerical experiments.

In the near future (as a part of my new job at Iowa State University), I will be investigating the use of variational formulation methods for solving Fluid-Structure interaction equations (FSI).

BIBLIOGRAPHY

[1] V. Adolfsson and D. Jerison, *L^p-integrability of the second order derivatives for the Neumann problem in convex domains*, Indiana Univ. Math. J., 43(4):1123–1138, 1994.

[2] N .Ahmed, *On the grad-div stabilization for the steady Oseen and Navier-Stokes equations*, Calcolo, 54(1):471–501, 2017.

[3] Peter Alfeld *A trivariate Clough-Tocher scheme for tetrahedral data*, Computer Aided Geometric Design (1984) 1:169–181

[4] J. H. Argyris, I. Fried, D. W. Scharpf *The TUBA family of plate elements for the matrix displacement method*, Aero. J. Roy. Aero. Soc., 72:701–709, 1968.

[5] D.N. Arnold and J. Qin, *Quadratic velocity/linear pressure Stokes elements*, in Advances in Computer Methods for Partial Differential Equations VII, ed. R. Vichnevetsky and R.S. Steplemen, 1992.

[6] F. Assous, P. Ciarlet Jr., and S. Labrunie, *Theoretical tools to solve the axisymmetric Maxwell equations*, Math. Methods Appl. Sci., 25(1):49–78, 2002.

[7] Z. Belhachmi, C. Bernardi, and S. Deparis, *Weighted Clement operator and application to the finite element discretization of the axisymmetric Stokes problem*, Numer. Math., 105(2):217–247, 2006.

[8] Z. Belhachmi, C. Bernardi, and S. Deparis, *A truncated Fourier/finite element discretization of the Stokes equations in an axisymmetric domain*, Math. Models Methods Appl. Sci., 16(2):233–263, 2006.

[9] C. Bernardi, M. Dauge, and Y. Maday. *Spectral methods for axisymmetric domains, volume 3 of series in Applied Mathematics(Paris). Gauthier-Villars, Editions Scientifiques et Medicales Elsevier, Paris, North-Holland, Amesterdam, 1999. Numerical algorithms and tests due to Mejdi Azaiez.*

[10] D. Boffi, F. Brezzi and M. Fortin, *Finite elements for the Stokes problem*, in *Mixed Finite Elements, Compatibility Conditions, and Applications*, Lectures given at the C.I.M.E. Summer School, Springer-Verlag, Berlin, 2008.

[11] Boffi, Daniele and Brezzi, Franco and Fortin, Michel and others *Mixed finite element methods and applications*, Springer (2013) 44

[12] Boffi, Daniele and Guzman, Johnny and Neilan, Michael *Convergence of Lagrange finite elements for the Maxwell Eigenvalue Problem in 2D*, arXiv preprint arXiv:2003.08381 (2020)

[13] M. Braack, E. Burman, V. John, and G. Lube, *Stabilized finite element methods for the generalized Oseen problem*, Comput. Methods Appl. Mech. Engrg., 196(4-6):853–866, 2007.

[14] D. Braess. *Finite Elements, in Theory, Fast Solvers, and Applications in Solid Mechanics, 2nd ed., Cambridge University Press, Cambridge, UK, 2001*

[15] S. C. Brenner, L. R. Scott, *The Mathematical Theory of Finite Element Methods, Third Edition*, Springer, 2000.

[16] M. A. Case, V. J. Ervin, A. Linke, L. G. Rebholz *Connection between Scott–Voglius and grad-div stabilized Taylor–Hood FE approximations of the Navier–Stokes equations*, SIAM J. Numer. Anal., 49(4):1461–1481, 2011.

[17] S. Christiansen and K. Hu, *Generalized finite element systems for smooth differential forms and Stokes' problem*, Numer. Math., DOI:10.1007/s00211-018-0970-6, 2018.

[18] D. M. Copeland, J. Gopalakrishnan, and M. Oh, *Multigrid in a weighted space arising from axisymmetric electromagnetics*, Math. Comp. 79(272):2033–2058, 2010.

[19] D. M. Copeland, J. Gopalakrishnan, and J. E. Pasciak, *A mixed method for axisymmetric div-curl systems*, Math. Comp. 77 (2008), no. 264, 1941–1965.

[20] V. J. Ervin, *Approximation of axisymmetric Darcy flow using mixed finite element methods*, SIAM J. Numer. Anal., 51(3):1421–1442, 2013.

[21] V. J. Ervin, *Approximation of coupled Stokes-Darcy flow in an axisymmetric domain,* Comput. Methods Appl. Mech. Engrg., 258:96–108, 2013.

[22] Lawrence C. Evans. *Partial Differential Equations, Graduate Studies in Mathematics, Volume 19, AMS.*

[23] J .Evans, *Divergence-free B-spline discretizations for viscous incompressible flows*, The University of Texas at Austin, 2011.

[24] E. Fabes, O. Mendez, M. Mitrea, *Boundary layers on Sobolev-Besov spaces and Poisson's equation for the Laplacian in Lipschitz domains*, J. Funct. Anal., 159(2):323–368, 1998.

[25] R.S. Falk, M. Neilan, *Stokes complexes and the construction of stable finite elements with pointwise mass conservation*, SIAM J. Numer. Anal., 51(2):1308–1326, 2013.

[26] Floater, Michael S and Hu, Kaibo *A characterization of supersmoothness of multivariate splines*, arXiv preprint arXiv:1906.08164 (2019)

[27] J. de Frutos, B. Garcia-Archilla, V. John, and J. Novo, *grad-div stabilization for the evolutionary Oseen problem with inf-sup stable finite elements*, J. Sci. Comput., 66(3):991–1024, 2016.

[28] J. de Frutos, B. Garcia-Archilla, V. John, and J. Novo, *Analysis of the grad-div stabilization for the time-dependent Navier-Stokes equations with inf-sup stable finite elements*, Adv. Comput. Math., 44(1):195–225, 2018.

[29] K. J. Galvin, A. Linke, L. G. Rebholz, N. E. Wilson, *Stabilizing poor mass conservation in incompressible ow problems with large irrotational forcing and application to thermal convection*, Comput. Methods Appl. Mech. Engrg., 237/240 (2012), pp. 166-176,

[30] V. Girault, P.-A Raviart. *Finite Element Approximaton of the Navier-Stokes Equations*, Lecture Notes in Math. v. 749, Springer-Verlag, Berlin, 1979.

[31] V. Girault and P.-A Raviart *Finite element methods for Navier-Stokes equations. Theory and algorithms*, Springer (1986) 5

[32] Guzmán, J and Lischke, A and Neilan, M *Exact sequences on Powell–Sabin splits*, Calcolo (2020) 57:1–25

[33] Guzman, Johnny and Lischke, Anna and Neilan, Michael *Exact sequences on Worsey-Farin Splits*, arXiv preprint arXiv:2008.05431 (2020)

[34] Guzmán, Johnny and Neilan, Michael *Conforming and divergence-free Stokes elements in three dimensions*, IMA Journal of Numerical Analysis (2014) 34:1489–1508

[35] J. Guzmán and M. Neilan, *Inf-sup stable finite elements on barycentric refinements producing divergence–free approximations in arbitrary dimension*, SIAM J. Numer. Anal., 56(5):2826–2844, 2018.

[36] J. Guzman, R. Scott, *Cubic Lagrange elements satisfying exact incompressibility*, SMAI J. Comput. Math. 4:345–374, 2018.

[37] J. Guzman, R. Scott, *The Scott-Vogelius Finite Element revisited*, Math. Comp., 88(316):515–529, 2019.

[38] E.W. Jenkins, V. John, A. Linke, L. G. Rebholz *On the parameter choice in grad-div stabilization for the Stokes equations*, Adv Comput Math (2014) 40:491–516.

[39] V. John, A. Linke, C. Merdon, M. Neilan, and L.G. Rebholz, *On the divergence constraint in mixed finite element methods for incompressible flows*, SIAM Rev., 59(3):492–544, 2017.

[40] A. Kufner, A.-M. Sändig, *Some applications of weighted Sobolev spaces*, Teubner-Texte zur Mathematik, 100. BSB B. G. Teubner Verlagsgesellschaft, Leipzig, 1987.

[41] P. Lacoste, *Solution of Maxwell equation in axisymmetric geometry by Fourier series decomposition and by use of H(rot) conforming finite element*, Numer. Math., 84(4):577–609, 2000.

[42] M.-J. Lai and L. L. Schumaker, *Spline functions on triangulations*, Encyclopedia of Mathematics and its Applications, 110., Cambridge University Press, Cambridge, 2007.

[43] Y.-J. Lee and H. Li, *On stability, accuracy, and fast solvers for finite element approximations of the axisymmetric Stokes problem by Hood-Taylor elements*, SIAM J. Numer. Anal., 49(2):668–691, 2011.

[44] Y.-J. Lee and H. Li, *Axisymmetric Stokes equations in polygonal domains: regularity and finite element approximations*, Comput. Math. Appl., 64(11):3500–3521, 2012.

[45] A. Linke, M. Neilan, L.G. Rebholz, and N.E. Wilson, *A connection between coupled penalty projection timestepping schemes with FE spatial discretization for the Naiver-Stokes equations*, J. Numer. Math., 25(4):229–248, 2017.

[46] A. Linke, L.G. Rebholz, and N.E. Wilson, *On the convergence rate of grad-div stabilized Taylor-Hood to Scott-Vogelius solutions for incompressible flow problems*, J. Math. Anal. Appl., 381(2):612–626, 2011.

[47] Lischke, Anna *Exact smooth piecewise polynomials on Powell–Sabin and Worsey–Farin splits*, Ph.D. Thesis, Brown University (2020)

[48] G. Lube and M. A. Olshanskii, *Stable finite-element calculation of incompressible flows using the rotation form of convection*, IMA J. Numer. Anal., 22(3):437–461, 2002.

[49] V. P. Mikhailov, *Partial differential equations*, Translated from the Russian by P.C. Sinha. Revised from the 1976 Russian ed., Moscow: Mir Publishers, p. 396

[50] P. Monk, *Finite Element Methods for Maxwell's Equations, Numerical Mathematics and Scientific Computation*, Oxford Science Publications, 2003.

[51] M. Neilan and A. Zytoon, *Low-order Raviart–Thomas approximations of axisymmetric Darcy flow*, JMAA, 473 (2), 905 – 917, 2019

[52] R. .H. Nochetto, E. Otárola, and A. J. Salgado, *Piecewise polynomial interpolation in Muckenhoupt weighted Sobolev spaces and applications*, Numer. Math., 132(1):85–130, 2016.

[53] M. Olshanskii, G. Lube, T. Heister, and J. Löwe *grad-div stabilization and subgrid pressure models for the incompressible Navier-Stokes equations*, Comput. Methods Appl. Mech. Engrg., 198(49–52):3975–3988, 2009.

[54] M. Olshanskii and A. Reusken, *grad-div stabilization for Stokes equations*, Math. Comp., 73:1699–1718, 2004.

[55] M. J. D. Powell and M. A. Sabin, *Piecewise quadratic approximations on triangles*, ACM Trans. Math. Software 3(4):316–325, 1977.

[56] Qin, Jinshui *On the convergence of some low order mixed finite elements for incompressible fluids*, Ph.D. Thesis, Citeseer (1994)

[57] Qin, Jinshui and Zhang, Shangyou *Stability and approximability of the P1-P0 element for Stokes equations*, International journal for numerical methods in fluids (2007) 54:497–515

[58] L. R. Scott, M. Vogelius, *Conforming finite element methods for incompressible and nearly incompressible continua, in Large-Scale Computations in Fluid Mechanics, Part 2.* Lectures in Appl. Math. 22-2, Amer. Math. Soc., Providence, RI, 1985, pp. 221–244.

[59] Scott, L. R. and Vogelius, M. *Norm estimates for a maximal right inverse of the divergence operator in spaces of piecewise polynomials*, RAIRO Modélisation Mathématique et Analyse Numérique (1985) 19:111–143

[60] R. Stenberg. *Analysis of mixed finite element methods for the Stokes problems: A unified approach, Math. Comp., 42 (1984), pp. 9–23.*

[61] G. Strang, G. J. Fix, *An Analysis of the Finite Element Method*, byWellesley-Cambridge Press, Wellesley, MA; Cambridge, MA, 1973.

[62] Zhang, Shangyou *A new family of stable mixed finite elements for the 3D Stokes equations*, Mathematics of computation (2005) 74:543–554

[63] Zhang, Shangyou *On the $P1$ Powell-Sabin divergence-free finite element for the Stokes equations*, Journal of Computational Mathematics (2008) pages : 456–470

[64] Zhang, Shangyou *A family of 3D continuously differentiable finite elements on tetrahedral grids*, Appl. Numer. Math. (2009) 59:219–233

[65] Zhang, Shangyou *Quadratic divergence-free finite elements on Powell-Sabin tetrahedral grids*, Calcolo. A Quarterly on Numerical Analysis and Theory of Computation (2011) 48:211–244